N73-24034

NASA CONTRACTOR REPORT

NASA CR-2251

NASA CR-2251

CASE FILE COPY

ANALYSIS AND TESTING OF TWO-DIMENSIONAL SLOT NOZZLE EJECTORS WITH VARIABLE AREA MIXING SECTIONS

by Gerald B. Gilbert and Philip G. Hill

Prepared by
DYNATECH R/D COMPANY
Cambridge, Mass.
for Ames Research Center

NATIONAL AERONAUTICS AND SPACE ADMINISTRATION • WASHINGTON, D. C. • MAY 1973

1. Report No. NASA CR-2251	2. Government Accession No.	3. Recipient's Catalog No.
4. Title and Subtitle "Analysis and Testing of Two-Dimensional Slot Nozzle Ejectors with Variable Area Mixing Sections"		5. Report Date May 1973
		6. Performing Organization Code
7. Author(s) Gerald B. Gilbert and Philip G. Hill		8. Performing Organization Report No.
		10. Work Unit No.
9. Performing Organization Name and Address Dynatech R/D Company Cambridge, Massachusetts		11. Contract or Grant No. NAS 2-6660
		13. Type of Report and Period Covered Contractor Report
12. Sponsoring Agency Name and Address National Aeronautics & Space Administration Washington, D.C.		14. Sponsoring Agency Code

15. Supplementary Notes

16. Abstract

Finite difference computer techniques have been used to calculate the detailed performance of air to air two dimensional ejectors with symmetric variable area mixing sections and co-axial converging primary nozzles. The analysis of the primary nozzle assumed correct expansion of the flow and is suitable for subsonic and slightly supersonic velocity levels. The variation of the mixing section channel walls is assumed to be gradual so that the static pressure can be assumed uniform on planes perpendicular to the axis. An x-ψ^2 coordinate system is used in the solution of the momentum and energy equations to remove a singularity condition at the wall.

A test program was run to provide two-dimensional ejector test data for verification of the computer analysis. A primary converging nozzle with a discharge geometry of 0.125" x 8.0" was supplied with 600 SCFM of air at about 35 psia and 180°F. This nozzle was combined with two mixing section geometries with throat sizes of 1.25" x 8.0" and 1.875" x 8.0" and was tested at a total of 11 operating points.

The comparisons of wall static pressures, centerline velocity, centerline temperature, and velocity profiles between experimental and analytical results at the same flow rate were generally very good.

17. Key Words (Suggested by Author(s))	18. Distribution Statement
Ejector Computer Program Finite Difference Experimental	UNCLASSIFIED - UNLIMITED

19. Security Classif. (of this report)	20. Security Classif. (of this page)	21. No. of Pages	22. Price*
Unclassified	Unclassified	129	$3.00

* For sale by the National Technical Information Service, Springfield, Virginia 22151

TABLE OF CONTENTS

Section | TABLE OF CONTENTS | Page

LIST OF FIGURES

LIST OF FIGURES (continued)

LIST OF TABLES

ANALYSIS AND TESTING OF TWO-DIMENSIONAL SLOT NOZZLE EJECTORS WITH VARIABLE AREA MIXING SECTIONS

By

Gerald B. Gilbert, Philip G. Hill

SUMMARY

Finite difference computer techniques have been used to calculate the detailed performance of air to air two dimensional ejectors with symmetric variable area mixing sections and co-axial converging primary nozzles. The successful completion of this program completes a step in the development of a computer program to analyze the ejector of the augmentor wing lift augmentation system for STOL aircraft.

The finite difference computer program analyzes two dimensional mixing in converging-diverging jets. The analysis of the primary nozzle assumes correct expansion of the flow and is suitable for subsonic and slightly supersonic velocity levels. The variation of the mixing section channel walls is assumed to be gradual so that the static pressure can be assumed uniform on planes perpendicular to the axis. An x-ψ^2 coordinate system is used in the solution of the momentum and energy equations to remove a singularity condition at the wall. Different assumptions for eddy viscosity are made for each distinctly different region of the flow based on information available in the literature.

A test program was run to provide two-dimensional ejector test data for verification of the computer analysis. Geometry and primary air operating conditions similar to a typical augmentor wing ejector were selected for the tests. A primary converging nozzle with a discharge geometry of 0.125" x 8.0" was supplied with 600 SCFM of air at about 35 psia and 180°F. This nozzle was combined with two mixing section geometries with throat sizes of 1.25" x 8.0" and 1.875" x 8.0" and was tested at a total of 11 operating points. Secondary flow was varied by adding three steps of increased restriction to the ejector discharge. For each test mass flow rate, wall static pressures and several velocity traverses were recorded for comparison with analytical results.

The comparisons of wall static pressures, centerline velocity, centerline temperature, and velocity profiles between experimental and analytical results at the same flow rate were generally very good. The computer program presented in this report accurately predicts the performance of the simple two-dimensional ejectors and thereby successfully completes the objectives of this program.

Section 1

INTRODUCTION

1.1 Background

The augmentor wing concept under investigation by NASA for STOL aircraft lift augmentation is powered by an air to air ejector. The wing boundary layer is drawn into the deflected double flap augmentor channel at the trailing edge of the wing and is pressurized by a high velocity slot jet which is oriented at an angle to the augmentor channel. To predict the performance and to optimize the design of the complete augmentor wing, an analytical method is needed to predict the performance of the air ejector which powers the augmentor flap section.

Under contract NAS2-5845 a computer analysis was developed for single nozzle axisymmetric ejectors with variable area mixing sections using integral techniques(1). The ejectors of primary interest in that program and earlier programs were high entrainment devices using small amounts of supersonic primary flow to pump large amounts of low pressure secondary flow. Good agreement was achieved between analytical and experimental results.

The integral analytical techniques used to analyze the axisymmetric ejector configurations are also valid for the analysis of two dimensional ejectors. However, the augmentor wing configuration may include asymmetric geometries, inlet flow distortions, wall slots, and primary nozzles that are at large angles to the axis of the augmentor mixing section. The integral techniques are not easily adaptable to these more complex flows. Finite difference techniques can be used to analyze these more complex flow geometries at the expense of increased computer time.

1.2 Objectives of Program

The specific objectives of this investigation are the following:

(1) to develop a finite difference computer program for the analysis of two-dimensional, air ejectors with symmetric variable area mixing sections and with co-axial converging primary nozzles.

(2) to obtain test results with two-dimensional ejector configurations so that the analytical methods can be checked.

By modifying the present analysis additional complicating features of the actual augmentor wing ejector may be incorporated into the computer program until the complete augmentor wing ejector can be successfully analyzed.

Section 2

NOMENCLATURE

A_N	Nozzle discharge area
A_{n-1}	Coefficient appearing in the finite difference equations 26 and 36
B_{n-1}	Coefficient appearing in the finite difference equations 26 and 36
$\overline{C}_p$	Time average specific heat at constant pressure
C_{po}	Specific heat at constant pressure evaluated at a reference temperature T_o
C_p^*	Dimensionless constant pressure specific heat, $\frac{\overline{C}_p}{C_{po}}$
C_L	Eckert number, $\frac{(\gamma - 1) M_{ir}^2}{\frac{T_{wr}}{T_o} - 1}$
C_N	Nozzle discharge coefficient
C_{n-1}	Coefficient appearing in the finite difference equations 26 and 36
D_{n-1}	Coefficient appearing in the finite difference equations 26 and 36
E	Dimensionless eddy viscosity, $\frac{\epsilon}{\nu_o}$
$\overline{k}$	Time average thermal conductivity
k_o	Thermal conductivity evaluated at T_o
k^*	Dimensionless thermal conductivity, $\frac{\overline{k}}{k_o}$
g_o	Dimensional Constant, 32.2 lbm-ft/lbf-sec^2
ℓ_m	Prandtl mixing length
L_m	Dimensionless mixing length, $\frac{\ell_m u_o}{\nu_o}$
m	Node points along a streamline
n	Streamline designation
M_{ir}	Dimensionless Mach number, $\frac{u_o}{(\gamma R T_o)^{1/2}}$
p_b	Barometric pressure

NOMENCLATURE
(continued)

p_N	Nozzle pressure
$\overline{p}$	Time average static pressure
P_{rt}	Turbulent Prandtl number, $\frac{\epsilon}{\epsilon_H}$
P_{ro}	Prandtl number, $\frac{u_o C_{po}}{k_o}$
P	Dimensionless pressure, $\frac{\overline{p}}{1/2\ \rho_o u_o^2}$
q	Heat Transfer
q_T	Turbulent heat transfer, $\overline{(\rho v)'\ T'}$
R	Gas constant
T_a	Atmospheric temperature
$\overline{T}$	Time average temperature
T'	Instantaneous fluctuating temperature
T_j	Jet temperature at the nozzle exit plane
T_o	Flow reference temperature
T_N	Nozzle temperature
T_{wr}	Wall reference temperature
$\overline{u}$	Time averaged velocity in x-direction
u'	Instantaneous fluctuating x component of velocity
u_o	Jet centerline velocity at the nozzle exit plane
$u_{2,n}$	Unknown velocity at the n^{th} grid point
u	Dimensionless velocity in x-direction, $\frac{\overline{u}}{u_o}$
u*	Friction velocity, $\frac{(\tau_w)^{1/2}}{\rho}$
$\overline{v}$	Time averaged flow velocity in y-direction

NOMENCLATURE
(continued)

v'	Instantaneous fluctuating y-component of velocity
W_m	Mixing section total flow rate
W_n	Nozzle flow rate
W_s	Secondary flow rate
x	Space co-ordinate in the axial direction
X	Dimensionless space co-ordinate in the axial direction, $\frac{u_o x}{\nu_o}$
ΔX	Step size in x-direction
y	Space co-ordinate perpendicular to axial direction
Y	Dimensionless space co-ordinate perpendicular to axial direction, $\frac{yu_o}{\nu_o}$
y_w	Duct half width or duct radius
$y+$	Dimensionless wall co-ordinate $\frac{y\,u^*}{\nu}$
α	Constant, unity for axisymmetric flow and zero for two-dimensional flow
γ	Ratio of specific heat, $\frac{\bar{C}_p}{\bar{C}_p}$
ψ	Transformed co-ordinate defined by equation 8
ψ_s	Regular stream coordinate
ψ^*	Dimensionless ψ co-ordinate $\psi^{*2} = \frac{\psi^2}{\nu_o \rho_o}$ for two-dimensional flow
$\bar{\rho}$	Time averaged fluid density
ρ_o	Fluid density evaluated at a reference temperature T_o
ρ^*	Dimensionless fluid density
$\bar{\mu}$	Time averaged absolute viscosity
μ_o	Absolute viscosity evaluated at a reference temperature T_o
μ^*	Dimensionless absolute viscosity, $\frac{\bar{\mu}}{\mu_o}$
τ	Mean average shear stress

NOMENCLATURE
(continued)

τ_T	Turbulent shear stress, $\overline{(\rho v)' u'}$
τ_w	Local wall shear stress
ϵ	Eddy viscosity
ϵ_H	Eddy conductivity
θ	Dimensionless temperature $\frac{T - T_o}{T_{wr} - T_o}$
ν	Kinematic viscosity at local temperature
ν_o	Reference kinematic viscosity evaluated at a reference temperature T_o
δ	Local wall boundary layer thickness or jet half width
Δ	Dimensionless boundary layer thickness, $\frac{u_o \delta}{\nu_o}$
κ	Mixing length constant
Φ	Mean value of dissipation

Section 3

ANALYSIS OF TWO-DIMENSIONAL JET MIXING

3.1 Introduction

This section is concerned with the essential physical features of a computation model for plane two-dimensional jet mixing in converging-diverging jets. A finite-difference computer program has been developed for treating the mixing of two parallel and compressible air streams, allowing for at least one of them to be supersonic. In all cases, the nozzle expansion is assumed "correct", i.e. nozzle exit plane pressure is matched to the ambient pressure at that station. Thus, expansion waves and shocks at the nozzle exit plane are assumed to be absent. Even though the correct expansion assumption may not be realized in a practical case, the downstream flow field will not likely be sensitive to small degrees of over - or under-expansion. The flows considered include compound flows of supersonic and subsonic streams; however, no provision is made for compound choking which may occur with an appropriate transverse distribution of Mach number. Such a condition is amenable to analytical treatment under simplified circumstances, but has not been encountered in experimental tests carried out so far.

This development is restricted to symmetric jet mixing in which the high speed jet is located on the axis of the channel and no provision is made for blowing or suction along the channel walls. The variation in channel geometry along the axis is assumed gradual, so that wall curvature is neglected and, on all planes normal to the axis, the pressure is assumed uniform.

In most calculations performed with this method to date, the velocity distribution at the nozzle exit plane was assumed to be rectangular, i.e., the wall boundary layer has been assumed to have zero thickness at that point; the initial thickness of the jet-secondary stream shear layer has also been assumed to be zero. This requirement is not necessary, however, and in general any initial distribution of velocity in the initial plane is permissible, under the assumption that pressure distribution across the plane is uniform.

Although previous work [1] has amply demonstrated that integral methods are capable of predicting symmetric jet mixing of compressible flow in jets, the finite difference method has been chosen for this problem. The finite difference method has advantages relative to the integral method of much greater flexibility in allowable flow inlet conditions, and wall boundary conditions, e.g., the use of wall jets or wall suction. Further the finite difference method offers the considerable advantage of mathematical precision in determining the overall consequences of any particular physical hypothesis regarding the shear stress distribution. With the integral method, the mathematical approximation due to the formation of integrals may contribute uncertainty in flow prediction in addition to the uncertainty introduced by a lack of precise physical knowledge. Thus, in developing a model to handle a certain class of flows, it is advantageous to have a method which is relatively precise mathematically, so that the effects of physical uncertainties may be assessed relatively clearly. The finite difference method is however, quite costly in its requirement for computer time. Further, as experience has shown, considerable care is required in adjusting the computation grid such that spacings are appropriately small in the region of the wall, and in any part of the flow where velocity gradients are quite large.

3.2 Basic Conservation Equations

In stream-wise coordinates, the momentum and energy equations[2] for the plane two-dimensional flow are:

$$\bar{u}\,\frac{\partial \bar{u}}{\partial x} = -\frac{1}{\bar{\rho}}\frac{d\bar{p}}{dx} + \bar{u}\,\frac{\partial \tau}{\partial \psi_s} \tag{1}$$

$$\bar{u}\,\frac{\partial(\bar{C}_p\,\bar{T})}{\partial x} = \frac{\bar{u}}{\bar{\rho}}\,\frac{d\bar{p}}{dx} + \bar{u}\,\frac{\partial q}{\partial \psi_s} + \frac{\Phi}{\bar{\rho}} \tag{2}$$

$$\Phi = \bar{\mu}\left(\frac{\partial \bar{u}}{\partial y}\right)^2 - \overline{(\rho v)'\ u'}\,\frac{\partial \bar{u}}{\partial y} = (\bar{\mu} + \bar{\rho}\epsilon)\left(\frac{\partial \bar{u}}{\partial y}\right)^2 \tag{3}$$

in which $\bar{u}$ is the velocity component in the x or principal flow direction, $\bar{p}$ is the static pressure, $\bar{\rho}$ the density and $\bar{T}$ is the temperature of the fluid. Using the eddy viscosity assumption, the mean average shear stress and heat transfer are defined by:

$$\tau = \bar{\mu}\,\frac{\partial \bar{u}}{\partial y} - \overline{(\rho v)'\,u'} = (\bar{\mu} + \bar{\rho}\epsilon)\,\frac{\partial \bar{u}}{\partial y} \tag{4}$$

$$q = \bar{k}\frac{\partial \bar{T}}{\partial y} - \bar{C}_p \; \overline{(\rho v)' T'} = (\bar{k} + \frac{\bar{\rho}\bar{C}_p \epsilon}{P_{rt}}) \frac{\partial \bar{T}}{\partial y} \tag{5}$$

in which ϵ is the kinematic eddy viscosity.

In developing the finite difference solution to this problem, the stream-wise coordinate system was attractive, not only in terms of the simplicity of the governing equations but also for possible development as a design procedure, in which the flow field pressure distribution could be specified and the required wall geometry determined, non-interatively, once the solution is obtained in stream coordinates. However, the difficulty with the stream wise coordinate is that it introduces a singularity in the governing equations in the vicinity of the wall. Given the definition of the stream function,

$$\frac{\partial \psi_s}{\partial y} = \bar{\rho}\bar{u} \tag{6}$$

it can be seen that the gradient

$$\frac{\partial \bar{u}}{\partial \psi_s} = \frac{1}{\bar{\rho}\bar{u}} \frac{\partial \bar{u}}{\partial y} \tag{7}$$

becomes undefined at the wall where the value of $\bar{u}$ approaches zero. The singularity can be removed as Denny[3] has shown by using the transformation

$$\frac{\partial \psi^2}{\partial y} = \bar{\rho}\bar{u}\,, \quad \frac{\partial \psi}{\partial y} = \frac{\bar{\rho}\,\bar{u}}{2\psi}\,, \text{ and } \frac{\partial \bar{u}}{\partial y} = \frac{\bar{\rho}\;\bar{u}}{2\psi}\frac{\partial \bar{u}}{\partial \psi} \tag{8}$$

instead of conventional stream function definition in which case the limiting value of the gradient $\frac{\partial \bar{u}}{\partial \psi}$ is finite and higher derivatives also exist. With this transformation then, the equations of motion may be written.

$$\bar{u}\frac{\partial \bar{u}}{\partial x} = -\frac{1}{\bar{\rho}}\frac{d\bar{p}}{dx} + \frac{\bar{u}}{2\psi}\frac{\partial}{\partial \psi}\left[(\bar{\mu} + \bar{\rho}\epsilon)\frac{\bar{\rho}\bar{u}}{2\psi}\frac{\partial \bar{u}}{\partial \psi}\right] \tag{9}$$

$$\bar{u}\,\frac{\partial(\bar{C}_p\bar{T})}{\partial x} = \frac{\bar{u}}{\bar{\rho}}\,\frac{d\bar{p}}{dx} + \frac{\bar{u}}{2\psi}\,\frac{\partial}{\partial\psi}\left[\left(\bar{k} + \frac{\bar{\rho}\bar{C}_p\epsilon}{P_{rt}}\right)\frac{\bar{\rho}\bar{u}}{2\psi}\,\frac{\partial\bar{T}}{\partial\psi}\right] + \left(\frac{\bar{\mu}+\bar{\rho}\epsilon}{\bar{\rho}}\right)\left(\frac{\bar{\rho}\bar{u}}{2\psi}\,\frac{\partial\bar{u}}{\partial\psi}\right)^2 \tag{10}$$

where ψ is now the transformed quantity according to Denney[3]. The transformation of these equations is shown in Appendix A.

3.3 Dimensionless Groups

Before solution of the finite-difference method, these equations are made dimensionless by the following steps.

The velocity $\bar{u}$ is normalized by dividing by the jet centerline velocity u_o. Also a reference Mach number is defined by:

$$M_{ir} = \frac{u_o}{\sqrt{\gamma R T_o}} \tag{11}$$

in which T_o is a reference temperature and γ is the specific heat ratio. A dimensionless temperature parameter is defined by:

$$\theta = \frac{\bar{T} - T_o}{T_{wr} - T_o} \tag{12}$$

in which T_{wr} is a second arbitrary reference temperature.

The fluid properties variables are made dimensionless by defining:

$$\begin{aligned} k^* &= \frac{\bar{k}}{k_o} & P_{ro} &= \frac{\mu_o C_{po}}{k_o} \\ C_p^* &= \frac{\bar{C}_p}{C_{po}} & E &= \frac{\epsilon}{\nu_o} \\ \mu^* &= \frac{\bar{\mu}}{\mu_o} & \rho^* &= \frac{\bar{\rho}}{\rho_o} \end{aligned} \tag{13}$$

in which k_o, C_{po}, μ_o, and ρ_o are fluid properties at reference values of pressure and temperature and $\mu_o = \rho_o \nu_o$.

In the program the reference values of temperature are

$$T_o = 520^{\circ}R$$

$$T_{wr} = 560^{\circ}R$$

and the reference fluid properties are evaluated at 520°R and 2115 psf.

The coordinate variables are transformed to:

$$X = \frac{u_o x}{\nu_o} \tag{14}$$

$$\psi^* = \frac{\psi}{\sqrt{\rho_o \nu_o}} \tag{15}$$

Then in dimensionless form the equations of motion become:

$$u \frac{\partial u}{\partial X} = - \frac{1}{2 \rho^*} \frac{dP}{dX} + \frac{u}{2 \psi^*} \frac{\partial}{\partial \psi^*} \left[(\mu^* + E\rho^*) \frac{\rho^* u}{2 \psi^*} \frac{\partial u}{\partial \psi^*} \right] \tag{16}$$

$$u \frac{\partial (C_p^* \theta)}{\partial X} = \frac{C_L u}{2 \rho^*} \frac{dP}{dX} + \frac{u}{2 \psi^*} \frac{\partial}{\partial \psi^*} \left[\left(\frac{k^*}{P_{ro}} + \frac{E\rho^* C_p^*}{P_{rt}} \right) \frac{\rho^* u}{2 \psi^*} \frac{\partial \theta}{\partial \psi^*} \right]$$

$$+ C_L \left(\frac{\mu^* + E\rho^*}{\rho^*} \right) \left(\frac{\rho^* u}{2 \psi^*} \frac{\partial u}{\partial \psi^*} \right)^2 \tag{17}$$

in which

$$C_L = \frac{(\gamma - 1) M_{ir}^2}{\frac{T_{wr}}{T_o} - 1} = \frac{u_o^2}{C_{po}(T_{wr} - T_o)} \tag{18}$$

The turbulent Prandtl number P_{rt} is taken to be 0.9. Neglecting the dependance of the specific heat on temperature, $C_p^* = 1.0$. The derivative of the dimensionless equations of motion is shown in Appendix A.

3.4 Evaluation of the Eddy Viscosity

In general, the eddy viscosity is evaluated by

$$\epsilon = \ell_m^2 \frac{\partial \bar{u}}{\partial y} \tag{19}$$

in which ℓ_m is the mixing length. In two-dimensional jet mixing, values of mixing length are not well known especially for the region in which the shear zone extends from wall to wall. In various zones of the flow, the mixing lengths have been evaluated as follows:

In the shear layer adjacent to the potential core zone of the primary jet the mixing length is evaluated from

$$\ell_m = 0.08\,\delta \tag{20}$$

in which δ is the shear layer width (including the zone between 1% and 99% of the total velocity difference between primary and secondary streams).

For the "fully-rounded" portion of the jet flowing coaxially with a secondary potential stream, the mixing length has been calculated from

$$\ell_m = 0.108\,\delta \tag{21}$$

in which δ is the half-width of the jet, evaluated from centerline to the point at which the difference between local and secondary velocity is only 1% of the difference between centerline and secondary velocity.

In the wall boundary layer, the mixing length has been evaluated from the lesser of:

$$\ell_m = 0.09\delta \quad \text{(outer part)} \tag{22}$$

or, using the Van Driest approximation,

$$\ell_m = 0.41 \left[1 - e^{-(y^+/26)}\right] y \quad \text{(inner part)} \tag{23}$$

in which

$$y^+ = \sqrt{\frac{\tau_w}{\rho}} \; \frac{y}{\nu} \tag{24}$$

For the region downstream of the point where the jet spreads to intersect the edge of the boundary layer the mixing length is evaluated, as a first approximation only, from

$$\ell_m = y_w \left[0.14 - 0.08 \left(\frac{y}{y_w} \right)^2 - 0.06 \left(\frac{y}{y_w} \right)^4 \right] \tag{25}$$

which is due to Nikuradse and is cited by Schlichting[4] for fully developed flow in round tubes. Near the wall ($y = y_w$) the mixing length is evaluated by the Van Driest approximation cited earlier, provided the local mixing length so calculated is less than that given by the Nikuradse formula.

3.5 Boundary Conditions

With prescribed wall geometry the boundary conditions at the outer wall are:

$$y = y_w(x)$$

$$\psi^* = \text{const.}$$

$$\frac{\partial \theta}{\partial \psi^*} = 0$$

$$u = 0$$

Along the channel axis of symmetry the boundary conditions are:

$$y = 0$$

$$\psi^* = 0$$

$$\frac{\partial \theta}{\partial \psi^*} = 0$$

$$\frac{\partial u}{\partial \psi^*} = 0$$

3.6 Finite Difference Procedure

By the finite-difference technique, the derivatives in the differential equations of motion are replaced by differences either along a streamline between two neighboring points X and X + ΔX or normal to it between two neighboring points ψ^* and $\psi^* + \Delta\psi^*$.

If one takes the velocity field at plane X as completely known then the velocity field at X + ΔX may be solved, using the implicit method, from the finite-difference form of the momentum equation which is of the form

$$A_{n-1}\, u_{2,n} + B_{n-1}\, u_{2,\, n+1} + C_{n-1}\, u_{2,n-1} = D_{n-1} \tag{26}$$

in which $u_{2,n}$ is the unknown velocity at the n^{th} grid point on plane X + ΔX and A_{n-1}, B_{n-1}, C_{n-1}, D_{n-1} are coefficients containing the mean pressure gradient between X and X + ΔX and the velocity and shear stress distributions at plane X.

As shown in the derivation in reference[5] and Appendix B, the coefficients in the finite difference form of the momentum equation are evaluated from:

$$A_{n-1} = Y8 + Y9 + \frac{u_{1,n}}{\Delta X} \tag{27}$$

$$B_{n-1} = - Y8 \tag{28}$$

$$C_{n-1} = - Y9 \tag{29}$$

$$D_{n-1} = - \frac{1}{4\rho^*_{1,n}} \left(\left.\frac{dP}{dX}\right|_{m=2} + \left.\frac{dP}{dX}\right|_{m=1} \right) + \frac{u^2_{1,n}}{\Delta X} \tag{30}$$

in which,

$$Y8 = \frac{u_{1,n}}{2\psi^*_n} \left(\frac{S_{n+1} + S_n}{\Delta\psi_1\, S1} \right) \tag{31}$$

$$Y9 = \frac{u_{1,n}}{2\psi^*_n} \left(\frac{S_n + S_{n-1}}{\Delta\psi_2\, S1} \right) \tag{32}$$

$$Sl = \Delta \psi_1 + \Delta \psi_2 \tag{33}$$

$$\Delta \psi_2 = \psi^*_n - \psi^*_{n-1}, \quad \Delta \psi_1 = \psi^*_{n+1} - \psi^*_n \tag{34}$$

$$S = \left(\frac{\mu^* + E\rho^*}{2\psi^*}\right) \rho^* u \tag{35}$$

In a similar way[5], the energy equation can be written in the finite difference form:

$$A_{n-1}\, \theta_{2,n} + B_{n-1}\, \theta_{2,n+1} + C_{n-1}\, \theta_{2,n-1} = D_{n-1} \tag{36}$$

where,

$$A_{n-1} = Y8' + Y9' + \frac{u_{1,n}}{\Delta X} \tag{37}$$

$$B_{n-1} = -Y8' \tag{38}$$

$$C_{n-1} = -Y9' \tag{39}$$

$$D_{n-1} = \frac{u_{1,n}\theta_{1,n}}{\Delta X} + \frac{C_L u_{1,n}}{4\rho^*_{1,n}} \left[\left.\frac{dP}{dX}\right|_{m=1} + \left.\frac{dP}{dX}\right|_{m=2} \right]$$

$$+ \frac{C_L S_{1,n} u_{1,n}}{2\psi^*} \left[R_2(u_{2,n+1} - u_{2,n}) + R_1 (u_{2,n} - u_{2,n-1}) \right]^2 \tag{40}$$

$$Y8' = \frac{u_{1,n}}{2\psi^*_n} \left[\frac{Q_{n+1} + Q_n}{\Delta \psi_1\, Sl} \right] \tag{41}$$

$$Y9' = \frac{u_{1,n}}{2\psi^*_n} \left[\frac{Q_n + Q_{n-1}}{\Delta \psi_2\, Sl} \right] \tag{42}$$

$$Q = \left[\frac{k^*}{P_{ro}} + \frac{E\rho^*}{P_{rt}} \right] \frac{\rho^* u}{2\psi^*} \tag{43}$$

$$R_1 = \frac{\Delta \psi_1}{\Delta \psi_2(\Delta\psi_2 + \Delta\psi_1)} \tag{44}$$

and

$$R2 = \frac{\Delta\psi_2}{\Delta\psi_1 (\Delta \psi_2 + \Delta\psi_1)} \tag{45}$$

The relationship between the x-ψ coordinates, and the physical plane in finite difference form, for any n, becomes,

$$Y_n = \left[Y_{n-1} + \frac{(\psi_n^{*2} - \psi_{n-1}^{*2})\ 2}{(\rho^* u)_n + (\rho^* u)_{n-1}} \right] \tag{46}$$

Finally the property relation becomes:

$$E_{2,n} = \frac{u_{1,n}\ \rho^*_{1,n}\ L_m^2}{2\psi^*} \left[\frac{u_{1,n+1} - u_{1,n-1}}{\psi^*_{n+1} - \psi^*_{n-1}} \right] \tag{47}$$

For a set of N ψ-lines and known boundary conditions, Equations (26) and (36) each provide a set of N-2 conditions to solve for the unknown velocities and temperatures. Each set of equations can be solved simultaneously if the pressure gradient is known or assumed. For calculation of flow between fixed channel walls, the pressure gradient is assumed and the velocities determined; then the location of the outer boundary is calculated from successive use of equation (46) across all N grid lines. If the calculated value of the outer boundary location does not agree satisfactorily with the actual wall geometry, a new value of the pressure gradient is chosen.

Since each set of equations can be represented by a tridiagonal matrix of coefficients, the Thomas Algorithm[5] is employed for speedy solution as shown in Appendix C which describes the solution procedure.

The structure of the computer program is given in Appendix D.

Section 4

TEST PROGRAM

A two-dimensional experimental rig was designed, fabricated, and installed in our laboratory. The purpose of the experimental work was to obtain test data for verification and adjustment of the computer analysis. The experimental program is described in this section.

4.1 Experimental Apparatus

4.1.1 Two-Dimensional Ejector

The two-dimensional ejector consisted of a slot type primary nozzle and a two-dimensional mixing section. The arrangement of the ejector system is shown on Figure 1.

A picture of the primary nozzle is shown on Figure 2. The discharge slot is 0.1215" $\pm$ .0005" by 8.00" with rounded corners. The side walls are quarter inch carbon steel and four internal supports are included to prevent widening of the discharge slot when the nozzle is pressurized. Dial indicator measurements show that the slot opened up by about 0.0008 inches in the center of the nozzle, about .0004" at the quarter width location and zero near the ends of the slot. This is equivalent to an increase in nozzle slot area of 0.33% when pressurized. Stagnation pressure measurements were made with a kiel probe from side to side in the nozzle discharge and were found to be uniform across the 8" width of the slot. The primary nozzle is positioned in the mixing section (see Figure 1 and Figure 3) so that the primary flow is discharged along the centerline of the straight symmetrical mixing section.

The mixing section as shown on Figure 1 consists of a rectangular variable area channel formed by two identically contoured aluminum plates and two flat side plates. The pictures in Figures 3 and 4 show two views of the mixing section. The two contoured plates can be positioned in two symmetrical locations about the centerline to form the two channels tested (throat heights of 1.25" and 1.875"). The width of the mixing section is 8.00" for the full length. The variation of channel height with distance from the nozzle discharge is given on Table 1 for the 1.875 throat mixing section. The geometry for the 1.25" throat height is obtained by subtracting 0.312" from each y value. Three plexiglass windows are installed along each side of the mixing section so the tufts of wool mounted inside can be observed for indications of flow separations and unsteadiness.

The screened mixing section inlet is shown on Figure 5. Initial tests without the extended inlet showed that highly swirling corner vortices were formed in the four corners of the bellmouth and extended into the test section. The extended inlet eliminated the corner vortices and improved the stability of the ejector flow and static pressures. The extended inlet shown on Figure 5 was used for all ejector tests.

4.1.2 Facilities for Ejector Tests

The schematic of the ejector test facilities on Figure 6 shows the three required subsystems needed for operation, control and measurement of the ejector:

- Primary Flow System
- Mixed Flow System
- Boundary Layer Suction System

The primary air flow is supplied by a 900 SCFM oil free screw compressor at 100 psig and an equilibrium operating temperature between $180^{\circ}F$ and $240^{\circ}F$. The primary air flow rate and pressure are controlled by a manual pressure regulator and bleed valve. The mass flow is measured by a standard 3 inch Danial orifice system. The air flow is delivered to the primary nozzle through a flexible hose.

The mixed flow system consists of a plenum chamber, an 8" orifice system and a throttle valve. Four different operating flow rates are achieved by the following equipment combinations.

1. Maximum Flow Rate -	Mixed flow discharges directly into laboratory from mixing section.
2. First Reduced Flow Rate -	The plenum is connected to the mixing section discharge.
3. Second Reduced Flow Rate -	The orifice is connected to the plenum.
4. Lowest Flow Rate -	The throttle valve is partially closed.

Orifice flow rates are obtained only for the two lowest flow rate conditions. Figure 7 and 8 show most of the experimental ejector installation. The large rectangular box connected to the mixing section by the large black flexible hose is the main plenum. The 8" orifice is not visible in the picture.

The suction system removes the boundary layer flow from each of the four corners of the mixing section to prevent wall boundary layer separation in the ejector. The pictures in Figures 7 and 8 show three 3/4 inch tubes connected to each corner of the mixing section. These 12 tubes collect the boundary layer flow from the corner suction slots which are 0.060 inches wide and are machined into the sides of the contoured plates (See figures 9 and 10). The four tubes at one X location are connected to a single large tube under the mounting table. The three large tubes are each connected to a large tank plenum through a separate throttle valve. A Roots blower draws the air through the suction system and through a three inch orifice system. The suction system is capable of removing about 1% to 2% of the mixing section flow rate. During the operation of the ejector rig, the boundary layer suction system was necessary to prevent flow separation in the mixing section diffuser. The presence of separation was easily observed from the violently flopping tufts, the large fluctuation in wall static pressures and audible pulsations. The operation of the suction system drastically reduced these symptoms.

The ejector system was operated by starting the primary air flow at low pressure and flow rate. The suction was turned on and then the primary pressure was increased to the desired test conditions. The large mixing section (1.875" throat height) was operated at 21 psig without separation in the mixing section. The small mixing section (1.25" throat height) could not be operated over 20 psig without separation for the high flow condition. The tests with the small mixing were therefore run at 17 psig.

4.2 Instrumentation and Data Reduction

4.2.1 Instrumentation

The following instrumentation was included on the test rig.

Primary Flow System

Flow Rate - Standard 3" orifice system
Nozzle Pressure - Pressure gage accurate to $\pm$ .25 psig
Nozzle Temperature - Thermocouple with digital readout

Mixed Flow System

Flow Rate -	8" orifice system for two lowest flow rate conditions
Static Pressures -	Wall static pressures down the center of the mixing section and some at other locations (see Figures 9 and 10). Manometers were used for measurement.
Traverse Data -	Stagnation pressure and temperature profiles were measured at up to 9 axial locations using a kiel temperature probe, a pressure transducer and direct digital readout, and a temperature direct digital readout (see Figure 8).

Suction Flow System

Flow Rate -	3" orifice system
Suction Pressure-	a mercury manometer

4.2.2 Data Reduction Procedures

Three types of data reduction calculations were needed in this program:

- Standard orifice calculations
- velocity profile calculations
- integration of velocity profiles to calculate flow rate

The orifice calculations were carried out using standard orifice equations and ASME orifice coefficients. The velocity profiles were calculated from the well known compressible flow relationships between Mach number and the ratio of stagnation pressure to static pressure that can be found in most fluid mechanics text books. The local velocity is calculated from the Mach number and the local speed of sound which is dependent on the local static temperature. The static temperature is calculated from the measured stagnation temperature profiles and the compressible flow relation between temperature ratio and Mach number.

To calculate an integrated mass flow rate for each traverse location a time sharing data reduction computer program was written to integrate the product of local velocity and local density over a two-dimensional section of unit width. The program also calculated the "mass-momentum" stagnation pressure at each traverse section using the equations presented on page 52 and 53 of reference 6. The mass-momentum method determines the flow conditions for a uniform velocity profile which has the same integrated values of mass flow rate, momentum, and energy as the non-uniform velocity profile actually present.

4.2.3 Experimental Uncertainty

Orifice Calculations

The techniques presented in reference 7 were applied to the primary flow orifice calculations and the mixed flow orifice calculations. The following uncertainty results were obtained:

Orifice	Nozzle Pressure psig	Uncertainty
Primary	17.0 and 21	$\pm$ 0.8%
Mixed	slightly above atmospheric	$\pm$ 1.3%

Static Pressures

Uncertainty in the wall static pressures mainly occurs because of unsteadiness in the manometer liquid columns caused by unsteadiness in the flow. The lowest flow rate condition which had the most system resistance downstream of the mixing section had a wall static pressure unsteadiness of about $\pm$3/8 inches of water. The amount of unsteadiness increased as the flow rate was increased by removing system resistance. For the unrestricted maximum flow rate condition the wall static pressure unsteadiness was $\pm$ 2.0 inches of water. These values are also a measure of the uncertainty.

Integrated Mass Flow Rate

The mass flow rate calculated by integrating the results of the stagnation pressure and temperature traverses is influenced by many items and is therefore very difficult to estimate. The following items all contribute to the uncertainty in integrated mass flow rate:

1. unsteady wall static pressures
2. unsteady traverse stagnation pressures
3. instrument accuracy of the pressure transducer and digital readout
4. inaccuracies due to the effect of steep velocity gradients on sensed pressure
5. inaccuracies due to probe effect near the mixing section walls
6. inaccuracy in probe position
7. assumptions and inaccuracies associated with the data reduction computer program
8. data recording errors or computer data input errors
9. errors caused by loose connections in the pneumatic sensing tube between the probe and the transducer
10. Non-two-dimensional flow distribution across the width of the 8 inch mixing section.

All of these effects could combine to give both a $\pm$ uncertainty band and a fixed error shift.

One measure of the uncertainty due to these effects is obtained from the limits of individual integrated mass flows for each test run. These values are listed on Table 2 for all of the test runs with traverse data. The results presented on Table 2 show an average variation of + 3.6% and -2.8% or a total spread of 6.4%. These values only include the effect of variable uncertainty and exclude the uncertainty due to probe errors in steep gradients and near walls and integration assumptions. Both of the excluded errors probably cause the intergrated mass flows to be too large because the probe tends to measure too high near the wall and the integration program neglects wall boundary layers.

From the above discussion it is concluded that the average integrated mass flow rates may have a fixed error of +1% to 2% and an uncertainty of about ±3% to ±4%.

4.3 Test Results

A total of eleven ejector tests were carried out on two mixing section configurations (1.25" and 1.875" throat height). The data presented in this report falls into the following categories:

Test Conditions and Mass Flows
Static Pressures
Centerline Velocities and Temperatures
Velocity Profiles
Temperature Profiles
Eddy viscosity Sensitivity
Flow Rate Sensitivity

Table 3 shows which figures and tables show the data for each test run. Most of the figures and tables present both test data and comparative analytical results. The comparisons will be discussed in section 5.0.

Section 5

COMPARISON OF ANALYTICAL AND EXPERIMENTAL RESULTS

5.1 Test Conditions and Mass Flows

Table 4 presents a tabulation of the measured nozzle conditions, the integrated mass flow rate from the measured pressure and temperature profiles, and the integrated "mass momentum" stagnation pressure.

The nozzle mass flow rate was calculated from standard orifice readings which were shown in section 4.2.3 to have an uncertainty of about $\pm 0.8\%$. Using the orifice flow rate, the nozzle pressure, the nozzle temperature, and the nozzle discharge area, a nozzle discharge coefficient (C_N) was calculated for each test run. These values all fall within a range of +0.007 and -0.0085 around an average of 0.973 which is consistent with the calculated uncertainty. If there were no error in the nozzle calculations all of the C_N values would be identical. From these results it is safe to assume that the listed nozzle flow rates are accurate to at least $\pm 1\%$.

The tabulated mixing section flow rates were calculated as described in section 4.2.2 by integrating the measured pressure and temperature profiles. As described in section 4.2.3, these results probably have a fixed error of between +1% and +2% and an uncertainty of between $\pm 3\%$ and $\pm 4\%$. Table 5 presents a comparison between three separate mass flow determinations:

- integrated from traverse data
- measured by orifice
- computer mass flow giving the best wall static pressure comparison

Only 4 of the tests could be measured with the large orifice, but all of these four tests agree with the computer mass flow within $\pm 0.9\%$ as shown on table 5. Section 4.2.3 shows that the expected uncertainty in orifice mass flow is about $\pm 1.3\%$ making it much more accurate than the integrated traverse values. The wall static pressures are in fact a function of the average mass flow represented by the orifice value rather than a local velocity profile down the center of the two-dimensional mixing section. This is true because the mixing section flow patterns can not support a side-to-side pressure gradient along the 8 inch width of the mixing section which was verified by test measurements. Therefore it is concluded that the measured orifice mass flows and the computer mass flow for best match of wall static pressures are the correct mass flow values. The integrated mass flows are in error and in some cases inconsistent. Table 5 shows that the integrated mass flow values spread over a range of -2.9% to +6.4% around the computer determined value. Figures 11 and 12 show all of the mass flow values on Table 5 plotted versus the mixing section throat static pressure. Figure 11 for Runs 1-5 shows the good agreement between computer analytical mass flows and orifice mass flows and shows the wide scatter of integrated traverse mass flows. Figure 12 for Runs 6-10 again shows good agreement between analytical and orifice values and this time shows a consistent trend of integrated traverse mass flows which are now offset by about +3.2% on a line parallel to the other more accurate mass flow values.

The "mass-momentum" stagnation pressure listed on table 4 suffers from the same inaccuracies as the integrated mass flow rate discussed above. The plotting of mass-momentum stagnation pressure versus mass flow will therefore show some discrepancies.

5.2 Mixing Section Wall Static Pressure Variation

The wall static pressure distributions are shown on Figures 13 and 14 and Table 6 as specified on Table 3. Runs 4, 8, and 11 on Table 6 were extra tests for which no analytical solutions were obtained. Test Run 11 was a repeat of test Run 9 and gives results that are essentially the same.

Figures 13 and 14 show there is a good comparison between experimental wall static pressures (shown as data points) and the analytical static pressures (solid lines) at essentially the same mass flow (see discussion in section 5.1). The analytical results have assumed that the mixing length constant in equation 20 is 0.08 and in equation 21 is 0.108. These values influence the mixing process through the eddy viscosity. The influence on wall pressures is relatively minor as will be discussed in section 5.5 where these values are varied over a reasonable range. The comparison between test and analytical values is generally excellent. Both the data and analytical results show changes in shape at points where the geometry changes. The two areas where some disagreement occurs is in the entrance region and in the last half of the diffuser.

The difference in the bellmouth section occurs because the analytical program calculates a centerline static pressure and assumes the static pressure constant at each x distance from the nozzle discharge whereas the experimental data are wall static pressures and can be influenced by curving streamlines. At $x = 0$ the bellmouth walls still have a significant curvature which causes flow streamline curvature in this region. The result is a reduced wall static pressure and an elevated centerline static pressure. Between 1 and 2 inches downstream of the nozzle discharge the wall curvature is reduced to very small values and the data and analytical results agree very closely.

The second area where minor differences occur is in the last half of the diffuser for the higher flow rate test runs. The reason for this difference could be an underestimation of the pressure losses due to wall friction, mixing, and diffusion. Substantiation of this can be seen by comparing the slope of the pressure data to the analytical results in the constant area throat section between 8 and 11 inches. For the low flow rate Runs 2, 6 and 7 where the slopes are essentially equal, the test and analytical diffuser wall pressures are almost identical. For the other runs the test data slope between 8 and 11 inches is always more negative than the analytical results. For frictionless uniform flow in a short constant area duct, the static pressures would be equal all along the duct. For frictionless non-uniform flow in a short constant area duct the static pressure can increase as mixing takes place. For non-uniform flow in a constant area duct with friction, the static pressure will tend to decrease along the duct and the slope will become less positive or more negative as flow rate (and therefore losses) increases. From these observations, it would appear that the flow dependent losses for the analytical solution may be underestimated in the constant area and diffusing sections. This may be the cause of the difference between the test and analytical wall static pressures in the diffuser section.

5.3 Centerline Velocity and Temperature Variations

Figures 15 and 16 present the variation of maximum velocity and maximum temperature as a function of distance from the nozzle discharge. The temperature comparison is generally good for all test runs. The velocity comparison is also good. However the experimental maximum velocities tend to be higher than the analytical values in the first 4 inches downstream of the nozzle discharge. In the throat section and diffuser, the experimental values tend to be lower than the analytical values. In general the comparisons are very good. Differences may occur due to the eddy viscosity and mixing length distributions assumed (see section 3.4) or due to measurement inaccuracies.

5.4 Velocity Profiles and Temperature Profiles

A total of 45 sets of traverse measurements were taken during the experimental test program. Table 3 shows the figure numbers that present the comparison of the test data and analytical results for each test run. These results are presented on Figures 17 through 26.

In general the comparison of profile shape and velocity magnitude is very good between the analytical and experimental profiles. The comparisons for Runs 6 through 10 (Figures 21-24) match very closely. The only differences that are noticeable are that the experimental velocity profiles within 5.0 inches of the nozzle discharge are off center by about 0.025" and slightly higher in maximum velocity than the correspoinding analytical velocities. The nonsymmetry has disappeared for all traverses at distances greater than 5 inches. The good match of velocity profiles for Runs 6 through 10 goes along with the good comparison of static pressures and the consistent trend in integrated traverse mass flow rate discussed previously.

The comparison of experimental and analytical velocity and temperatures is not as good for Runs 1 through 5 as it was for Runs 6 through 10. The comparisons are also not as consistent from run to run which also coincides with some of the static pressure and mass flow differences noted previously for these runs. The following observations apply only to Runs 1 through 5.

1. The experimental jet is off center by about 0.057" but the non-symmetry has disappeared for profiles at distances of greater than 5.0".

2. For x of 3.0" or less the peak experimental velocities are greater than the analytical values for Run 3 and Run 2 and are slightly less for Runs 1 and 5.

3. The spread width of the velocity profiles compares very well at distances from the nozzle of 7.0 inches or less. For distances between 7 inches and 16 inches, the experimental profiles tend to spread faster and have a flatter profile.

4. The experimental temperature profiles in Figure 25 are spread significantly more than the analytical values at x = 3.0" and x = 10.5", the only two profiles plotted.

5. The comparisons for Run 1 are better than for the other runs for the 1.25" throat mixing section.

Both sets of data (for the 1.25" and 1.875" throat height) were calculated using the same eddy viscosity assumptions for mixing (0.08 for eq. 20, 0.108 for eq. 21). The test Runs 6 through 10 have lower average throat Mach numbers (.39 to .52), slightly higher primary nozzle velocities, higher wall static pressures, and larger mixing section dimensions. The eddy viscosity assumptions may be more suitable for these operating conditions than for those of test Runs 1 through 5. In any event, the agreement between experimental and analytical results is better for the Runs 6 through 10.

5.5 Sensitivity of Computer Analysis

The sensitivity of the computer analysis to changes in eddy viscosity and flow rate were investigated to obtain a measure of the amount of performance change that can result from small changes in assumed values.

5.5.1 Eddy Viscosity

The results for the eddy viscosity changes are shown on Figures 27, 28, and 29. The eddy viscosity is directly proportional to the square of the mixing length according to equation 19. The changes in mixing length were confined to the mixing region prior to the point where the jet mixing reaches the developing wall boundary layer. In this region the mixing length is defined by equations 20 and 21 as a constant times a mixing zone dimension (see section 3.4)

Equation 20 is used to calculate the mixing length in the region close to the nozzle discharge where the primary jet still has a flat potential core (probably confined to the first 0.5" to 1.0" of mixing). Most of the calculations have been carried out using a constant of 0.08 in equation 20. For the results presented in this section the comparative runs were made with the constant equal to 0.094 which gives about a 38% increase in eddy viscosity in this small region.

Equation 21 is used to calculate the mixing length in the region where the primary jet is "fully rounded" but has not intersected with the wall boundary layer. This region extends for about 4" to 6" into the mixing section for the 1.25" throat configuration and extends for about 6" to 8" for the 1.875" throat configuration. Most of the calculations have been carried out using a constant of 0.108 in equation 21. For the results presented in this section, the comparative runs were made with a constant equal to 0.120 which gives about a 23% increase in eddy viscosity.

The velocity and temperature results shown on Figures 28 and 29 for Runs 3 and 6 show that the amount of mixing increases with eddy viscosity. This results in reduced centerline velocities, increased velocities near the walls and increased wall static pressures (see Figure 27). All of the changes are small.

The effect of mixing length changes in the rest of the mixing section as defined by equation 25 was not investigated but it is expected that the results would be similar. Section 3.4 points out that equation 25 was obtained by Nikuradse for fully developed flow in round tubes and should be considered to give only approximate results. Changes in this equation could provide a better match of static pressures for some of the high flow test runs as discussed in Section 5.2.

5.5.2 Flow Rate

Figure 27 shows the effect on wall static pressures of a 2.2% change in total mass flow for Runs 3 and 6. The wall pressure decrease as flow rate is increased is about double for Run 3 as compared to Run 6. The reason for this is that the average Mach number for Run 3 (1.25" throat) is larger than for Run 6 (1.875" throat) even though the Run 6 mass flow is larger. Figure 30 shows the influence of throat Mach number on throat static pressure level. The local slope of this line indicates the rate of change of throat pressure with Mach number. Run 6 happens to be the lowest Mach number test run and Run 3 has one of the largest Mach numbers. A comparison of the local slopes for Run 3 and Run 6 on Figure 30 gives results consistent with Figure 27.

Section 6

CONCLUSIONS

(1) The finite difference computer analysis developed to analyze two-dimensional co-axial slot ejectors with variable area mixing sections predicts the performance of the experimental configurations tested under this program very closely.

(2) The analytical and experimental results compared are at essentially the same flow rate within the accuracy of our measurements. The correct mixing section mass flow rates for each test are best represented by the orifice measured values and the computer analytical mass flow for best comparison of measured wall static pressures. These two values agree within $\pm$ 0.9%. The integrated traverse mass flows are less accurate and range between -2.9% and 6.4% of the other values.

(3) The experimental and analytical wall static pressure distributions agree within 1 or 2 inches of water over most of the mixing section for most of the test runs.

(4) The experimental and analytical velocity profiles compare very well in both velocity level and amount of jet spread due to mixing.

Appendix A

BASIC EQUATIONS OF MOTION

The momentum and energy equations as shown in equations 1 and 2 in the main text can be transformed to the $x\text{-}\psi^2$ coordinates according to Denny[3] by the following steps.

Momentum Equation:

The stream function transformation is defined by:

$$\frac{\partial \psi^2}{\partial y} = \bar{\rho}\,\bar{u} \qquad \frac{\partial \psi}{\partial y} = \frac{\bar{\rho}\,\bar{u}}{2\psi} \tag{A-1}$$

then:

$$\frac{\partial \bar{u}}{\partial y} = \frac{\partial \psi}{\partial y}\,\frac{\partial \bar{u}}{\partial \psi} = \frac{\bar{\rho}\,\bar{u}}{2\psi}\quad\frac{\partial\,\bar{u}}{\partial\,\psi} \tag{A-2}$$

The third term of the momentum equation becomes:

$$\bar{u}\,\frac{\partial \tau}{\partial \psi_s} = \frac{\bar{u}}{2\,\psi}\,\frac{\partial \tau}{\partial \psi} = \frac{\bar{u}}{2\,\psi}\quad\frac{\partial}{\partial \psi}\left[(\bar{\mu} + \bar{\rho}\,\epsilon)\,\frac{\partial\,\bar{u}}{\partial\,y}\right] \tag{A-3}$$

$$\frac{\bar{u}\,\partial \tau}{\partial\,\psi_s} = \frac{\bar{u}}{2\,\psi}\quad\frac{\partial}{\partial\,\psi}\left[(\bar{\mu} + \bar{\rho}\epsilon)\,\frac{\bar{\rho}\,\bar{u}}{2\,\psi}\quad\frac{\partial\,\bar{u}}{\partial\,\psi}\right] \tag{A-4}$$

The substitution of equation A-4 into equation 1 of the main text results in equation 9 of the main text.

Energy Equation

The third term of the energy equation (equation 2) is transformed as follows:

$$\bar{u}\,\frac{\partial\,q}{\partial\,\psi_s} = \frac{\bar{u}}{2\,\psi}\,\frac{\partial q}{\partial\,\psi} = \frac{\bar{u}}{2\,\psi}\quad\frac{\partial}{\partial\psi}\left[(\bar{k} + \frac{\bar{\rho}\,\bar{C}_p\epsilon}{P_{rt}})\,\frac{\partial\,\bar{T}}{\partial\,y}\right] \tag{A-5}$$

$$\frac{\partial\,\bar{T}}{\partial\,y} = \frac{\partial \psi}{\partial\,y}\,\frac{\partial\,\bar{T}}{\partial\,\psi} = \frac{\bar{\rho}\,\bar{u}}{2\,\psi}\quad\frac{\partial\,\bar{T}}{\partial\,\psi} \tag{A-6}$$

The substitution of equation A-6 into A-5 completes the transformation of the third term of the energy equation as shown in equation A-7.

$$\bar{u}\,\frac{\partial q}{\partial \psi_s} = \frac{\bar{u}}{2\psi}\,\frac{\partial}{\partial \psi}\left[\left(\bar{k} + \frac{\bar{\rho}\bar{C}_p \epsilon}{P_{rt}}\right)\frac{\bar{\rho}\bar{u}}{2\psi}\,\frac{\partial \bar{T}}{\partial \psi}\right] \tag{A-7}$$

The fourth term of the energy equation (equation 2 and 3) is transformed by substituting equation A-2 into equation 3 as follows:

$$\frac{\Phi}{\bar{\rho}} = \left(\frac{\bar{\mu} + \bar{\rho}\epsilon}{\bar{\rho}}\right)\left(\frac{\bar{\rho}\bar{u}}{2\psi}\,\frac{\partial \bar{u}}{\partial \psi}\right)^2 \tag{A-8}$$

The substitution of equations(A-7) and (A-8) into equation 2 of the main text results in equation 10 of the main text.

Dimensionless Momentum Equation

The equations 11 through 15 of the main text define the dimensionless groups used to non-dimensionalize both the momentum and energy equations.

The first term of the momentum equation (equation 9) is non-dimensionalized as follows:

$$\bar{u}\,\frac{\partial \bar{u}}{\partial x} = \left(\frac{u_o^3}{\nu_o}\right) u\,\frac{\partial u}{\partial X} \tag{A-9}$$

The second term of the momentum equation is non-dimensionalized as follows;

$$-\frac{1}{\bar{\rho}}\,\frac{d\bar{p}}{dx} = -\frac{1}{\rho_o}\left(\frac{\rho_o u_o^2}{2}\,\frac{u_o}{\nu_o}\right)\frac{1}{\rho^*}\,\frac{dP}{dX} \tag{A-10}$$

$$-\frac{1}{\bar{\rho}}\,\frac{d\bar{p}}{dx} = -\left(\frac{u_o^3}{\nu_o}\right)\frac{1}{2\rho^*}\,\frac{dP}{dX} \tag{A-11}$$

The third term of the momentum equation is non-dimensionalized as follows:

$$\frac{\bar{u}}{2\psi}\frac{\partial}{\partial\psi}\left[(\bar{\mu}+\bar{\rho}\epsilon)\frac{\bar{\rho}\,\bar{u}}{2\psi}\frac{\partial\bar{u}}{\partial\psi}\right]$$

$$=\frac{u_o u}{2\rho_o\nu_o\psi^*}\frac{\partial}{\partial\psi^*}\left[(\mu_o\mu^*+\rho_o\rho^* E\,\nu_o)\frac{\rho_o\rho^* u_o u\, u_o}{2\rho_o\nu_o\psi^*}\frac{\partial u}{\partial\psi^*}\right]$$

$$=\left(\frac{u_o^3}{\nu_o}\right)\frac{u}{2\psi^*}\frac{\partial}{\partial\psi^*}\left[(\mu^*+\rho^* E)\frac{\rho^* u}{2\psi^*}\frac{\partial u}{\partial\psi^*}\right] \qquad \text{(A-12)}$$

The non-dimensionalized form of the momentum equation (equation 16) is obtained by substituting equations A-9, A-11, and A-12 into equation 9 of the main text and eliminating the factor (u_o^3/ν_o) from each term.

Dimensionless Energy Equation

The first term of the energy equation (equation 10) is non-dimensionalized as follows:

$$\bar{u}\frac{\partial(\bar{C}_p\bar{T})}{\partial x}=\frac{u_o^2\,u\,C_{po}(T_{wr}-T_o)}{\nu_o}\frac{\partial(C_p^*\theta)}{\partial X}$$

$$=\left[\frac{u_o^2 C_{po}(T_{wr}-T_o)}{\nu_o}\right]u\frac{\partial(C_p^*\theta)}{\partial X} \qquad \text{(A-13)}$$

The second term of the energy equation is non-dimensionalized as follows:

$$\frac{\bar{u}}{\bar{\rho}}\frac{d\bar{p}}{dx}=\frac{u_o u}{\rho_o\rho^*}\frac{\rho_o u_o^2 u_o}{2\nu_o}\frac{dP}{dX}$$

$$=\left(\frac{u_o^4}{\nu_o}\right)\frac{u}{2\rho^*}\frac{dP}{dX} \qquad \text{(A-14)}$$

The third term of the energy equation is non-dimensionalized as follows:

$$\frac{\bar{u}}{2\psi}\frac{\partial}{\partial\psi}\left[(\bar{k}+\frac{\bar{\rho}\,\bar{C}_p\,\epsilon}{P_{rt}})\frac{\bar{\rho}\,\bar{u}}{2\,\psi}\frac{\partial\bar{T}}{\partial\,\psi}\right]$$

$$= \frac{u_o u}{2\,\rho_o\nu_o\psi^*}\frac{\partial}{\partial\,\psi^*}\left[(k_o k^* + \frac{\rho_o\rho^* C_{po}C_p^* E\nu_o}{P_{rt}})\frac{\rho_o\rho^* u_o u}{2\rho_o\nu_o\psi^*}\right.$$

$$\left.(T_{wr}-T_o)\frac{\partial\,\theta}{\partial\,\psi^*}\right]$$

$$= (\frac{u_o^2 C_{po}(T_{wr}-T_o)}{\nu_o})\frac{u}{2\,\psi^*}\frac{\partial}{\partial\,\psi^*}\left[(\frac{k^*}{P_{ro}}+\frac{\rho^* C_p^* E}{P_{rt}})\frac{\rho^* u}{2\psi^*}\frac{\partial\,\theta}{\partial\,\psi^*}\right] \tag{A-15}$$

The fourth term of the energy equation is non-dimensionalized as follows:

$$(\frac{\bar{\mu}+\bar{\rho}\epsilon}{\bar{\rho}})(\frac{\bar{\rho}\,\bar{u}}{2\,\psi}\frac{\partial\,\bar{u}}{\partial\,\psi})^2$$

$$= (\frac{\mu_o\mu^* + \rho_o\rho^* E\,\nu_o}{\rho_o\rho^*})(\frac{\rho_o\rho^*\,u_o u\,u_o}{2\,\rho_o\nu_o\psi^*}\frac{\partial\,u}{\partial\,\psi^*})^2$$

$$= (\frac{u_o^4}{\nu_o})(\frac{\mu^* + E\,\rho^*}{\rho^*})(\frac{\rho^* u}{2\,\psi^*}\frac{\partial\,u}{\partial\,\psi^*})^2 \tag{A-16}$$

Each of the four terms of the energy equation is then divided by the quantity:

$$\frac{u_o^2\,C_{po}(T_{wr}-T_o)}{\nu_o} \tag{A-17}$$

which results in the following combination of quantities in the second and fourth terms of the energy equation:

$$\frac{u_o^2}{C_{po}(T_{wr}-T_o)} \quad \text{which equals } C_L.$$

The substitution of equations A-13, A-14, A-15, and A-16 into equation 10, the division by the quantity in (A-17) and the substitution of C_L into the second and fourth terms results in equation 17 of the main text.

Appendix B

FINITE DIFFERENCE EQUATIONS

This Appendix provides the detailed derivations of the finite difference equivalents of the momentum and energy conservation equations, (16) and (17) respectively. For convenience the following definitions are introduced:

$$Q = \left[\frac{k^*}{P_{ro}} + \frac{E\rho^* C_p^*}{P_{rt}}\right] \frac{\rho^* u}{2\,\psi^*}$$

and

$$S = \left[\frac{\mu^* + E\rho^*}{2\psi^*}\right] \rho^* u$$

These definitions and the assumption that $C_p^* = 1.0$ permit the momentum and energy equations to be expressed as

$$u\,\frac{\partial\, u}{\partial\, X} = -\,\frac{1}{2\rho^*}\,\frac{dP}{dX} + \frac{u}{2\psi^*}\,\frac{\partial}{\partial\,\psi^*}\left[S\,\frac{\partial\, u}{\partial\,\psi^*}\right] \tag{B-1}$$

$$u\,\frac{\partial\,\theta}{\partial\, X} = \frac{C_L}{2\rho^*}\,u\,\frac{dP}{dX} + \frac{C_L uS}{2\psi^*}\left[\frac{\partial\, u}{\partial\,\psi^*}\right]^2 + \frac{u}{2\psi^*}\,\frac{\partial}{\partial\,\psi^*}\left[Q\,\frac{\partial\,\theta}{\partial\,\psi^*}\right] \tag{B-2}$$

Before approximating these equations with finite difference relations a system of grid lines parallel to the X and ψ^* axes must be introduced. As illustrated in figure B-1, a nodal point coincides with each intersection of these lines. Lines parallel to the ψ^* axis are termed m-lines and those parallel to X axis n-lines. Each node is given a double subscript, the first being the number of the m-line passing through it, and the second the n-line number.

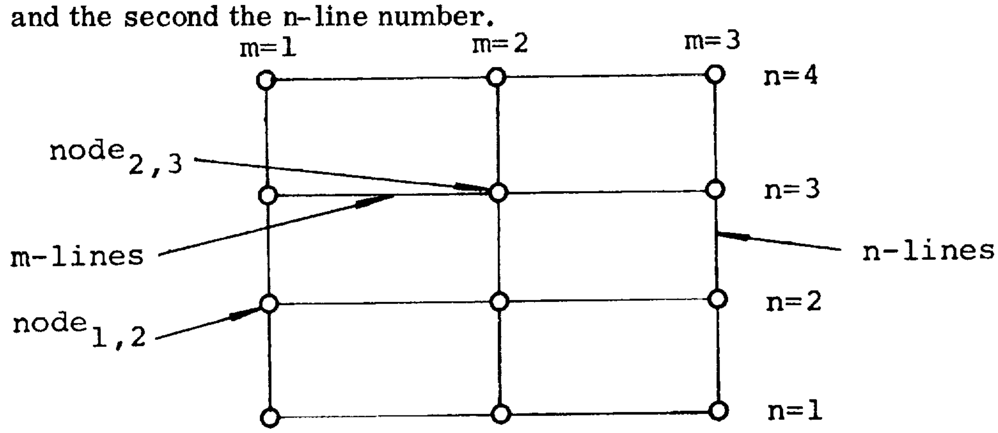

Figure B-1 Definition of Grid Lines for Finite Difference Solution

The values of the variables on the m=1 line are the known initial conditions. The conservation equations express for each node on the m=2 line its inter-relation with other nodes on the m=2 line and nodes on the m=1 line. If m=2 line nodes are only related to nodes which lie on the m=1 line, the finite difference scheme is termed explicit. If an m=2 node is also related to a number of other m=2 nodes, the scheme is termed implicit (See figure B-2).

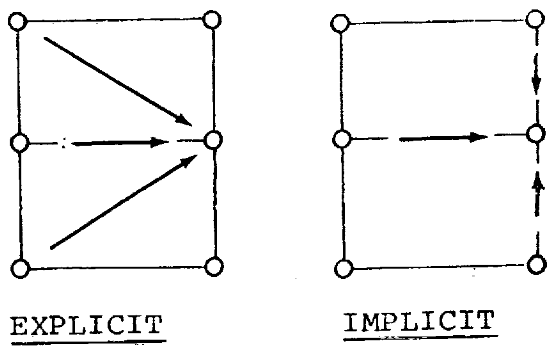

Figure B-2
Diagrams of Explicit and Implicit Solutions

The implicit form of finite difference schemes leads to a series of N simultaneous algebraic equations relating the known initial conditions on the m=1 line and the unknown variables on each of the N nodes on the m=2 line. After solution of these simultaneous equations, the variables on the m=3 line are expressed in terms of the known values on the m=2 line. Proceeding in this manner, a solution to the complete flow field is marched out. Although simpler to program, the explicit scheme shows unstable characteristics if the m-lines are widely spaced relative to the n-line spacing. Implicit schemes show much more stable characteristics and therefore allow much larger m-line spacings, thus reducing computation times. The computer procedure presented in this report employs a system of implicit finite difference approximations which are defined using the notation described in figure B-3.

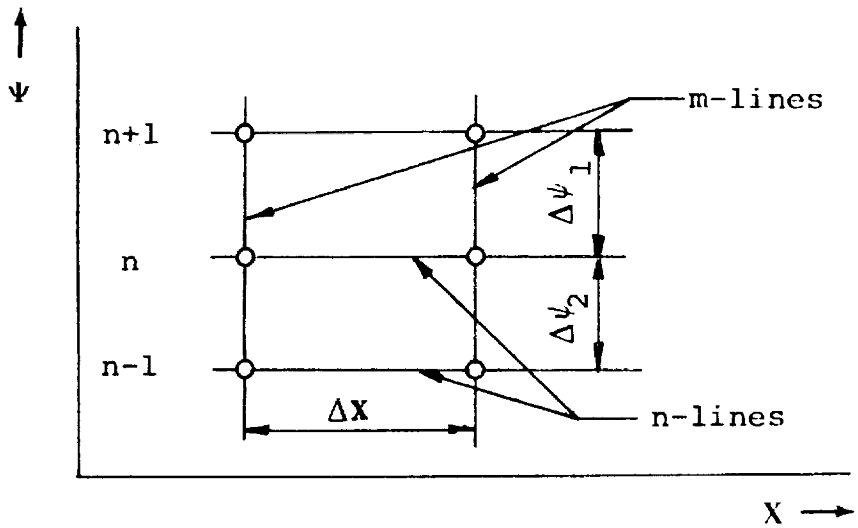

Figure B-3

Implicit Finite Difference Term Definition

The velocity at nodes n+1 and n-1 can be expressed in terms of a Taylor series expanded about node n, on the same m-line,

$$u_{n+1} = u_n + \Delta\psi_1 \left.\frac{\partial u}{\partial \psi^*}\right|_n + \frac{(\Delta\psi_1)^2}{2} \left.\frac{\partial^2 u}{\partial \psi^{*2}}\right|_n + \text{higher order terms} \qquad \text{(B-3)}$$

$$u_{n-1} = u_n - \Delta\psi_2 \left.\frac{\partial u}{\partial \psi^*}\right|_n + \frac{(\Delta\psi_2)^2}{2} \left.\frac{\partial^2 u}{\partial \psi^{*2}}\right|_n + \text{higher order terms} \qquad \text{(B-4)}$$

Combining these equations to eliminate $\left.\frac{\partial^2 u}{\partial \psi^{*2}}\right|_n$ yields,

$$\frac{(\Delta\psi_2)^2}{2} u_{n+1} - \frac{(\Delta\psi_1)^2}{2} u_{n-1} = \frac{u_n}{2}(\Delta\psi_2^2 - \Delta\psi_1^2) + \left.\frac{\partial u}{\partial \psi^*}\right|_n \frac{1}{2}(\Delta\psi_1 \Delta\psi_2^2 + \Delta\psi_2 \Delta\psi_1^2)$$

$$+ \text{higher order terms}$$

Neglecting terms of the order $(\Delta\psi)^3$ and higher, yields

$$\left.\frac{\partial u}{\partial \psi^*}\right|_n = \frac{\left(\frac{\Delta\psi_2}{\Delta\psi_1}\right) u_{n+1} - \left(\frac{\Delta\psi_1}{\Delta\psi_2}\right) u_{n-1} - \left(\frac{\Delta\psi_2}{\Delta\psi_1} - \frac{\Delta\psi_1}{\Delta\psi_2}\right) u_n}{\Delta\psi_2 + \Delta\psi_1}$$

Defining $R_1 = \frac{\Delta\psi_1}{\Delta\psi_2(\Delta\psi_2 + \Delta\psi_1)}$

and

$$R_2 = \frac{\Delta\psi_2}{\Delta\psi_1(\Delta\psi_2 + \Delta\psi_1)}$$

yields,

$$\left.\frac{\partial u}{\partial \psi^*}\right|_n = R_2\ (u_{n+1} - u_n) + R_1\ (u_n - u_{n-1}) \qquad \text{(B-5)}$$

Similarly

$$\left.\frac{\partial \theta}{\partial \psi^*}\right|_n = R_2\ (\theta_{n+1} - \theta_n) + R_1\ (\theta_n - \theta_{n-1}) \qquad \text{(B-6)}$$

The second derivative term in the momentum equation is approximated using the following Taylor series expansions,

$$\left(S\frac{\partial u}{\partial \psi^*}\right)_{n+\frac{1}{2}} = \left(S\frac{\partial u}{\partial \psi^*}\right)_n + \frac{\Delta\psi_1}{2}\frac{\partial}{\partial \psi^*}\left[\left(S\frac{\partial u}{\partial \psi^*}\right)_n\right] + \frac{\Delta\psi^2_1}{4}\frac{\partial^2}{\partial \psi^{*2}}\left[\left(S\frac{\partial u}{\partial \psi^*}\right)_n\right]$$

$$+ \text{ higher order terms} \tag{B-7}$$

$$\left(S\frac{\partial u}{\partial \psi^*}\right)_{n-\frac{1}{2}} = \left(S\frac{\partial u}{\partial \psi^*}\right)_n - \frac{\Delta\psi_2}{2}\frac{\partial}{\partial \psi^*}\left[\left(S\frac{\partial u}{\partial \psi^*}\right)_n\right]$$

$$+ \frac{\Delta\psi^2_1}{4}\frac{\partial^2}{\partial \psi^{*2}}\left[\left(S\frac{\partial u}{\partial \psi^*}\right)_n\right] + \text{ higher order terms} \tag{B-8}$$

Neglecting terms of the order of $\frac{\Delta\psi^2}{4}$ and higher yields,

$$\frac{\partial}{\partial \psi^*}\left(S\frac{\partial u}{\partial \psi^*}\right)_n = \left\{\left(S\frac{\partial u}{\partial \psi^*}\right)_{n+\frac{1}{2}} - \left(S\frac{\partial u}{\partial \psi^*}\right)_{n-\frac{1}{2}}\right\}\left\{\frac{2}{\Delta\psi_1 + \Delta\psi_2}\right\}$$

$$= \frac{1}{\Delta\psi_1 + \Delta\psi_2}\left[\frac{(S_{n+1} + S_n)(u_{n+1} - u_n)}{\Delta\psi_1} - \frac{(S_n + S_{n-1})(u_n - u_{n-1})}{\Delta\psi_2}\right] \tag{B-9}$$

Similarly,

$$\frac{\partial}{\partial\psi^*}\left[Q\frac{\partial\theta}{\partial\psi^*}\right]_n = \frac{1}{\Delta\psi_1+\Delta\psi_2}\left[\frac{(Q_{n+1}+Q_n)(\theta_{n+1}-\theta_n)}{\Delta\psi_1} - \frac{(Q_n+Q_{n-1})(\theta_n-\theta_{n-1})}{\Delta\psi_2}\right] \tag{B-10}$$

The velocity at a node located at the intersection of the downstream m-line and any n-line $u_{2,n}$ can be expressed in terms of the following Taylor series,

$$u_{2,n} = u_{1,n} + \left.\frac{\partial u}{\partial X}\right|_n \Delta X + \left.\frac{\partial^2 u}{\partial X^2}\right|_n (\Delta X)^2 + \text{higher order terms} \tag{B-11}$$

Use of the boundary layer equations implies that gradients in the X-direction are much smaller than those in the ψ^*-direction. Therefore it is permissible to use a simplier approximation of the X-direction derivatives.

Neglecting terms of $(\Delta X)^2$ and higher yields,

$$\left.\frac{\partial u}{\partial X}\right|_n = \frac{u_{2,n} - u_{1,n}}{\Delta X} \tag{B-12}$$

This approximation is termed "backward-difference".

Similarly,

$$\left.\frac{\partial\theta}{\partial X}\right|_n = \frac{\theta_{2,n} - \theta_{1,n}}{\Delta X} \tag{B-13}$$

The only terms in the energy and momentum equations which cannot be approximated using the preceeding equations are those containing the pressure gradient $\frac{dP}{dX}$. Assuming this gradient varies linearly throughout the ΔX interval yields,

$$\frac{dP}{dX} = \frac{1}{2}\left(\left.\frac{dP}{dX}\right|_{m=1} + \left.\frac{dP}{dX}\right|_{m=2}\right) \tag{B-14}$$

Momentum Equation

Combining equations (B-1), (B-9), (B-12) and (B-14) yields

$$u_{1,n}\frac{(u_{2,n} - u_{1,n})}{\Delta X} = -\frac{1}{4\rho^*_{1,n}}\left[\frac{dP}{dX}_{m=1} + \frac{dP}{dX}_{m=2}\right] + \frac{u_{1,n}}{2\psi^*_n}\left(\frac{1}{\Delta\psi_1 + \Delta\psi_2}\right)$$

$$\left[\frac{(S_{n+1} + S_n)(u_{2,n+1} - u_{2,n})}{\Delta\psi_1} - \frac{(S_n + S_{n-1})(u_{2,n} - u_{2,n-1})}{\Delta\psi_2}\right] \tag{B-15}$$

This equation can be expressed in the form

$$A_{n-1}\, u_{2,n} + B_{n-1}\, u_{2,n+1} + C_{n-1}\, u_{2,n-1} = D_{n-1} \tag{B-16}$$

in which the coefficients are defined by equations 27 through 34 of the main text.

Energy Equation

Combining equations (B-2), (B-5), (B-10), (B-13) and (B-14) yields

$$\frac{u_{1,n}(\theta_{2,n} - \theta_{1,n})}{\Delta X} = \frac{C_L\, u_{1,n} S_{1,n}}{2\psi^*}\left[R_2\,(u_{2,n+1} - u_{2,n}) + R_1\,(u_{2,n} - u_{2,n-1})\right]^2$$

$$+ \frac{u_{1,n}}{2\psi^*_n}\left[\frac{1}{\Delta\psi_1 + \Delta\psi_2}\right]\left[\frac{(Q_{n+1} + Q_n)(\theta_{2,n+1} - \theta_{2,n})}{\Delta\psi_1}\right.$$

$$\left. - \frac{(Q_n + Q_{n-1})(\theta_{2,n} - \theta_{2,n-1})}{\Delta\psi_2}\right] + \left(\frac{C_L u_{1,n}}{4\rho^*_{1,n}}\right)\left[\frac{dP}{dX}_{m=1} + \frac{dP}{dX}_{m=2}\right]$$

(B-17)

This equation can be expressed in the form

$$A_{n-1} \cdot \theta_{2,n} + B_{n-1} \cdot \theta_{2,n+1} + C_{n-1} \cdot \theta_{2,n-1} = D_{n-1} \tag{B-18}$$

in which the coefficients are defined by equations 37 through 45 of the main text.

Appendix C

Solution Procedure

The calculation procedure starts at the upstream flow boundary, where the values of all flow variables must be known or assumed. Specification of the velocity and temperature distribution, dimensionless eddy viscosity, duct and nozzle inlet dimensions, and working fluid, defines all initial conditions.

The known initial conditions, m=1 line, are related to the unknown conditions, m=2 line, by the previously derived equations, and assumed boundary conditions. These inter-relations form a set of N-2 simultaneous algebraic equations, where N is the number of n-lines, and the equations are shown in Appendix B. The resultant matrix of coefficients is tridiagonal in form except for the initial and final rows which only contain two terms. Rapid, exact solutions to this type of matrix are obtained using the Thomas Algorithm, a successive elimination technique, which is described in this Appendix.

The solution for the variables on the m=2 line is iterative, because of the presence of the unknown pressure in the momentum equation. The procedure adopted was to estimate the pressure gradient, and solve the equations, using the algorithm. The equations automatically satisfy conservation of mass, momentum, and energy, but only one pressure gradient yields the correct wall geometry. The duct dimension corresponding to the estimated pressure gradient was calculated from the m=2 line variables. The pressure gradient was then incremented by a small percentage of its initial estimated value, and the calculation process repeated for a new duct dimension. A third estimate of the pressure gradient was obtained by interpolation between the two calculated, and the actual duct dimension. In almost all the calculations performed to date, this value has been acceptably close, within 0.001%, to the actual duct dimension. If this criterion is not met, a further iteration is applied, and a fourth solution obtained.

The now known variables on the m=2 line become the new m=1 line variables and the procedure is repeated for another set of m=2 line variables. Thus a solution to the complete flow field is marched out.

The difference form of the momentum and energy equation is:

$$A_{n-1} X_n + B_{n-1} X_{n+1} + C_{n-1} X_{n-1} = D_{n-1} \tag{C-1}$$

where X is either u or θ. If the number of n-lines is N, there are N-2 equations of the form (1) and two equations expressing the boundary conditions. The first and the last equations represent the boundary conditions, which in difference form along the axis of symmetry are:

$$\frac{\partial u}{\partial \psi^*} = 0 \text{ or } u_{2,2} = u_{2,1} \tag{C-2}$$

and

$$\frac{\partial \theta}{\partial \psi^*} = 0 \text{ or } \theta_{2,2} = \theta_{2,1} \tag{C-3}$$

Equations (C-2) and (C-3) can be written in terms of X as follows:

$$X_1 = X_2 \tag{C-4}$$

At the duct wall the boundary conditions are

$$u_N = 0 \tag{C-5}$$

$$\theta_{2,N} = \theta_{2,N-1} \tag{C-6}$$

Equations (C-5) and (C-6) can be written in terms of X as follows:

$$X_N = K\,X_{N-1} \tag{C-7}$$

where K is 0 for the momentum equation and unity for the energy equation. Thus, the matrix form of the equation (C-1) is shown on the following page (Table C-1).

The second equation is

$$C_1X_1 + A_1X_2 + B_1X_3 = D_1 \tag{C-9}$$

Substituting equation (C-4) into this equation yields:

$$A'_1X_2 + B_1X_3 = D_1 \tag{C-10}$$

where $A'_1 = C_1 + A_1$

The N^{th} -1 equation is

$$C_{n-2}\,X_{N-2} + A_{N-2}\,X_{N-1} + B_{N-2}\,X_N = D_{N-2} \tag{C-11}$$

Substituting equation (C-7) into this equation yields:

$$C_{N-2}\,X_{N-2} + A'_{N-2}\,X_{N-1} = D_{N-2} \tag{C-12}$$

where $A'_{N-2} = A_{N-2} + K\cdot B_{N-2}$

Thus the N equations (C-8) can be reduced to the N-2 equations shown on Table C-2.

Table C-1

Matrix Form of Equation C-1 Designated As Equation C-8

$$
\begin{bmatrix}
1 & -1 & 0 & 0 & 0 & - & 0 & 0 & 0 & - & 0 & 0 & 0 \\
C_1 & A_1 & B_1 & 0 & 0 & - & 0 & 0 & 0 & - & 0 & 0 & 0 \\
0 & C_2 & A_2 & B_2 & 0 & - & 0 & 0 & 0 & - & 0 & 0 & 0 \\
0 & 0 & C_3 & A_3 & B_3 & - & 0 & 0 & 0 & - & 0 & 0 & 0 \\
- & - & - & - & - & - & - & - & - & - & - & - & - \\
0 & 0 & 0 & 0 & 0 & - & C_{n-1} & A_{n-1} & B_{n-1} & - & 0 & 0 & 0 \\
- & - & - & - & - & - & - & - & - & - & - & - & - \\
0 & 0 & 0 & 0 & 0 & - & 0 & 0 & 0 & - & C_{N-2} & A_{N-2} & B_{N-2} \\
0 & 0 & 0 & 0 & 0 & - & 0 & 0 & 0 & - & 0 & -K & 1
\end{bmatrix}
\begin{bmatrix}
X_1 \\ X_2 \\ X_3 \\ X_4 \\ X_{n-1} \\ X_n \\ X_{n+1} \\ X_{N-1} \\ X_N
\end{bmatrix}
=
\begin{bmatrix}
0 \\ D_1 \\ D_2 \\ D_3 \\ D_{n-2} \\ D_{n-1} \\ D_n \\ D_{N-2} \\ 0
\end{bmatrix}
$$

Table C-2

Matrix Form of Equation C-8 with Simplified Terms Designated as Equation C-13

$$
\begin{bmatrix}
A'_1 & B_1 & 0 & 0 & - & 0 & 0 & 0 & - & 0 & 0 & 0 \\
C_2 & A_2 & B_2 & 0 & - & 0 & 0 & 0 & - & 0 & 0 & 0 \\
0 & C_3 & A_3 & B_3 & - & 0 & 0 & 0 & - & 0 & 0 & 0 \\
- & - & - & - & - & - & - & - & - & - & - & - \\
0 & 0 & 0 & 0 & - & C_{n-1} & A_{n-1} & B_{n-1} & - & 0 & 0 & 0 \\
- & - & - & - & - & - & - & - & - & - & - & - \\
0 & 0 & 0 & 0 & - & 0 & 0 & 0 & - & C_{N-3} & A_{N-3} & B_{N-3} \\
0 & 0 & 0 & 0 & - & 0 & 0 & 0 & - & 0 & C_{N-2} & A'_{N-2}
\end{bmatrix}
\begin{bmatrix}
X_2 \\ X_3 \\ X_4 \\ X_{n-1} \\ X_n \\ X_{n+1} \\ X_{N-2} \\ X_{N-1}
\end{bmatrix}
=
\begin{bmatrix}
D_1 \\ D_2 \\ D_3 \\ D_{n-2} \\ D_{n-1} \\ D_n \\ D_{N-3} \\ D_{N-2}
\end{bmatrix}
$$

The Thomas Algorithm

Starting with the first equation, X_2 can be expressed in terms of X_3. The second equation gives X_3 in terms of X_4. Continuing through all the equations until the N^{th} -3 equation gives X_{N-2} in terms of X_{N-1}. Combining this with the last equation gives X_{N-1}. Working backwards through the equations then allows the remaining unknowns to be found. This procedure is most easily applied by defining the following:

$$W_1 = A'_1$$

$$g_1 = \frac{D_1}{W_1}$$

$$Q_{n-1} = \frac{B_{n-1}}{W_{n-1}} \qquad n = 2,3---(N-2) \qquad \text{(C-14)}$$

$$W_n = A_n - C_n Q_{n-1} \qquad n = 2,3---(N-2)$$

$$g_n = D_n - \frac{C_n g_{n-1}}{W_n} \qquad n = 2,3---(N-2)$$

Equations (C-13) then reduce to:

$$X_{N-1} = g_{N-2} \text{ and } X_n = g_{n-1} - Q_{n-1} X_{n+1} \quad n=(N-2),\ (N-3),---2 \qquad \text{(C-15)}$$

If the values of W, Q and g are calculated in order of increasing n using equations (C-14), then equations (C-15) can be used to calculate the values of X in order of decreasing X starting with X_{N-1}. To clarify this procedure, the method is now used to solve the following four simultaneous equations:

$$
\begin{bmatrix} A'_1 & B_1 & 0 & 0 \\ C_2 & A_2 & B_2 & 0 \\ 0 & C_3 & A_3 & B_3 \\ 0 & 0 & C_4 & A'_4 \end{bmatrix} \cdot \begin{bmatrix} X_2 \\ X_3 \\ X_4 \\ X_5 \end{bmatrix} = \begin{bmatrix} D_1 \\ D_2 \\ D_3 \\ D_4 \end{bmatrix}
$$

$$A'_1 \; X_2 + B_1 \; X_3 = D_1$$

$$W_1 = A'_1$$

$$Q_1 = \frac{B_1}{W_1}$$

$$g_1 = \frac{D_1}{W_1}$$

hence $X_2 = g_1 - Q_1 \; X_3$

$$A_2 \; X_3 + B_2 \; X_4 + C_2 \; X_2 = D_2$$

$$W_2 = A_2 - C_2 \; Q_1$$

$$Q_2 = \frac{B_2}{W_2}$$

$$g_2 = \frac{D_2 - C_2 \; g_1}{W_1}$$

hence $X_3 = g_2 - X_4 \; Q_2$ (C-16)

$$A_3 \quad X_4 \quad + \quad B_3 \quad X_5 \quad + \quad C_3 \quad X_3 \quad = \quad D_3$$

$$W_2 \quad = \quad A_3 \quad - \quad C_3 \quad Q_2$$

$$Q_3 \quad = \quad \frac{B_3}{W_3}$$

$$g_3 \quad = \quad \frac{D_3 \quad - \quad C_3 \quad g_2}{W_3}$$

hence $X_4 \quad = \quad g_3 \quad - \quad Q_3 \quad X_5$ (C-17)

$$A'_4 \quad X_5 \quad + \quad C_4 \quad X_4 \quad = \quad D_4$$

$$W_4 \quad = \quad A_4 \quad - \quad C_4 \quad Q_3$$

$$g_4 \quad = \quad \frac{D_4 \quad - \quad C_4 \quad g_3}{W_4}$$

hence $X_5 \quad = \quad g_4$ (C-18)

Substituting in equation (C-16) yields X_3. Equations (C-17) and (C-18) are special forms of equations (C-15) for N=6 and n=4.

Appendix D

COMPUTER PROGRAM

The computational procedure consists of a main program, which is divided into ten sections, and six subroutines. The program Flow Chart is shown on Figure D-1. The functions of each section of the main program are as follows:

Section (1): Input and Initialization

(a) Constants which have single, initial value for most applications are defined with data statements.

(b) The parameters which specify the test conditions are inputed from data cards.

(c) Dimensional parts of the data are non-dimensionalized.

Section (2): Initial Profiles Generated

(a) The initial u, θ, μ^*, ρ^*, E, Y, and ψ^* distributions are calculated.

(b) The shear layer and wall boundary layer thickness are calculated using a search technique applied to the m = 1 line velocity profile.

Section (3): Turbulence Model

(a) The dimensionless eddy viscosity, which will subsequently be used in calculating the variables on the m = 2 line, is calculated from m = 1 velocity profile and one of the turbulence models detailed in the main text.

Section (4): Choice of X-Step

(a) The distance between the m = 1 and m = 2 lines is chosen. Initially, this distance is related to the shear layer width but after this layer impinges on the wall boundary layer, it becomes a constant fraction of the duct radius or width.

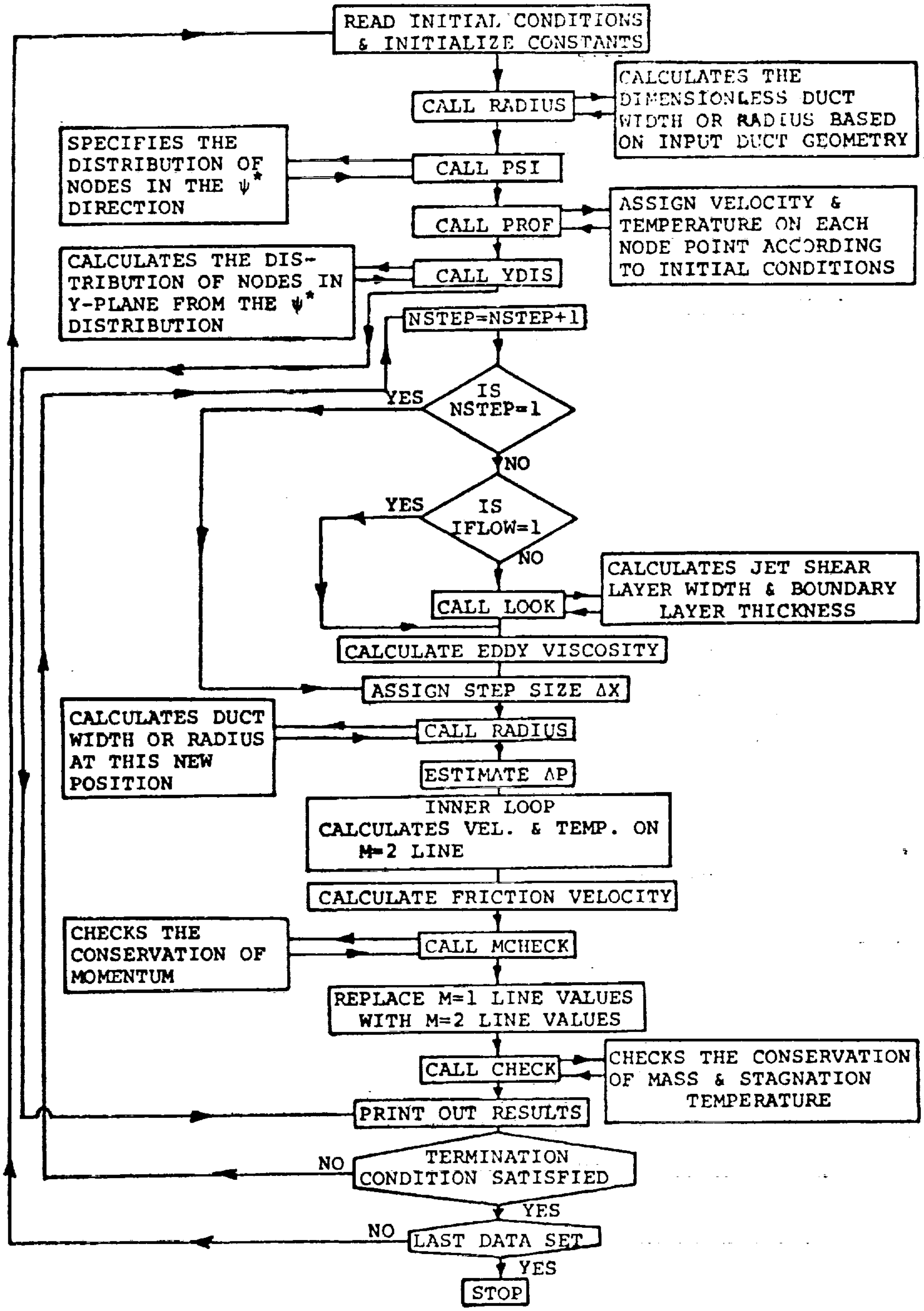

Figure D-1

Computer Program Flow Chart

FLOW CHART - INNER LOOP

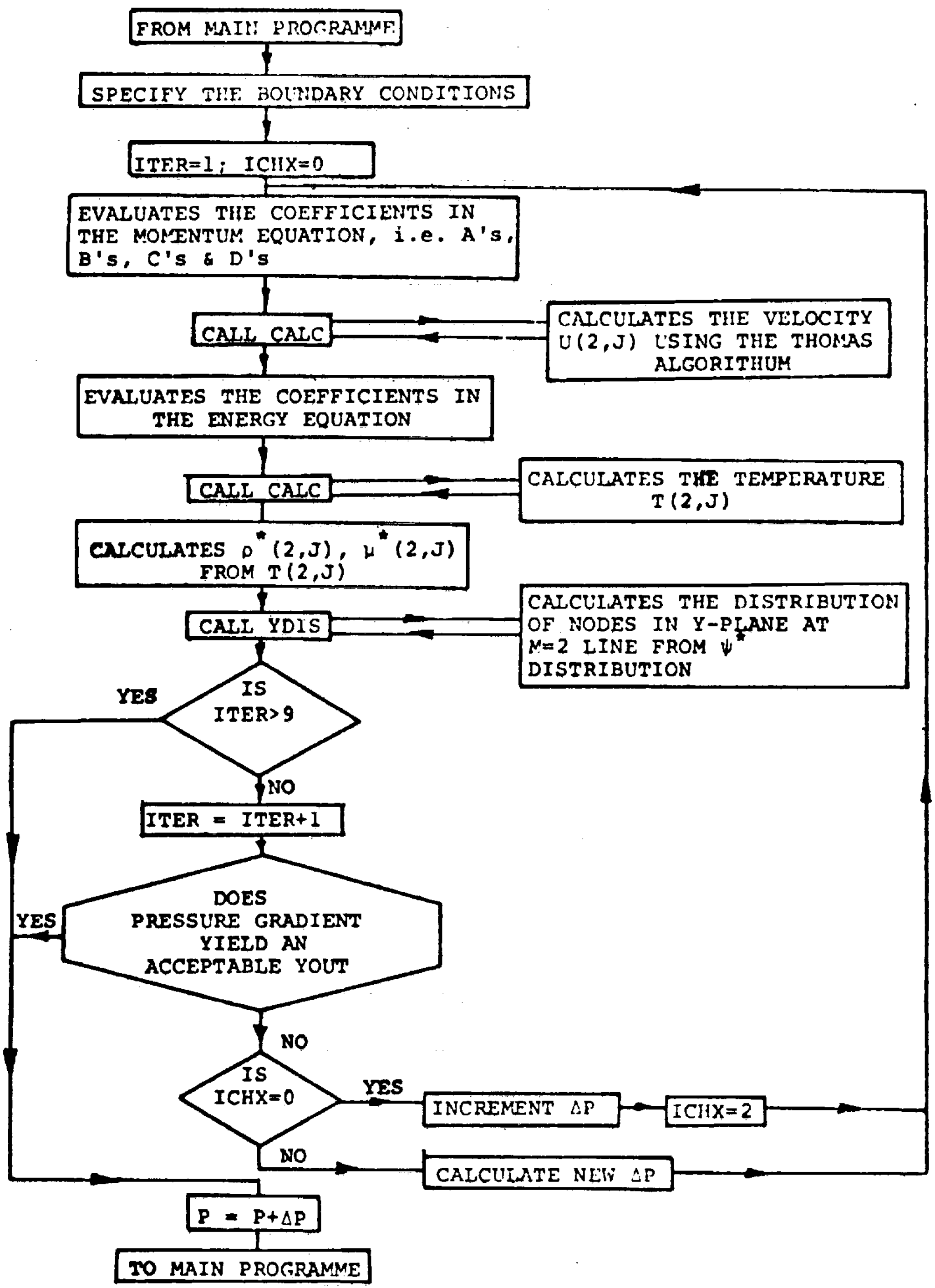

Figure D-1 (continued)

Section (5): Calculation of Velocity on m = 2 Line

(a) The duct radius or width at the m = 2 line, is interpolated from the input data.

(b) Initially, the m = 2 line pressure gradient is set equal to the average of the pressure gradients at the previous two m lines.

(c) The distribution of velocity on the m = 2 line is calculated.

Section (6): Calculation of Temperature on m = 2 Line

(a) The distribution of temperature on the m = 2 line, is calculated, and from it the distributions of density and molecular viscosity.

Section (7): Pressure Gradient Modification

(a) The position of the nth node, in the y-plane, is calculated from the m = 2 line profiles. If this value is acceptably close to the duct wall, the pressure is incremented by dp.

(b) Alternatively if this requirement is not satisfied, then an improved estimate of the pressure gradient is made.

(c) Using this estimate, section 5(c) and section (6) are repeated.

Section (8): Transference

(a) The values of u and θ calculated on the m = 2 line are transferred to the storage space previously used for conditions on the m = 1 line, in preparation for the advance to the next m-line.

Section (9): Output

(a) The velocity and temperature profiles are printed out at defined intervals, and several flow variables are printed at every step.

Section (10): Termination Test

(a) If the maximum x-value has not been reached, execution is returned to Section (3), in order to advance to the next m-line. The functions of each sub-routine are as follows:

CALC: This evaluates u and θ using the Thomas algorithm.

RADIUS: The duct shape is inputed to the calculation procedure, through this routine. It interpolates this data and calculates the local duct radius at every m-line.

TEMP: If the dimensionless temperature variation is a known boundary condition , it is specified in the routine. This routine is redundant with the present boundary conditions.

YDIS: The position of the grid nodes in the y-plane is calculated with this routine.

PSI: The position of the grid nodes in the ψ-plane is assigned in this routine. The initial flow conditions determine the form of this routine, i.e. single stream flow, two-stream and mass ratio.

LOOK: The shear layer and boundary layer width are calculated using a search technique applied to the m = 1 line velocity profile.

CHECK: This routine checks the conservation of mass and energy.

MCHECK: This routine checks the conservation of momentum between adjacent m-lines.

PROF: Calculates the initial velocity and temperature profiles.

FORTRAN SYMBOLS	MEANING
A(I)	A_{n-1}
B(I)	B_{n-1}
BB	Minimum value of step size ΔX
BE	Dimensionless jet shear layer inner edge
BH	Dimensionless jet shear layer width, BY-BE
BY	Dimensionless jet shear layer outer edge
CC	κ
C(I)	C_{n-1}
D(I)	D_{n-1}
DELTA	Δ
DP1	$\frac{dP}{dX}$ at m = 1 line
DP2	$\frac{dP}{dX}$ at m = 2 line
DP11	$\frac{dP}{dX}$ at m = 0 line
DX	ΔX
E(I)	E
ENERG	$\sum_{i=1}^{N} \theta u \rho^* \Delta Y$
FDUCT	Mass flow in duct
FPRIM	Mass flow in nozzle
GAMA	γ
IFLOW	Control variable (zero upstream of point where wall boundary layer and shear layer meet, otherwise one)
ITER	Iteration counter for inner loop
JFLOW	Control variable with the value one for single-stream flow and two for two-stream flow

FORTRAN SYMBOLS	MEANING
LVH	Dimensional local velocity head, $\bar{\rho}\bar{u}^2/2g_o$
LZ	L_m
N	Total number of node points on each m-line
NL, NP, NPP, SQP	Control variables for axisymmetric flow NL=1, NP= 2, NPP= 0 and SQP= 0.5; and for plane flow NL= 0, NP = 0, NPP=1 and SQP = 1
NJ	Number of node points in jet
NSTEP	Number of downstream steps
NTEST	Test number
PAMB	Ambient pressure
PCUM	Local dimensionless pressure
PE	Pressure at nozzle exit plane
PH2O	Local dimensional pressure
PS(I)	ψ^*_n
PR	P_r
PRT	P_{rt}
PSN	Total ψ^* in the duct
PSNJ	Total ψ^* in the jet
RHO(m, I)	ρ^*
RM	M_{ir}
RNU	μ_o
ROREF	ρ_o
RR(I)	Duct width or diameter
T(m, I)	θ
TCLI	T_j
TFLOW	Total mass, flow rate, $\sum_{i=1}^{N} \rho^* u \, \Delta Y$

TREF	T_o
TSEC	Temperature of secondary flow at nozzle exit plane
TTP(J)	$\bar{T}$
TTT(J)	Dimensional stagnation temperature at each node, $\bar{T} + \frac{\bar{\rho}\bar{u}^2}{2g_o}$
TWREF	T_{wr}
U(m, I)	u
UCLI	u_o
UPOT	Velocity at inflection point
URR	u^*
USE	Secondary velocity at nozzle exit
UUU(I)	$\bar{u}$
VHEAD	Reference velocity head, $\rho_o u_o^2/2g_o$
VIS(I)	μ^*
X	X
XX	Distance from duct inlet at which calculation ends
XX(I)	Distance from duct inlet at which duct width, RR(I) are provided
XRO	Non-dimensional downstream distance with respect to the initial duct half width or radius
Y(I)	Y
YJ	Half nozzle width or radius at nozzle exit
YS	y^+

Definition of the Input and Output Parameters

Part (a) Input data

The input data to the program must be prepared according to the following sequence:

Card No.	Parameters	Format
1	SQP, NP, NPP, NL	F5.0, 3I5
2	DP1, DP2, DP11	3E13.6
3	X, xx	8F10.0
4	MK	I5
5	PROFE(I), I = 1, MK	8F10.0
6		
7	NTEST	I5
8	P01, TO1, PAMB, TOO, AMASS1, AMASSO, RD, YJ	8F10.0
9		
10	(PS(I), I = 53, 70)	6E13.6
11		
12	NS	I2
13		
14	(RR(I), I = 1, NS)	8F10.0
15		
16		
17	(XX(I), I = 1, NS)	8F10.0
18		
19	SQP, NP, NPP, NL	F5.0, 3I5

Card 19 is the last card to end the calculation of the Program, on which NPP must be set a value larger than 1.

Cards 1 through 18 are required for each set of data. For data more than one set, cards 1 through 18 must be repeated in the same sequence.

An example of input data for two sets of data are shown on Table A-1. The input parameters are:

SQP, NP, NPP, NL	Control Card for axisymmetric flow SQP = 0.5, NP = 2, NPP = 0, NL = 1, for plane flow SQP = 1.0, NP = 0, NPP = 1, NL = 0.
DP1, DP2, DP11	Initial guessed dimensionless pressure gradients on m=1, 2 and zero lines respectively. The initial guesses of the values of DP1, DP2, DP11 at the initial plane may be assumed equal at any plus or minus dimensionless value of the order of 10^{-7} to 10^{-8}.
X -	Distance from duct inlet to nozzle exit plane at which calculation begins, inches.
XX-	Distance from duct inlet at which calculation stops
MK-	A number which indicates the number of velocity and temperature detail being printed out.
PROFE(I)-	An array contains MK value of downstream positions in inches where the velocity and temperature detail are required to be printed out.
NTEST-	Test or Run number identity
PO1-	Stagnation pressure of the primary flow, psia
TO1-	Stagnation temperature of the primary flow, ^{o}R
PAMB	Ambient pressure (i.e., stagnation pressure of the secondary flow), psia
TOO-	Stagnation temperature of the secondary flow, ^{o}R
AMASS1-	Primary mass flow rate.
AMASS0-	Secondary Mass flow rate. For axisymmetric flow, lbm/sec. For plane flow, lbm/sec-in.
RD-	Half duct width at nozzle discharge plane, inches
YJ-	Full jet width, inches, (Outside dimension of nozzle exit)

```
Card No.
 1    1.          0       1      0
 2   -0.100000E-03-0.100000E-08-0.100000E-08
 3    0.                 23.5
 4         9
 5    .99       1.98      2.98      4.98      6.98      10.45     12.98     16.98
 6    19.98
 7         3
 8    31.61     706.      14.61     553.       .075      .2763    1.206      .162
 9    0.540000E 00 0.722000E 00 0.815000E 00 0.877000E 00 0.918000E 00 0.945000E 00
10    0.963000E 00 0.975100E 00 0.983200E 00 0.989600E 00 0.993200E 00 0.995600E 00
11    0.997200E 00 0.998300E 00 0.999000E 00 0.999500E 00 0.999800E 00 1.000000E 00
12   21
13    1.206     1.173     1.139     1.109     1.081     1.053     1.027     1.005
14    .975      .931      .887      .849      .817      .764      .745      .729
15    .711      .694      .625      .625      1.28
16    0.        .125      .25       .375      .5        .625      .75       .875
17    1.0       1.25      1.5       1.75      2.0       2.5       2.75      3.0
18    3.5       4.0       8.        11.       23.5
19    1.          0       1      0
20   -0.100000E-03-0.100000E-08-0.100000E-08
21    0.        23.5
22         9
23    .99       .198      2.98      4.98      6.98      10.45     12.98     16.98
24    19.98
25         6
26    35.8      649.      14.8      547.      .0882     .3320     1.519     .162
27    0.540000E 00 0.722000E 00 0.815000E 00 0.877000E 00 0.918000E 00 0.945000E 00
28    0.963000E 00 0.975100E 00 0.983200E 00 0.989600E 00 0.993200E 00 0.995600E 00
29    0.997200E 00 0.998300E 00 0.999000E 00 0.999500E 00 0.999800E 00 1.000000E 00
30   21
31    1.519     1.486     1.452     1.422     1.394     1.366     1.34      1.318
32    1.288     1.244     1.2       1.162     1.13      1.077     1.058     1.042
33    1.024     1.007     .938      .938      1.593
34    0.        .125      .25       .375      .5        .625      .75       .875
35    1.0       1.25      1.5       1.75      2.0       2.5       2.75      3.0
36    3.5       4.0       8.        11.       23.5
37    1.          0       5      0
```

Table D-1

Input Data Example for Runs 3 and 6

PS(I)- To take care of the boundary layer problem, the last 18 values to the wall are required to be specified in the SUBROUTINE PSI. SUBROUTINE PS(I) already includes the values needed for the computer calculation. The computer values were selected to satisfy the following:

(1) grid spacing of the wall should not correspond to a value of y^+ greater than 3.

(2) neighboring grid spacings should not differ in size by more than 50%.

(3) close spacing is also required in any region away from the wall where the velocity gradient is large.

NS - Indicates the total number of duct geometry to be read in the SUBROUTINE RADIUS

RR(I) - An array contains the total number (NS) of duct width, inches

XX(I) - An array contains the total number (NS) of axial downstream distance, where RR(I) are provided, inches

Part (b) Output Parameters

The first section of the output repeats the most important input data for different test or run number.

$$\text{Velocity ratio} = \frac{\text{initial velocity of secondary flow}}{\text{initial velocity of primary flow}}$$

$$\text{Width ratio} = \frac{\text{initial duct width}}{\text{nozzle width}}$$

$$\text{Mass flow ratio} = \frac{\text{secondary mass flow}}{\text{primary mass flow}}$$

J - Indicates node point counting from centerline to wall

Y(J) - Dimensionless Y coordinate with respect to the local half duct width.

U(J) - Dimensional velocity on Jth node, ft/sec

TO(J) -	Dimensional stagnation temperature on Jth node, ^{o}F
I -	Print step counter at approximately XIN increases 0.25 inches
XIN -	downstream distance from nozzle exit plane where calculation begins, inches
X/BO -	ratio of downstream distance with respect to initial half duct width.
B/BO -	ratio of the local duct width with respect to initial duct width.
PH2O -	Local wall static pressure, 9 inches of water
UCENT -	velocity of the flow at centerline, ft/sec
TOCENT -	centerline stagnation temperature of the flow, ^{o}F
AUGMENT -	Local momentum flux, $2 \int_{o}^{y_w} \bar{\rho}\, \bar{u}^2\, dy$, divided by initial jet momentum
USTER -	Local friction velocity, ft/sec

The selection of intervals at which calculations are made is determined by a subroutine in the computer program. The data is printed out at approximately quarter inch intervals. The locations where temperature and velocity profiles are printed out are specified by the user in PROFE(I) described in the input data.

PROGRAM LISTING

The program listing included in this report is for the program as run on a CDC/6600. The program was initially developed on an IBM 360/50. The deck is the one successfully run on the CDC/6600.

The essential changes to the program necessary to recover the IBM 360/50 deck are:

1. Certain variables should be in a real*8 mode

Add

Card	
JMX40	REAL*8 Y, DABS, DLOG, YB1, YB2
YIS20	REAL*8 ZY, Y
CHE20	REAL*8 Y
BLC20	REAL*8 Y
LEF20	REAL*8 Y

Change

Functions ABS( ), and ALOG( ), should be changed to DABS( ), and DLOG( ). These occur in cards

JMX2710	JMX3750	JMX4450
JMX3030	JMX4340	JMX4460

Card YIS50 should be Y(1) = 0.0D0

Output Hollerith symbols should be changed from * to These occur in cards

JMX460	JMX660	JMX730	JMX2120	JMX5640
JMX470	JMX700	JMX740	JMX5190	JMX5650
JMX520	JMX710	JMX2090	JMX5200	JMX5660
JMX530	JMX720	JMX2110	JMX5590	JMX5670
GEM110	CHE330	BLC190		
GEM120	CHE340	BLC200		

Deck characters are BCD.

Figure D-2

COMPUTER PROGRAM LISTING

```
RUN VERSION 2.3 --PSR LEVEL 298--

              PROGRAM NAS(INPUT,OUTPUT,TAPE5=INPUT,TAPE6=OUTPUT)
000003        REAL  LZ
000003        COMMON NP,SQP,NPP,NL
000003        DIMENSION U(2,70 ),TTT(70), T(2,70 ),S1(70 ),S2(70 ),S3(70 ),
             1PS(70 ),R2(70 ),E1(70 ),P1(70 ),         Y(70 ),E(70 ),
             2RHO(2,70),VIS(70),TTP(70),AA(70), D(70)
             3,A(70 ),B(70 ),C(70 ),H(70 ),BBB(70)
             4 ,TOLD(2),AUGM(70),PROFE(20),UJ(70) ,YRL(70)
000003         F(X1,Y1)=((2./2.4)*(1.+.2*X1**2))**3-Y1*X1
        C
        C   *    *    *    SECTION 1    *    *    *
        C
        C     KJ IS A CONTROL VARIABLE. 1 FOR SINGLE STREAM FLOW WITH INITIAL WA
        C     BOUNDARY LAYER, 2 FOR SINGLE STREAM FLOW WITHOUT W.B.L. OR TWO STR
        C     FLOW WITH A TOP HAT PROFILE
        C
        C      X =DISTANCE FROM THE DUCT INLET TO NOZZLE EXIT INCHES
        C     USE= U SECONDARY (FT/SEC)
        C      XX=DISTANCE FROM THE DUCT INLET  AT WHICH CALCULATIONS STOP (INCH
        C      RNU= REFERENCE VISCOSITY  FT/SEC2
        C      PE=NOZZLE EXIT PLANE PRESSURE LBF/FT2 GAUGE
        C      ROREF=REFERENCE DENSITY LBM/FT3
        C      FDUCT=TOTAL MASS FLOW RATE   (LBM/SEC )
        C      PR=PRANTL NUMBER
        C      PRT= TURBULENT PRANTL NUMBER
        C      TWREF=WALL REFERENCE TEMPERATURE DEG R
        C      TCLI= JET TEMPERATURE AT NOZZLE EXIT  DEG R
        C     YJ= EFFECTIVE NOZZLE EXIT RADIUS(INCHES)
        C      UCLI =JET VELOCITY AT NOZZLE EXIT FT/SEC
        C      GAMA=GAS CONSTANT= 1.4 FOR AIR
        C      RM= REFERENCE MACH NUMBER
        C      TSEC=SECONDARY TEMPERATURE (DEG R)
        C      PREF=REFERENCE PRESSURE LBF/FT2 A
        C      PAMB=AMBIENT PRESSURE LBF/FT2
        C     NOZZLE RADIUS IN INCHES
000016        DATA RNU,ROREF,PREF,GAMA/.0001580,.0763,2115.,1.4/
000016        DATA PR,PRT,TREF,TWREF/0.7,0.9,520.0,560.0/
000016   8888   CONTINUE
000016        READ(5,8019) SQP,NP,NPP,NL
000032   8019  FORMAT(F5.0,3I5)
000032         IF(NPP- 1) 737,838,883
000035    838 WRITE(6,279)
000041    279 FORMAT(1H1,//,10X,*TWO-DIMENSIONAL DUCT FLOW*,/,10X,*--- ---------
             1-- ---- -----*,//)
000041          TWREF =540.
000043        CC = .08
000044         GO TO 1021
000045    737   WRITE(6,829)
000051    829 FORMAT(1H1,//,10X, *AXISYMMETRIC DUCT FLOW*,/,10X,*------------ --
             1-- -----*,//)
000051         TWREF = 560.
000053         CC = .07
        C       INPUT SECTION
000054   1021  CONTINUE
```

RUN VERSION 2.3 --PSR LEVEL 298-- NAS

```
000054          READ(5,7817) DP1,DP2,DP11
000066   7817   FORMAT(3E13.6)
000066          READ(5,  73) X,XX
000076          READ(5,37) MK
000104          READ(5,73) (PROFE(I),I=1,MK)
000117          READ(5,37) NTEST
000125     37 FORMAT(I5)
000125          WRITE(6,39) NTEST
000133    39    FORMAT(//,25X,* INPUT DATA     RUN NO. *,I5,//)
000133          READ(5,73) PO1,TO1,PAMB,TOO,AMASS1,AMASSO,RD,YJ
000157    73    FORMAT(8F10.0)
000157          WRITE(6,7) PO1,TO1,PAMB,TOO,AMASS1,AMASSO,RD,YJ
000203     7    FORMAT(15X,*PO1 = *,F8.4,*  PSIA*,/,15X,*TO1 = *,F8.4,*  DEG R* ,
               1/,15X,*PAMB = *,F8.4,*  PSIA*,/,15X,*TOO = *,F8.4,*  DEG. R*,
               2/,15X,*AMASS1 = *,F8.4,*  LBM/S-IN.*,/,15X,*AMASSO = *,F8.4,*  LBM
               3/S-IN.*,/,15X,*RO(HALF DUCT WIDTH) = *,F8.4,*  IN.*,/,15X,*YJ(FULL
               4 JET WIDTH) = *,F8.4,*  IN.*,/)
000203          IF(NP .EQ. 2) GO TO 2001
000205          A2 = 2.*RD -YJ
000210          GO TO 1201
000211   2001   A2 = 3.1416/4.*((2.*RD)**2-YJ**2)
000216   1201   CONTINUE
000216          ASTAR=(AMASSO/PAMB)*SQRT(TOO*(53.3/(1.4*32.2)))*1.2**3
000226          Y1 = A2/ASTAR
000230          X11 = 1.
000231          X22 = .03
000233          TOL = .0001
000234         TEST1=F(X11,Y1)
000237         TEST2=F(X22,Y1)
000241    22    HALF = (X11+X22)/2.
000244         CHEK1=F(HALF,Y1)
000247         IF(ABS(CHEK1).LE.TOL) GO TO 23
000252         IF(ABS(TEST1-CHEK1)-ABS(TEST1)) 19,23,29
000256    29     X22 = HALF
000260         TEST2=CHEK1
000261          GO TO 22
000262    19    X11 = HALF
000264         TEST1=CHEK1
000265          GO TO 22
000266    23    RM2 = HALF
000270          P1 = PAMB/((1.+.2* RM2**2)**3.5)
000276          PA1 = (PO1/P1)**((GAMA-1)/GAMA)
000305          RM = SQRT((PA1 -1.)*(2./(GAMA-1.)))
000314          TCLI = TO1/PA1
000316          UCLI = RM*SQRT(1.4*32.2*53.3*TCLI)
000323          PA2=(PAMB /P1)**((GAMA-1.)/GAMA)
000332          TSEC = TOO/PA2
000334          USEC = SQRT(2.*.24*778.*32.2*(TOO-TSEC))
000341          PE = (P1-PAMB)*144.
000344          PAMB= PAMB*144.
000345          UJR = USEC/UCLI
000347          AMR = AMASSO/AMASS1
000351           YJ = YJ/2.
000352         N=70
000353         NTT=N-2
```

```
RUN VERSION 2.3 --PSR LEVEL 298--                          NAS
000355           NN= N-1                                                JMX 1130
000357           PREF = 2115.                                           JMX 1140
000360           PI = 0.                                                JMX 1150
000361           TOLD(1) = 0.                                           JMX 1160
000362           ITER = 0                                               JMX 1170
000363           BY=0.                                                  JMX 1180
000364           IL= 0                                                  JMX 1190
000365           JFLOW=2                                                JMX 1200
000366           UREF = .001                                            JMX 1210
000367           IURES=0                                                JMX 1220
000370           BH=0.                                                  JMX 1230
000371           PH20 = 0.                                              JMX 1240
000372           NSTEP=0                                                JMX 1250
000373           IFLOW = 0                                              JMX 1260
000374           URR = 1.                                               JMX 1270
000375           ICORE=0                                                JMX 1280
000376           TOLD(2) =0.                                            JMX 1290
000377           DELTA=0.                                               JMX 1300
000400           KJ=2                                                   JMX 1310
           C     UJR=U SECONDARY/U PRIMARY                              JMX 1320
000401           REN=UCLI/(24.*RNU)                                     JMX 1330
000404           IF (NP .EQ. 2) GO TO 118                               JMX 1340
000406           AMASS1 = AMASS1*12.                                    JMX 1350
000407           FDUCT = AMASS0*12.+ AMASS1                             JMX 1360
000412           PSN = FDUCT/(2.*RNU*ROREF)                             JMX 1370
000415           PSNJ=AMASS1 /(2.*RNU*ROREF)                            JMX 1380
000417           FDUCT = PSN                                            JMX 1390
000420           GO TO 117                                              JMX 1400
000421       118 CONTINUE                                               JMX 1410
000421           YOUT = RD*2.*REN                                       JMX 1420
000424           FDUCT = AMASS1   +AMASS0                               JMX 1425
000426           PSN    =FDUCT*UCLI/(6.284*RNU**2*ROREF)                JMX 1430
000432           PSNJ = AMASS1*UCLI/(6.284*RNU**2*ROREF)                JMX 1440
000437           FDUCT=FDUCT*UCLI/(ROREF*3.142*YOUT**2*RNU**2)          JMX 1450
000444       117 CONTINUE                                               JMX 1460
           C                                                            JMX 1470
           C     SPECIFY   STREAM FUNCTION DISTRIBUTION                 JMX 1480
           C                                                            JMX 1490
000444           CALL PSI( N, PSN,NJ,PS,PSNJ)                           JMX 1500
           C                                                            JMX 1510
000450           DO  8   J=2,NN                                         JMX 1520
000452           JP1=J+1                                                JMX 1530
000454           JM1=J-1                                                JMX 1540
000455           S1(J)=PS(JP1)-PS(J)                                    JMX 1550
000460           S2(J)=PS(J)-PS(JM1)                                    JMX 1560
000463           S3(J)=PS(JP1)-PS(JM1)                                  JMX 1570
000466           R1(J)=S1(J)/S2(J)/S3(J)                                JMX 1580
000471           R2(J)=S2(J)/S1(J)/S3(J)                                JMX 1590
000474         8 CONTINUE                                               JMX 1600
000476           DO  9 I=1,N                                            JMX 1610
           C                                                            JMX 1630
000500         9  F(I) = 0.                                             JMX 1620
000503           X =X *UCLI/(RNU*12.)                                   JMX 1640
000507           XX=XX*UCLI/(RNU*12.)                                   JMX 1650
000510           YJ=YJ*UCLI/(RNU*12.)                                   JMX 1660
```

```
000512           CALL RADIUS(X,YOUT,1,REN)
000515           YT=YOUT
000517           NTP=N-3
000521            BLEND = 4.*YT
          C       BLENDING LENGTH IN RADII
000523           XBLEND=0.
000524           XRO=X/YOUT
          C      *N*TIALISATION OF CONSTANTS
000526           IF(UJR.GT..990)JFLOW=1
000531           IF(JFLOW.EQ.1)NJ=N
000535           IF(JFLOW.EQ.1)CC=0.09
          C      INITIALISATION OF DP/DX VARIABLES
000540           VHEAD=UCLI**2*ROREF/64.4
000543           TJR=(TSEC-TCLI)/(TWREF-TCLI)
000547           PREF=PREF /VHEAD
000550           PAMB=PAMB /VHEAD
000551           PCUM=PE/VHEAD
000553           NN=N-1
000555            URR = 1.
          C
          C
          C
          C   *    *    *    SECTION 2    *    *    *
          C
          C      *    *    *    *    *    *    *    *    *    *    *    *    *    *    *    *    *
          C       INITIAL FLOW CHARACTERISTICS AT M=1 LINE.
          C       VELOCITY AND TEMPERATURE ON M=1 LINE
000556           CALL PROF(U,T,NJ,N,UJR,TJR,KJ,UCLI)
          C
000566           CONA=(TWREF-TCLI)/TREF
000571           CONB=TCLI/TREF
000572           CONF=198.7/TREF
000574           COND=1.+CONE
000576           CONL    =(GAMA-1.)*RM    **2./(TWREF/TCLI-1.)
000607           DO 51 I=1,N
000610           RHO(1,I)=(PCUM+PAMB)/(PREF*(CONA*T(1,I)+CONB))
000621           RHO(2,I)=RHO(1,I)
000623       51  VIS(I)=(T(1,I)*CONA+CONB)**1.5*COND/(T(1,I)*CONA+CONB+CONE)
          C
000641           CALL YDIS(Y,PS,RHO,U,N)
000645           DJR=YOUT/YJ
000647            WRITE(6,1051)
000653     1051   FORMAT(1H1,*           .PRINT OUT INITIAL VALUES*,//)
000653            WRITE(6,7232) UJR,DJR,AMR
000665     7232   FORMAT(20X,*VELOCITY RATIO = *,F14.4,/,20X,*WIDTH(DIA) RATIO = *,
              1F14.4,/,20X,*MASS FLOW RATIO = *,F14.4,/)
          C     JJK IS THE NUMBER OF THE GRID NODE AT YJ PLUS 2
000665           JJK=NJ+2
          C      *    *    *    *    *    *    *    *    *    *    *    *    *    *    *    *    *
          C       PRINT OUT INITIAL VALUES
          C
000667           GO TO 1748
          C      *    *    *    *    *    *    *    *    *    *    *    *    *    *    *    *    *
          C      INITIALISATION ENDS +OUTER LOOP BEGINS
000670    100    CONTINUE
```

```
000670           NSTEP=NSTEP+1
          C
          C      CALCULATE FRICTION VELOCITY
          C
000672           IF(NSTEP.EQ.1)GO TO 631
          C
          C
000673           IF(IFLOW.EQ.1)GO TO 88
          C
000674           CALL LOOK(JJK,NN,U,Y,DELTA,BH,BY,N,CC,IFLOW,XBLEND,YJ,BE)
          C       EVALUATES SHEAR LAYER WIDTH ECT.
          C
000711       88  CONTINUE
          C
          C      SECTION 3 INSERTED HERE
          C    *    *    *    SECTION 3    *    *    *
          C
          C     *  EVALUATE  TURBULENT VISCOSITY  USING MIXING LENGTH  *
          C      VERSION FOR PIPE FLOW  (AS PER APRIL 17, 1972 )
          C
000711           IF(IFLOW.EQ.1)GO TO 778
000713           IF(JFLOW.EQ.1)GO TO 778
          C      JFLOW=1 INDICATES A PIPE FLOW
000715           BDELTA=Y(N)-DELTA
000717           INM=0
000720           AZ1 = .09*DELTA
000722           DO 45 I=2,NN
000723           IP1=I+1
000725           IM1=I-1
000726     162   DELU=ABS((U(1,IP1)-U(1,IM1))/U(1,I))
000735           IF(DELU.LE..  0010)GO TO 1360
000737           IF(Y(I).LT.BE)GO TO 1360
000742           IF(I.EQ.2)GO TO 796
          C       IF POINT IS BETWEEN SHEAR LAYER AND WALL B. L. GO TO 1360
000744           IF(Y(IM1).GT.BY.AND.Y(I).LT.BDELTA)GO TO 1360
          C       IF POINT IS IN WALL B. L. GO TO 1373
000755           IF(Y(I).GE.BDELTA)GO TO 1373
000757           GO TO 796
          C       WALL VISCOSITY
000760    1373   CONTINUE
000760           YS=(Y(N)-Y(I))*UREF
000764           LZ=0.41*(1.0-EXP(-YS/26.0))*(Y(N )-Y(I ))
000777           IF(LZ.LT.AZ1) INM=INM+1
001003           IF(LZ.GT.AZ1)LZ=AZ1
001006           GO TO 762
001007    1360   E(I)=0.
001011           GO TO 45
          C       JET VISCOSITY
001011     796   LZ=CC *BH
001013     762   E(I)= ABS((Y(I)-Y(IM1))*(U(1,IP1)-U(1,I))/((Y(IP1)-Y(I))*
               1 (Y(IP1)-Y(IM1)))+(Y(IP1)-Y(I))*(U(1,I)-U(1,IM1))/((Y(I)-Y(IM1))*
               2(Y(IP1)-Y(IM1))))*LZ*LZ
001044      45   CONTINUE
001047           GO TO 48
          C      PIPE FLOW MIXING LENGTH
```

```
001047    778  INM=-1
001050         IT=0
001051         AZ = .09*DELTA
001053         DO 10 J=2,NN
001055         I=N+1-J
001057         IP1=I+1
001061         IM1=I-1
001062         IF(IFLOW.EQ.1)GO TO 4172
001063         UNN=.0050*U(1,I)
001066         UN=ABS(U(1,IM1)-U(1,IP1))
001073         IF(UN.GT.UNN  )GO TO 8140
001076         GO TO 10
001076   4172  YD=Y(N)-Y(I)
001101          YD=1.-YD/Y(N)
001104         IF(XBLEND.LT.BLEND) GO TO 4173
001107         AZ=( .14-.08*YD**2-.06*YD**4)*Y(N)
001116         GO TO 8140
001116   4173  AZ  =CC *BH+((.14-.08*YD**2-.06*YD**4)*Y(N)-CC *BH)*XBLEND/BLEND
001132   8140  IF(IT.EQ.1)GO TO 832
001134         YS=(Y(N)-Y(I))*UREF
001140          LZ =.41*(1.-EXP(-YS/26.))*(Y(N)-Y(I))
001153         INM=INM+1
001154         IF(LZ.GE.AZ)IT=1
001160         AZ1=LZ
001161         IF(LZ.LT.AZ)GO TO 11
001163    832  AZ1=AZ
001165     11  F(I)= ABS((Y(I)-Y(IM1))*(U(1,IP1)-U(1,I))/((Y(IP1)-Y(I))*
              1 (Y(IP1)-Y(IM1)))+(Y(IP1)-Y(I))*(U(1,I)-U(1,IM1))/((Y(I)-Y(IM1))*
              2(Y(IP1)-Y(IM1))))*AZ1*AZ1
001216     10  CONTINUE
001221     48    CONTINUE
         C
         C        FINAL CARD OF SECTION 3
001221    631   CONTINUE
         C      SECTION 4 INSERTED HERE
         C   *    *    *    SECTION 4    *    *    *
         C
         C        EVALUATE DX STEP   (FOR EJECTOR FLOW AS PER  FEB. 19)
         C
001221         DX=BH*.4
001223         BB=.040*Y(N)
001226         IF(DX.LT.BB)DX=BB
001231         ZK=Y(N)/8.
001234         IF(DX.GT.ZK)DX=ZK
001236         IF(NSTEP.LT.10)DX=.5*DX
001242         IF(NSTEP.LT.20)DX=.2*DX
001246         IF(NSTEP.LT.30)DX=.5*DX
001252         IF(IURES.EQ.1)DX=.3*DX
001256         IF(XRO.GT.12.0)DX=DX*2.
001262         IURES=0
001263    12   X=X+DX
001265         XBLEND=XBLEND+DX
001267         XRO=X/YT
         C
         C      FINAL CARD OF SECTION 4
```

```
             C
             C   *    *    *    SECTION 5    *    *    *
             C
             C       DETERMINE BOUNDARY CONDITIONS ON N+1 LINE
001270               U(2,N)=0.0
001272               Y(1)=0.
001273               CALL RADIUS(X,YOUT,2,REN)
001276               DP2=(DP11+DP1)/2.
001301               ICHX=0
001302               ITER=1
             C
             C       CALCULATE VELOCITY U ON N+1 LINE
             C
001303                E1(1) = 0.
001304                DO 7347 J =2,N
001305        7347 E1(J)=Y(J)**NP *U(1,J)*RHO(1,J)/(2.*PS(J))
001326               NTK=NTT-1
             C
             C        ITERATION STARTS
             C
001330        6001 CONTINUE
001330               DO 13 J=2,NTT
001332               JP1=J+1
001334               JM1=J-1
001335               Y1=E1(JP1)*(VIS(JP1)+RHO(1,JP1)*E(JP1))
001342               Y2=E1(JM1)*(VIS(JM1)+RHO(1,JM1)*E(JM1))
001347               Y3=E1(J)*(VIS(J)+RHO(1,J)*E(J))
001354               Y4=(Y1+Y3)/S1(J)
001357               Y5=(Y3+Y2)/S2(J)
001362               Y6=Y4/(S3(J)*2.)
001365               Y7=Y5/(S3(J)*2.)
001367               Y8=Y6*U(1,J)/PS(J)
001372               Y9=Y7*U(1,J)/PS(J)
001375               A(JM1)=U(1,J)/DX+Y8+Y9
001402               B(JM1)=-Y8
001404               C(JM1)=-Y9
001405          13   D(JM1)=U(1,J)**2/DX-DP2        /(2.*RHO(1,J))
001417               A(1)=A(1)+C(1)
001421               IF(NP .EQ. 2) GO TO 119
001423               DIG= (Y(NN)-Y(N))/(Y(NTT)-Y(N))
001432               DBAR=DP1*(Y(NN)**2-Y(N)**2-( Y(NTT)**2-Y(N)**2)*DIG)/4./VIS(NN)
001446                GO TO 219
001447         119    CONTINUE
001447               DIG=ALOG(Y(NN)/Y(N))/ALOG(Y(NTT)/Y(N))
001463                 DBAR=DP1*(Y(NN)**2-Y(N)**2-(Y(NTT)**2-Y(N)**2)*DIG)/8./VIS(NN)
001477         219    CONTINUE
001477               A(NTK)=A(NTK)+DIG*B(NTK)
001503               D(NTK)=D(NTK)-DBAR*B(NTK)
001506               CALL CALC(A,B,C,D,H,NN)
001512               DO 1934 J=2,NTT
001514               U(2,J)=H (J-1)
001516               IF(U(2,J).LE..001)IURES=1
001522               IF(U(2,J).LE..001)U(2,J)=.001
001527        1934 CONTINUE
001532               U(2,1)=U(2,2)
```

```
001533           U(2,NN)=U(2,NTT)*DIG+DBAR
           C   *    *    *    SECTION 6    *    *    *
           C      EVALUATE TEMPERATURE,VISCOSITY,AND DENSITY FIELDS
           C      THIS SECTION SHOULD FOLLOW  SECTION 7 FOR INCOMPRESSIBLE FLOW
           C
001540           DO 1935 J=2,NN
001541           JP1=J+1
001543           JM1=J-1
001544           Y1=E1(JP1)*(VIS(JP1)/PR+E(JP1)*RHO(1,JP1)/PRT)
001553           Y2=E1(JM1)*(VIS(JM1)/PR+E(JM1)*RHO(1,JM1)/PRT)
001562           Y3=E1(J)*(VIS(J)/PR+(E(J)*RHO(1,J))/PRT)
001570           Y4=(Y1+Y3)/S1(J)
001573           Y5=(Y3+Y2)/S2(J)
001576           Y6=Y4/(S3(J)*2.)
001601           Y7=Y5/(S3(J)*2.)
001603           Y8=Y6*U(1,J)/PS(J)
001606           Y9=Y7*U(1,J)/PS(J)
001611           A(JM1)=U(1,J)/DX+Y8+Y9
001616           B(JM1)=-Y8
001620           C(JM1)=-Y9
001621      1935 D(JM1)=T(1,J)*U(1,J)/DX+CONL   *DP2 *      U(1,J)/(2.*RHO(1,J))
                1+(VIS(J)+E(J)*RHO(1,J))*RHO(1,J)*CONL*
                2(R2(J)*(U(2,JP1)-U(2,J))+R1(J)*(U(2,J)-U(2,JM1)))**2*
                3Y(J)**NP *U(1,J)*U(1,J)/(4.*PS(J)*PS(J))
001672           DIG=1.
001674           BOUND=(Y(N-1)-Y(N-2))*(Y(N)*2.-Y(N-1)-Y(N-2))/4.
001704           DBAR=CONL*PR*BOUND*(UREF*VIS(N-1))**4./(RHO(1,N-1)**2.)
001720           IF(NSTEP.EQ.1)DBAR=0.
001723           A(NTK)=A(NTK)+DIG*B(NTK)
001727           D(NTK)=D(NTK)-DBAR*B(NTK)
001732           A(1)=A(1)+C(1)
001734           CALL CALC(A,B,C,D,H,NN)
001740           DO 16 J=2,NTT
001742      16   T(2,J)=H (J-1)
001750           T(2,NN)=T(2,NTT)*DIG+DBAR
001755           T(2,N)=T(2,N-1)
001761           T(2,1)=T(2,2)
001762           DO 50 I=1,N
001763           RHO(1,I)=RHO(2,I)
001767           RHO(2,I)=(PCUM+PAMB)/(PREF*(CONA*T(2,I)+CONB))
001776       50  VIS(I)=(T(1,I)*CONA+CONB)**1.5*COND/(T(1,I)*CONA+CONB+CONE)
           C   *    *    *    SECTION 7    *    *    *
           C
           C     *    *    *    *    CALCULATE PRESSURE GRADIENT
002014           CALL YDIS(Y,PS,RHO,U,N)
002020           IF(ITER.GT.9)GOTO 6732
002024           ITER=ITER+1
002025           YTEST= ABS(YOUT-Y(N))
002030           YPPT=YOUT*.00001
002032           IF(YTEST.LT.YPPT   )GO TO 6732
           C
002034           IF(ICHX.EQ.0)GO TO 4775
002035           GO TO 6000
002036      4775 DPB1=DP2
002040           YB1=Y(N)
```

```
002142          DP2=DP2*.9
002143     740  ICHX=2
002144          GO TO 6001
002145    6000  VS= ABS(YOUT-YB1)
002150          VNF= ABS(YOUT-Y(N))
002153          IF(VNF.GT.VS)GO TO 235
002157          YB2=YB1
002160          DPB2=DPB1
002161          YB1=Y(N)
002163          DPB1=DP2
002164          GO TO 236
002164     235  YB2=Y(N)
002166          DPB2=DP2
002170     236  DP2=DPB1+(YOUT-YB1)*(DPB2-DPB1)/(YB2-YB1)
002101          GO TO 6001
           C    ITERATION ENDS
           C
002101    6732  IF(NSTEP.EQ.1)DP1=DP2
002105          PCUM=PCUM+((DP2+DP1)*DX/2.0)
002112          J=NTT
002113          BZ=R2(J)*(U(2,J+1)-U(2,J))+R1(J)*(U(2,J)-U(2,J-1))
002123          BZ=BZ*E1(J)*(VIS(J)+RHO(1,J)*E(J))
002130          URR=(Y(J)**(NP+NPP)-Y(N)**(NP+NPP))*DP1/((2.+FLOAT(NP))*RHO
               *(1,J)*Y(N)**NL)-BZ/(RHO(1,J)*Y(N)**NL)
002161          URR=UCLI* SQRT(URR)
002164           TOLD(2) = URR/UCLI
002165          DELY=Y(N)-Y(NN)
002170          UREF=SQRT((U(1,NN)/DELY-DELY*DP1/4./VIS(NN))*RHO(1,NN)/
               *VIS(NN))
           C
           C    *    *    *    SECTION 8    *    *    *
           C    *    *    *    *    *    *    *    *    *    *    *    *    *    *    *    *    *
           C     REPLACE M LINE VALUES WITH M+1 LINE VALUES
           C
           C    *    *    *    SECTION 9    *    *    *
           C     *  OUTPUT SECTION   *   *
           C
002203    1748   XIN = XRO*YT/(2.*REN)
002207           IF( NSTEP .EQ. 0 ) GO TO 458
002210           IF(NSTEP .EQ. 1) GO TO 908
002212           IF(XIN .GE. PI) GO TO 908
002214           GO TO 7142
002215     908   CONTINUE
002215           IL = IL +1
002217           YIN= Y(N)/YT
002221           UCL = U(2,1)*UCLI
002223           TCL = T(2,1)*(TWREF-TCLI) + TCLI+ UCL**2/12000.- 460.
002233           AUGM(1) =0.
002234           DO 1111 I = 2,N
002235           IM1 = I-1
002237           AUGM(I) = AUGM(IM1) +(U(2,I)+U(2,IM1))*(PS(I)+PS(IM1))*(PS(I)-
               1 PS(IM1))
002251    1111   CONTINUE
002254           AUGMET = AUGM(N)/(PSNJ*2.*6.2836**NL)
002262           PH20 = PCUM*VHEAD *.1923
```

```
002265          DEL  = DELTA*RNU/(UCLI*ROREF)                                  JMX 4970
002270          WRITE(6,63)   IL,XIN,XRO,YIN,PH2O,UCL,TCL,AUGMET,URR           JMX 4980
002316    63    FORMAT(/,5X,I4,8F13.3)                                         JMX 4990
002316          PI = PI+ .25                                                   JMX 5000
002320          DO 57 I= 1,MK                                                  JMX 5010
002322          IF(XIN .GE. PROFE(I)) GO TO 902                                JMX 5020
002325    57    CONTINUE                                                       JMX 5030
002327          GO TO 7142                                                     JMX 5040
002327   458    CONTINUE                                                       JMX 5050
002327          WRITE(6,752)                                                   JMX 5060
002333         DO 909 J=1,N,1                                                  JMX 5070
002335          YRL(J) = Y(J)/YOUT                                             JMX 5080
002337          UJ(J) = U(2,J) *UCLI                                           JMX 5090
002342          LVH = UJ(J)**2/12000.-460.                                     JMX 5100
002346         TTP(J)=T(2,J)*(TWREF-TCLI)+TCLI                                 JMX 5110
002353         TTT(J)=TTP(J)+LVH                                               JMX 5120
002356   909    WRITE(6,61) J,YRL(J),UJ(J),TTT(J)                              JMX 5130
002374          WRITE(6,757)                                                   JMX 5140
002377          GO TO 7142                                                     JMX 5150
002400   902    CONTINUE                                                       JMX 5160
002400          PROFE(I) = 50.                                                 JMX 5170
002402          WRITE(6,351)                                                   JMX 5180
002406   351    FORMAT(//,15X,*VELOCITY AND TEMPERATURE DISTRIBUTION ARE PRINTED JMX 5190
               1 OUT AT THE CORRESPONDING X IN. POSTION*,/)                    JMX 5200
002406          WRITE(6,752)                                                   JMX 5210
002412         DO 709 J=1,N                                                    JMX 5220
002414          YRL(J) = Y(J)/YOUT                                             JMX 5230
002416          UJ(J) =U(2,J)*UCLI                                             JMX 5240
002421          LVH = UJ(J)**2/12000.-460.                                     JMX 5250
002425         TTP(J)=T(2,J)*(TWREF-TCLI)+TCLI                                 JMX 5260
002432         TTT(J)=TTP(J)+LVH                                               JMX 5270
002435   709    CONTINUE                                                       JMX 5280
002437          DO 1213 J= 1,N,2                                               JMX 5290
002440          WRITE(6,61) J,YRL(J),UJ(J),TTT(J)                              JMX 5300
002453          I= J+1                                                         JMX 5310
002455          IF(I .EQ. N) GO TO 4311                                        JMX 5320
002457          GO TO 1213                                                     JMX 5330
002457  4311    WRITE(6,61) I,YRL(I),UJ(I),TTT(I)                              JMX 5340
002473  1213    CONTINUE                                                       JMX 5350
        C THE FOLLOWING CARD IS INSERTED IF A MASS ,ENERGY CHECK REQUIRED      JMX 5360
        C      CALL CHECK(Y,E,U,RHO,YT,FDUCT,TTP,TTT,NN,UCLI,UJR)              JMX 5370
002476          CALL        BLCHEK(N,U,PS,Y,DX     ,DP2,UCLI,RBH,TOLD ,URR,RHO,AA)  JMX 5380
002511          CALL        CHECK(Y,E,U,RHO,YT,FDUCT,TTP,TTT,NN,UCLI,UJR)      JMX 5390
002524          WRITE(6,757)                                                   JMX 5400
002530  7142 DP11=DP1                                                          JMX 5410
002532         DP1=DP2                                                         JMX 5420
002533         DO 17 J=1,N                                                     JMX 5430
002534         U(1,J)=U(2,J)                                                   JMX 5440
002540     17 T(1,J)=T(2,J)                                                    JMX 5450
002544          TOLD(1) = TOLD(2)                                              JMX 5460
        C                                                                      JMX 5470
        C   *    *    *    SECTION 10  *    *    *                             JMX 5480
        C     *  TERMINATION TEST  *  *                                        JMX 5490
        C                                                                      JMX 5500
002545         IF (X .GT. XX) GO TO 18                                         JMX 5510
```

```
002551          GO TO 100                                                          JMX 5520
        C                                                                          JMX 5530
        C       RETURN TO START OF OUTER LOOP                                      JMX 5540
        C                                                                          JMX 5550
002551       18 CONTINUE                                                           JMX 5560
002551            GO TO 8888                                                       JMX 5570
002552      883 WRITE(6,7717)                                                      JMX 5580
002556     7717 FORMAT(//,*      END OF CALCULATION*,/*      ------------------*)  JMX 5590
        C                                                                          JMX 5600
        C       FORMAT STATEMENTS.                                                 JMX 5610
        C                                                                          JMX 5620
002556     61   FORMAT(25X,I6,6X,F10.6,6X,F14.5,2X,F14.5)                          JMX 5630
002556     757  FORMAT(//,5X,*   I          X IN.        X/B0          B/B0       PJMX 5640
          *     1H20      UCENT(F/S)   TOCENT(DEG.R)    AUGMENT     USTAR(F/S)*,/)  JMX 5650
002556     752   FORMAT(    25X,*       J              Y(J)              U(J)      JMX 5660
               1 T(J) *)                                                           JMX 5670
002556          STOP                                                               JMX 5680
002560          END                                                                JMX 5690
```

```
RUN VERSION 2.3 --PSR LEVEL 298--                              NAS

NAS

PROGRAM LENGTH INCLUDING I/O BUFFERS
013414

FUNCTION ASSIGNMENTS
F        -  000006

STATEMENT ASSIGNMENTS
7        -  002645    9        -  000500    10       -  001216    11       -  001165
12       -  001263    16       -  001742    18       -  002551    19       -  000262
22       -  000241    23       -  000266    29       -  000256    37       -  002633
39       -  002635    45       -  001044    48       -  001221    61       -  003044
63       -  003013    73       -  002643    88       -  000711    100      -  000670
117      -  000444    118      -  000421    119      -  001447    162      -  000726
219      -  001477    235      -  002064    236      -  002070    279      -  002603
351      -  003020    458      -  002327    631      -  001221    737      -  000045
740      -  002043    752      -  003067    757      -  003051    762      -  001013
778      -  001047    796      -  001011    829      -  002616    832      -  001163
838      -  000035    883      -  002552    902      -  002400    908      -  002215
1021     -  000054    1051     -  002744    1201     -  000216    1213     -  002473
1360     -  001007    1373     -  000760    1748     -  002203    1934     -  001527
2001     -  000211    4172     -  001076    4173     -  001116    4311     -  002457
4775     -  002036    6000     -  002045    6001     -  001330    6732     -  002101
7142     -  002530    7232     -  002752    7347     -  001305    7717     -  003035
7817     -  002631    8019     -  002577    8140     -  001132    8888     -  000016

BLOCK NAMES AND LENGTHS
         -  000004

VARIABLE ASSIGNMENTS
A        -  006035    AA       -  005621    AMASSO   -  007171    AMASS1   -  007170
AMR      -  007221    ASTAR    -  007175    AUGM     -  006575    AUGMET   -  007347
AZ       -  007305    AZ1      -  007277    A2       -  007174    B        -  006143
BB       -  007312    BBB      -  006465    BDELTA   -  007275    BE       -  007274
BH       -  007234    BLEND    -  007257    BOUND    -  007330    BY       -  007227
B7       -  007341    C        -  006251    CC       -  007153    CHEK1    -  007205
CONA     -  007265    CONB     -  007266    COND     -  007270    CONE     -  007267
CONL     -  007271    D        -  005727    DBAR     -  007327    DEL      -  007350
DELTA    -  007242    DELU     -  007302    DELY     -  007342    DIG      -  007326
DJR      -  007272    DPB1     -  007333    DPB2     -  007340    DP1      -  007154
DP11     -  007156    DP2      -  007155    DX       -  007311    E        -  005063
E1       -  004541    FDUCT    -  007245    GAMA     -  007146    H        -  006357
HALF     -  007204    I        -  007162    ICHX     -  007314    ICORE    -  007241
IFLOW    -  007237    IL       -  007230    IM1      -  007301    INM      -  007276
IP1      -  007300    IT       -  007304    ITER     -  007226    IURFS    -  007233
J        -  007252    JFLOW    -  007231    JJK      -  007273    JM1      -  007254
JP1      -  007253    KJ       -  007243    LVH      -  007351    LZ       -  003244
MK       -  007161    N        -  007222    NJ       -  007251    NL       -  000003C01
NN       -  007224    NP       -  000000C01 NPP      -  000002C01 NSTEP    -  007236
NTEST    -  007163    NTK      -  007315    NTP      -  007256    NTT      -  007223
PAMB     -  007166    PA1      -  007210    PA2      -  007214    PCUM     -  007264
PE       -  007217    PH2O     -  007235    PI       -  007225    PO1      -  007164
```

```
RUN VERSION 2.3 --PSR LEVEL 29A--                                   NAS

PR      -  007147   PREF    -  007145    PROFE   -  006703   PRT     -  007150
PS      -  004325   PSN     -  007246    PSNJ    -  007247   P1      -  007207
RO      -  007172   REN     -  007244    RHO     -  005171   RM      -  007211
RM2     -  007206   RNU     -  007143    ROREF   -  007144   R1      -  004647
R2      -  004433   SUP     -  000001C01 S1      -  004003   S2      -  004111
S3      -  004217   T       -  003567    TCL     -  007346   TCLI    -  007212
TEST1   -  007202   TEST2   -  007203    TJR     -  007263   TOL     -  007201
TOLD    -  006573   TOO     -  007167    TO1     -  007165   TREF    -  007151
TSEC    -  007215   TTP     -  005513    TTT     -  003461   TWREF   -  007152
U       -  003245   UCL     -  007345    UCLI    -  007213   UJ      -  006727
UJR     -  007220   UN      -  007307    UNN     -  007306   UREF    -  007232
URR     -  007240   USEC    -  007216    VHEAD   -  007262   VIS     -  005405
VNE     -  007336   VS      -  007335    X       -  007157   XBLEND  -  007260
XIN     -  007343   XHO     -  007261    XX      -  007160   X11     -  007177
X22     -  007200   Y       -  004755    YB1     -  007334   YB2     -  007337
YD      -  007310   YIN     -  007344    YJ      -  007173   YOUT    -  007250
YPPT    -  007332   YRL     -  007035    YS      -  007303   YT      -  007255
YTEST   -  007331   Y1      -  007176    Y2      -  007316   Y3      -  007317
Y4      -  007320   Y5      -  007321    Y6      -  007322   Y7      -  007323
Y8      -  007324   Y9      -  007325    ZK      -  007313

START OF CONSTANTS
002562

START OF TEMPORARIES
003100

START OF INDIRECTS
003166

UNUSED COMPILER SPACE
062200
```

```
RUN VERSION 2.3 --PSR LEVEL 29A--

                 SUBROUTINE YDIS(Y,PS,RHO,U,N)                                        YIS   10
000010           DIMENSION Y(70),PS(70),RHO(2,70),U(2,70)                             YIS   30
000010           COMMON NP,SQP,NPP,NL                                                 YIS   40
000010           Y(1)=0.0                                                             YIS   50
000011           DO 500 I=2,N                                                         YIS   60
000012           Z=(2.*FLOAT(NP))/(RHO(2,I-1)*U(2,I-1)+RHO(2,I)*U(2,I))               YIS   70
000023           ZY=Y(I-1)**(NP+NPP) + Z*(PS(I)*PS(I)-PS(I-1)*PS(I-1))                YIS   80
000040       500 Y(I) = ZY**SQP                                                       YIS   90
000050           RETURN                                                               YIS  100
000050           END                                                                  YIS  110


RUN VERSION 2.3 --PSR LEVEL 29A--                       YDIS

YDIS

SUBPROGRAM LENGTH
000106

FUNCTION ASSIGNMENTS

STATEMENT ASSIGNMENTS

BLOCK NAMES AND LENGTHS
       - 000004

VARIABLE ASSIGNMENTS
I      - 000103    NP    - 000000C01 NPP    - 000002C01 SQP    - 000001C01
Z      - 000104    ZY    - 000105

START OF CONSTANTS
000052

START OF TEMPORARIES
000054

START OF INDIRECTS
000073

UNUSED COMPILER SPACE
073300
```

```
RUN VERSION 2.3 --PSR LEVEL 298--

                SUBROUTINE CALC (A,B,C,D,H,J)
          C
          C                          AS PER     MAY 19          1971
          C
          C     *    *    *    THIS EVALUATES RESULTS USING THOMAS ALGORITHM    *
000011          DIMENSION A(70 ),B(70 ),C(70 ),D(70 ),H(70 ),W(70 ),Q(70 ),G(70 )
000011          N2=J-2
000012          N1=J-1
000014          W(1)=A(1)
000015          G(1)=D(1)/W(1)
000017          DO 1 K=2,N2
000020          K1=K-1
000021          Q(K1)=B(K1)/W(K1)
000025          W(K)=A(K)-C(K)*Q(K1)
000031        1 G(K)=(D(K)-C(K)*G(K1))/W(K)
000043          H(N2)=G(N2)
000044          N3=J-3
000046          DO 2 K=1,N3
000050          KK=N2-K
000051        2 H(KK)=G(KK)-Q(KK)*H(KK+1)
000062          RETURN
000062          END
```

```
RUN VERSION 2.3 --PSR LEVEL 298--                      CALC

CALC

SUBPROGRAM LENGTH
000437

FUNCTION ASSIGNMENTS

STATEMENT ASSIGNMENTS

BLOCK NAMES AND LENGTHS

VARIABLE ASSIGNMENTS
G     = 000323   K     = 000433   KK    = 000436   K1    = 000434
N1    = 000432   N2    = 000431   N3    = 000435   Q     = 000215
W     = 000107

START OF CONSTANTS
000064

START OF TEMPORARIES
000065

START OF INDIRECTS
000071

UNUSED COMPILER SPACE
073200
```

```
RUN VERSION 2.3 --PSR LEVEL 298--

                SUBROUTINE PROF(U,T,NJ,N,UJR,TJR,KJ,UCLI)
          C     VERSION FOR  SINGLE STREAM FLOW WITH A WALL BOUNDARY LAYER IF KJ=1
          C     VERSION FOR TWO STREAM FLOW (TOP-HAT PROFILE ) OR SINGLE
          C     STREAM FLOW WITHOUT A BOUNDARY LAYER IF KJ=2
          C
000013          DIMENSION U(2,70),T(2,70)
000013          IF(KJ.EQ.1)GO TO 12
000015          DO 10 I=1,N
000016          IF(I.GT.NJ )GO TO 5
000021          U(1,I)=1.0
000023          T(1,I)=0.0
000024          GO TO 10
000025        5 U(1,I)=UJR
000030          T(1,I)=TJR
000031       10 CONTINUE
000034          GO TO 8
000034       12 READ(5,13)(U(1,I),I=1,N)
000054       13 FORMAT(6E13.6)
000054          DO 15 I=1,N
000061       15 T(1,I)=0.0
000065        8 DO 20 I=1,N
000067          U(2,I)=U(1,I)
000073       20 T(2,I)=T(1,I)
000077          U(1,N)=0.0
000100          U(2,N)=0.0
000102          RETURN
000102          END

RUN VERSION 2.3 --PSR LEVEL 298--                              PROF

PROF

SUBPROGRAM LENGTH
000124

FUNCTION ASSIGNMENTS

STATEMENT ASSIGNMENTS
5      -  000025    8      -  000065    10     -  000031    12     -  000034
13     -  000107    15     -  000061

BLOCK NAMES AND LENGTHS

VARIABLE ASSIGNMENTS
I      -  000123    KJ     -  000000    UCLI   -  000001

START OF CONSTANTS
000104

START OF TEMPORARIES
000111

START OF INDIRECTS
000115

UNUSED COMPILER SPACE
073100
```

```
RUN VERSION 2.3 --PSR LEVEL 298--

                  SUBROUTINE PSI( N, PSN,NJ,PS,PSNJ)
            C
000010            DIMENSION PS(70)
            C      JN +1 IS THE NUMBER OF NODE POINTS  IN JET
000010            JN = 11
000010             NJ= JN+1
000012             PS(1) =0.0
000013             DO 30 I = 2,NJ
000015             PS(I) = PSNJ/2.*(1.-COS(3.1416/FLOAT(JN)*FLOAT(I-1)))
000032      30     CONTINUE
000034             FS = 0.1*(PSN-PSNJ)
000036             J =NJ+1
000040             K= NJ+JN
000042              DO 40 I = J,K
000044             PS(I) =PS( NJ) + FS*(1.-COS(3.1416/(2.*JN)*FLOAT(I-NJ)))
000063      40     CONTINUE
000065             DELPS =.85*(PSN-PSNJ)/FLOAT(N-K-18)
000071             J =K+1
000073             K = N-18
000075              DO 50 I = J,K
000077             PS(I) =PS(I-1) +DELPS
000102      50     CONTINUE
000105            FSA=.05*(PSN-PSNJ)
000107             J = K+1
000111             READ(5,200)  (PS(I),I=J,N)
000130     200     FORMAT(6E13.6)
000130             DO 60 I = J,N
000135             PS(I) = PS(K) + FSA*PS(I)
000141      60     CONTINUE
000143             DO 101 I=1,N
000145             PS(I) = SQRT(PS(I))
000155     101     CONTINUE
000160            RETURN
000160            END
```

```
RUN VERSION 2.3 --PSR LEVEL 298--                          PSI

PSI

SUBPROGRAM LENGTH
000226

FUNCTION ASSIGNMENTS

STATEMENT ASSIGNMENTS
200     -  000174

BLOCK NAMES AND LENGTHS

VARIABLE ASSIGNMENTS
DELPS  -  000224    FS     -  000221    FSA    -  000225    I      -  000220
J      -  000222    JN     -  000217    K      -  000223

START OF CONSTANTS
000162

START OF TEMPORARIES
000176

START OF INDIRECTS
000215

UNUSED COMPILER SPACE
072700
```

```
RUN VERSION 2.3 --PSR LEVEL 298--

                    SUBROUTINE RADIUS(X,YOUT,KZ,REN)
            C                     AS PER     MAY 19           1971
000007              DIMENSION RR(25),XX(25)
000007              GO TO(1,2),KZ
000014            1 READ(5,6)NS
000022            6 FORMAT(I2)
000022              READ(5,3)(RR(I),I=1,NS)
000035              READ(5,3)(XX(I),I=1,NS)
000050          3    FORMAT(8F10.0)
000050               WRITE(6,20)
000054          20  FORMAT(//,25X,*DUCT GEOMETRY*,//,5X,*DUCT DIAMETER OR HEIGHT
                   1     DISTANCE FROM NOZZLE EXIT (IN)*,//)
000054               DO 25  I= 1,NS
            C .      THE FOLLOWING CARD IS INSERT IF HALF WIDTH OF THE DUCT IS USED
000060               RR(I) =RR(I)*2.
000062               WRITE(6,7) RR(I),XX(I)
000072          7    FORMAT(10X,F10.5,25X,F10.5)
000072         25    CONTINUE
000077              DO 4 I=1,NS
000101              RR(I)=RR(I)*REN
000103            4 XX(I)=XX(I)*REN*2.
000107              I=1
000110            2 IF(X.GT.XX(NS))GO TO 5
000114              IF(X.GT.XX(I+1))I=I+1
000120              YOUT=RR(I)+(X-XX(I))*(RR(I+1)-RR(I))/(XX(I+1)-XX(I))
000131            5 RETURN
000132              END


RUN VERSION 2.3 --PSR LEVEL 298--                          RADIUS


RADIUS

SUBPROGRAM LENGTH
000266

FUNCTION ASSIGNMENTS

STATEMENT ASSIGNMENTS
1       -  000014    2      -  000110    3      -  000140    5      -  000131
6       -  000136    7      -  000160    20     -  000143

BLOCK NAMES AND LENGTHS

VARIABLE ASSIGNMENTS
I       -  000265    NS     -  000264    RR     -  000202    XX     -  000233

START OF CONSTANTS
000134

START OF TEMPORARIES
000164

START OF INDIRECTS
000174

UNUSED COMPILER SPACE
073000
```

```
RUN VERSION 2.3 --PSR LEVEL 29A--

                 SUBROUTINE CHECK(Y,E,U,RHO,YT,FDUCT,TTP,TTT,NN,UCLI,UJR)
000014            COMMON NP,SUP,NPP,NL
000016           DIMENSION Y(70),E(70),U(2,70),RHO(2,70),TTP(70),TTT(70)
000016           ENERG=0.
000017           TFLOW=0.
000020           VISCIN=0.
000021           DEL2=0.
000022           DO 3471 J=1,NN
000023           JP1=J+1
000025           TFLOW =TFLOW + (Y(JP1)**(NP+NPP) -Y(J)**(NP+NPP))
                1*(RHO(2,JP1)+RHO(2,J))
                2*(U(2,JP1)+U(2,J))/4.
000056           VISCIN=VISCIN+(Y(JP1)+Y(J))*(E(JP1)+E(J))*(U(2,JP1)-U(2,J))
                1/(TTP(J+1)+TTP(J))/2.
000102           DEL2=DEL2+(U(2,JP1)+U(2,J))*(Y(JP1)**(NP+NPP)-Y(J)**(NP+NPP))
                1*((U(2,JP1)+U(2,J))*(.5/UJR)-1.)*.5/UJR
000134           ENERG=ENERG+(TTT(J)+TTT(JP1))*(Y(JP1)**(NP+NPP)-Y(J)**(NP+NPP))
                1*(U(2,JP1)+U(2,J))*(RHO(2,JP1)+RHO(2,J))/8.
000172      3471 CONTINUE
000175           IF (NP .EQ. 0) GO TO 219
000176           ENERG=ENERG/(FDUCT*YT**2)
000200           TFLOW=TFLOW/(FDUCT*YT**2)
000201           GO TO 319
000202       219 CONTINUE
000202           PSN = FDUCT
000203           ENERG=ENERG/PSN
000205           TFLOW=TFLOW/PSN
000206       319 CONTINUE
000206           VISCIN=VISCIN*.000158**2
000210           DEL2=DEL2 **.5*.000158/UCLI
000216           WRITE(6,3472)ENERG,TFLOW,VISCIN,DEL2
000232      3472 FORMAT(/,6X,*TO-F  = *,E14.6,6X,*TOTAL FLOW = *,E14.6,
                16X,*VISCIN=*,E14.6,2X,*DEL2=*,E14.6)
000232           RETURN
000233           END
```

```
RUN VERSION 2.3 --PSR LEVEL 29A--                       CHECK

CHECK

SUBPROGRAM LENGTH
000405

FUNCTION ASSIGNMENTS

STATEMENT ASSIGNMENTS
219    -  000202    319    -  000206    3472    -  000245

BLOCK NAMES AND LENGTHS
       -  000004

VARIABLE ASSIGNMENTS
DEL2   -  000401    ENERG  -  000376    J      -  000402    JP1    -  000403
NN     -  000002    NP     -  000000C01 NPP    -  000002C01 PSN    -  000404
TFLOW  -  000377    TTP    -  000000    TTT    -  000001    UCLI   -  000003
UJR    -  000004    VISCIN -  000400

START OF CONSTANTS
000235

START OF TEMPORARIES
000260

START OF INDIRECTS
000344

UNUSED COMPILER SPACE
072500
```

```
RUN VERSION 2.3 --PSR LEVEL 298--

                SUBROUTINE BLCHEK(N,U,PS,Y,DX     ,DP2,UCLI,BBB,TOLD ,URR,RHO,AA)
000017           DIMENSION U(2,70),PS(70), DUX(70),RHO(2,70) ,AA(70),Y(70),BBB(70)
               * ,TOLD(2)
000017          COMMON NP,SQP,NPP,NL
000017          DO 1 J = 1,N
000020          DUX(J) = (U(2,J)-U(1,J))/DX
000034     1    CONTINUE
000037            AA(1) = 0.
000041          DO 2 J= 2, N
000042          JM1 = J-1
000044          AA(J)=AA(J-1)+(DUX(J)*PS(J)+DUX(JM1)*PS(JM1))*(PS(J)-PS(JM1))
000061          BBB(J) =DP2    *Y(J)**(NP+NPP)/(2.*FLOAT(NP+NPP))
000075     2    CONTINUE
000100          B=-RHO(2,1)*( TOLD(2) +TOLD(1)       ) **2*Y(N)**NL*.25
000114          AOB=BBB(N)/(B-AA(N))
000121           BC = B-AA(N)
000124           WRITE(6,40)  BC,BBB(N),AOB
000142    40     FORMAT(/,10X,*FLUID FORCES = *,E13.6,*       PRESS. FORCES  = *,
               1 E13.6,*        RATIO OF THESE TWO = *,E13.6,/)
000142   100    RETURN
000143          END


RUN VERSION 2.3 --PSR LEVEL 298--                                 BLCHEK


BLCHEK

SUBPROGRAM LENGTH
000342

FUNCTION ASSIGNMENTS

STATEMENT ASSIGNMENTS
40      -  000151    100     -  000142

BLOCK NAMES AND LENGTHS
        -  000004

VARIABLE ASSIGNMENTS
AA      -  000005    AOB     -  000340    B       -  000337    BBB     -  000001
BC      -  000341    DUX     -  000227    J       -  000335    JM1     -  000336
NL      -  000003C01 NP      -  000000C01 NPP     -  000002C01 RHO     -  000004
TOLD    -  000002    UCLI    -  000000    URR     -  000003

START OF CONSTANTS
000145

START OF TEMPORARIES
000165

START OF INDIRECTS
000210

UNUSED COMPILER SPACE
072700
```

```
              SUBROUTINE LOOK(JJK,NN,U,Y,DELTA,BH,BY,N,CC,IFLOW,XBLEND,YJ,BE)
        C
        C     FOR EJECTOR FLOW  AS PER FEB. 19
        C
000020        DIMENSION U(2,70),Y(70)
        C     SEARCH FOR INFLECTION POINT
000020        DO 770 J=JJK,NN
000021        M=J+1
000023        K=J+2
000025        DZ=(U(1,J)-U(1,M))/(Y(J)-Y(M))-(U(1,M)-U(1,K))/(Y(M)-Y(K))
000044        IF(DZ.GT.0.)GO TO 771
000046    770 CONTINUE
000050    771 IF(DZ.LT.0.)GO TO 776
        C     NO INFLECTION POINT
000052        JJ=N-M -1
000055        UPOT=U(1,M)
000057        IF(Y(M).LE.BY)GO TO 776
000062        BELTA=Y(N)-DELTA
000065        IF(Y(M).GE. BELTA)GO TO 776
        C     SEARCH FOR SHEAR LAYER OUTER EDGE
000070        MY=M-1
000072        DO 1319 I=1,MY
000073        UTY=(U(1,M-I)-UPOT)/(U(1,1)-UPOT)
000103        IF(UTY.GT..003)GO TO 1320
000106   1319 CONTINUE
000110   1320 MP=M-I+1
000113        JJK=MP
000114        BY=(Y(MP-1)-Y(MP))*(.003*(U(1,1)-UPOT)-
             1U(1,MP-1)+UPOT)/(U(1,MP-1)-U(1,MP))+Y(MP-1)
        C     SEARCH FOR SHEAR LAYER INNER EDGE
000133        DO 772 I=3,M
000134        UTT=(U(1,1)-U(1,I))/(U(1,1)-UPOT)
000140        IF(UTT.GT..003)GO TO 773
000144    772 CONTINUE
000146    773 BE=Y(I-1)+(Y(I)-Y(I-1))*(U(1,1)-U(1,I-1)-
             1.003*(U(1,1)-UPOT))/(U(1,I)-U(1,I-1))
000166        IF(I.EQ.3)BE=0.
000171        BFRAC=BE/YJ
000173        IF(BFRAC.LE..050) CC=.108
000177        BH=BY-BE
        C     SEARCH FOR EDGE OF WALL BOUNDARY LAYER
000202        DO 774 I=1,JJ
000203        UKK=(UPOT-U(1,M+I))/UPOT
000211        IF(UKK.GT..010)GO TO 775
000214    774 CONTINUE
000216    775 KI=M+I-1
000221        BELTA=Y(KI)-(Y(KI+1)-Y(KI))*(U(1,KI)-.990*
             1UPOT)/(U(1,KI+1)-U(1,KI))
000236        IF(BY.GE.BELTA)GO TO 776
000240        DELTA=Y(N)-BELTA
000243        MZ=KI-MP
000245        IF(MZ.LE.1)GO TO 776
000247        GO TO 777
        C IFLOW=1 THERE IS NO INFLECTION POINT
```



```
000250    776 IFLOW=1
000252        XBLEND=0.
000253    777 RETURN
000254        END
```

```
RUN VERSION 2.3 --PSR LEVEL 298--                          LOOK


LOOK

SUBPROGRAM LENGTH
000325

FUNCTION ASSIGNMENTS

STATEMENT ASSIGNMENTS
771      -  000050    773      -  000146    775      -  000216    776      -  000250
777      -  000253    1320     -  000110

BLOCK NAMES AND LENGTHS

VARIABLE ASSIGNMENTS
BE       -  000006    BELTA    -  000313    BFRAC    -  000321    BY       -  000000
CC       -  000002    DZ       -  000310    I        -  000315    IFLOW    -  000003
J        -  000305    JJ       -  000311    K        -  000307    KI       -  000323
M        -  000306    MP       -  000317    MY       -  000314    MZ       -  000324
N        -  000001    UKK      -  000322    UPOT     -  000312    UTT      -  000320
UTY      -  000316    XBLEND   -  000004    YJ       -  000005

START OF CONSTANTS
000256

START OF TEMPORARIES
000264

START OF INDIRECTS
000277

UNUSED COMPILER SPACE
072400
```

REFERENCES

1. Hickman, K.E., Hill, P.G., and Gilbert, G. B.: "Analysis and Testing of Compressible Flow Ejectors with Variable Area Mixing Tubes," NASA CR-2067 and ASME Paper 72-FE-14.

2. Patankar, S.V., and Spalding, D.B.,: "Heat and Mass Transfer in Boundary Layers," Morgan-Grampian, London 1967,

3. Denny, V.E., and Landis, R.B.,: "An Improved Transformation of the Patankar-Spalding Type for Numerical Solution of Two-Dimensional Boundary Layer Flows," Int. J. Heat Mass Transfer, Vol. 14, pp. 1859-1862, Pergamon Press, 1971.

4. Schlichting, H.,: "Boundary Layer Theory," McGraw-Hill Book Company, Inc., New York, 1968,

5. Hedges, K.R., and Hill, P.G.,: "A Finite Difference Method for Compressible Jet Mixing in Converging-Diverging Ducts," Queen's University Thermal Sciences Report No.3/72, June 1, 1972, Department of Mechanical Engineering, Kingston, Ontario, Canada.

6. Hickman, K.E., Gilbert, G.B., and Carey, J.H.,: "Analytical and Experimental Investigation of High Entrainment Jet Pumps," NASA CR-1602, July 1970.

7. Kline, S.J., and McClintock, F.A.,: "Describing Uncertainties in Single Sample Experiments," Mechanical Engineering, 1953.

Table 1

Mixing Section Dimensions for 1.875" Throat Size

x Inches	±y Inches	x Inches	±y Inches	x Inches	±y Inches
-3.000		-0.937	1.960	1.062	1.280
-2.937	4.496	-0.875	1.922	1.125	1.268
-2.875	4.288	-0.812	1.886	1.187	1.256
-2.812	4.128	-0.750	1.850	1.250	1.244
-2.750	3.982	-0.687	1.814	1.312	1.234
-2.687	3.860	-0.625	1.782	1.375	1.222
-2.625	3.740	-0.562	1.746	1.437	1.210
-2.562	3.628	-0.500	1.715	1.500	1.200
-2.500	3.510	-0.437	1.688	1.562	1.192
-2.437	3.412	-0.375	1.658	1.625	1.182
-2.375	3.310	-0.312	1.632	1.687	1.174
-2.312	3.226	-0.250	1.608	1.750	1.162
-2.250	3.140	-0.187	1.586	1.812	1.154
-2.187	3.064	-0.125	1.562	1.875	1.146
-2.125	2.998	-0.062	1.540	1.937	1.138
-2.062	2.918	0.000*	1.519	2.000	1.130
-2.000	2.840	0.062	1.502	2.125	1.116
-1.937	2.778	0.125	1.486	2.250	1.100
-1.875	2.708	0.187	1.470	2.375	1.086
-1.812	2.646	0.250	1.452	2.500	1.077
-1.750	2.586	0.312	1.438	2.625	1.066
-1.687	2.520	0.375	1.422	2.750	1.058
-1.625	2.464	0.437	1.406	2.875	1.048
-1.562	2.404	0.500	1.394	3.000	1.042
-1.500	2.350	0.562	1.380	3.125	1.038
-1.437	2.296	0.625	1.366	3.250	1.034
-1.375	2.246	0.687	1.354	3.375	1.030
-1.312	2.196	0.750	1.340	3.500	1.024
-1.250	2.152	0.812	1.328	3.625	1.018
-1.187	2.110	0.875	1.318	3.750	1.014
-1.125	2.070	0.937	1.304	3.875	1.010
-1.062	2.030	1.000	1.288	4.000	1.007
-1.000	1.990			8.000	0.938
				11.000	0.938
				23.500	1.593

*Nozzle discharge plane at x = 0.000

Table 2

Variation of Individual Integrated
Traverse Mass Flows For Each Test Run

Run	Variation of Integrated Traverse Mass Flow Rate Around An Average Value	Number of Traverse Locations
1	+2.2%, -3.0%	4
2	+3.5%, -2.3%	5
3	+3.4%, -3.9%	9
5	+0%, -0%	3
6	+2.3%, -2.8%	4
7	+4.1%, -2.8%	5
9	+5.6%, -2.6%	5
10	+4.0%, -2.2%	5
11	+3.8%, -2.6%	5
Average w/o Run 5	+3.6%, -2.8%	

Table 3

Location of Test Data for Each Test Run

	Run 1	Run 2	Run 3	Run 4	Run 5	Run 6	Run 7	Run 8	Run 9	Run 10	Run 11
Test Conditions and Mass Flows	T4 → T5 F11	T5 F11	T5 F11	- -	T5 F11	T5 F12	T5 F12	- -	T5 F12	T5 F12	- -
Static Pressures	F13	F13	F13	T6	F13	F14	F14	T6	F14	F14	T6
Centerline Velocities and Temperatures	F15	F15	F15	-	F15	F16	F16	-	F16	F16	-
Velocity Profiles	F17	F18	F19a F19b	-	F20	F21	F22	-	F23a F23b	F24	-
Temperature Profiles	-	-	F25	-	-	-	-	-	F26	-	-
Eddy Viscosity Sensitivity	-	-	F27 F28 F29	-	-	F27 F28 F29	-	-	-	-	-
Flow Rate Sensitivity	-	-	F27	-	-	F27	-	-	-	-	-

T Stands for Table

F Stands for Figure

Table 4

Summary of Experimental Test Conditions and Flow Rates

Run No.	Nozzle Pressure psia	Nozzle Temp. °R	Nozzle Throat Area in²	Nozzle Throat Co-efficient	Baro-metric Pressure psia	Atmo-spheric Temp °R	Measure Nozzle Flow Rate lb/sec	Measure Nozzle Flow Rate lb/sec. in	Mixing Section Flow lb/sec in	Secondary Flow Rate lb/sec.in.	Flow Ratio	Mixing Section Throat Size	Mass-Momentum Stagnation Pressure at x = 10.5" psia
Symbol	p_N	T_N	A_N	C_N	p_b	T_a	–	W_N	W_m	W_s	W_s/W_N		
1	31.69	641	0.9688	0.9674	14.69	538	0.6240	0.0780	0.408	.330	4.23	1.25"	16.15
2	31.60	637		0.9645	14.60	543	0.6263	0.0782	0.341	.2627	3.36		16.19
3	31.61	706		0.978	14.61	553	0.5997	0.0750	0.357	.2820	3.76		15.91
4	35.61	659		0.978	14.61	553	0.6993	0.0874	0.396	.3086	3.53		-----
5	31.71	648		0.980	14.71	544	0.6293	0.0787	0.384	.3053	3.88		15.86
6	35.80	649		0.974	14.80	547	0.7056	0.0882	0.434	.3458	3.92	1.875"	16.23
7	35.80	647		0.974	14.80	543	0.7069	0.0884	0.458	.3696	4.18		16.20
8	31.80	642		0.968	14.80	543	0.6256	0.0782	0.424	.3458	4.42		-----
9	85.73	644		0.975	14.73	550	0.7072	0.0884	0.501	.4126	4.67		16.06
10	35.70	660		0.976	14.70	547	0.6993	0.0874	0.525	.4376	5.006		15.96
11	35.68	652		0.973	14.68	548	0.7006	0.0876	0.506	.4184	4.777		16.05

Table 5

Comparison of Experimental and Analytical Mass Flow Rates

Run No.	Throat Width (inches)	Mixing Section Mass Flow Rate From Traverse Data lb/sec. in. ①	Mixing Section Mass Flow Rate From Orifice Data lb/sec. in. ②	Percent Difference In Measured Data (① - ②)/①	Analytical Mass Flow For Best Static Pressure Match lb/sec. in. ③	Comparison Of Traverse To Analytical Mass Flow (① - ③)/①	Comparison Of Orifice To Analytical Mass Flow (② - ③)/②
1	1.25	0.408	--	--	0.382	+ 6.4%	--
2	↓	0.341	0.320	+ 6.7%	0.322	+ 5.6%	- .6%
3	↓	0.357	0.3535	+ 1.0%	0.351	+ 1.7%	+ .7%
5	↓	0.384*	--	--	0.395	- 2.9%	--
6	1.875	0.434	0.417	+ 4.0%	0.420	+ 3.2%	- .7%
7	↓	0.458	0.447	+ 2.5%	0.443	+ 3.3%	+ .9%
9	↓	0.501	--	--	0.485	+ 3.2%	--
10	↓	0.525	--	--	0.508	+ 3.2%	--

* Transducer Battery May Have Been Going Bad During This Test

Table 6

Tabulation of Static Pressures For

Runs 4, 8, and 11

Distance From Nozzle Discharge inches	Run No.	4	8	11
	Nozzle Pressure psia	35.61	31.80	35.68
	Throat Height	1.25"	1.875"	1.875"
	Wall Static Pressure in Inches of Water Gage			
-1.62		-8.05	-6.8	-10.4
-1.25		-11.2	-9.1	-13.7
-0.87		-13.7	-10.7	-16.3
-0.46		-17.1	-13.0	-19.5
+0.03		-19.5	-14.2	-21.5
+0.56		-19.5	-13.9	-20.9
+0.99		-20.7	-14.2	-21.5
+1.50		-21.5	-13.9	-22.4
+2.00		-28.0	-16.5	-26.6
+2.50		-32.2	-17.7	-28.6
+3.00		-35.7	-18.6	-30.1
+3.50		-37.5	-18.3	-30.1
+4.00		-39.5	-18.6	-31.0
+4.50		-40.7	-18.3	-31.3
+5.00		-41.9	-18.3	-31.6
+5.50		-42.7	-18.0	-31.9
+6.00		-43.1	-18.0	-32.5
+7.00		-48.7	-18.6	-33.6
+8.00		-54.3	-19.2	-35.4
+9.00		-55.8	-18.5	-35.4
+10.50		-58.1	-17.7	-35.1
+12.00		-42.2	-13.0	-28.6
+13.00		-30.1	-9.1	-23.3
+15.00		-13.2	-2.5	-15.1
+17.00		- 2.3	+2.2	- 8.3
+19.00		+ 4.9	+5.9	- 5.1
+21.00		+ 9.9	+8.6	+ 0.7
+23.00		+13.2	+10.9	+ 3.7

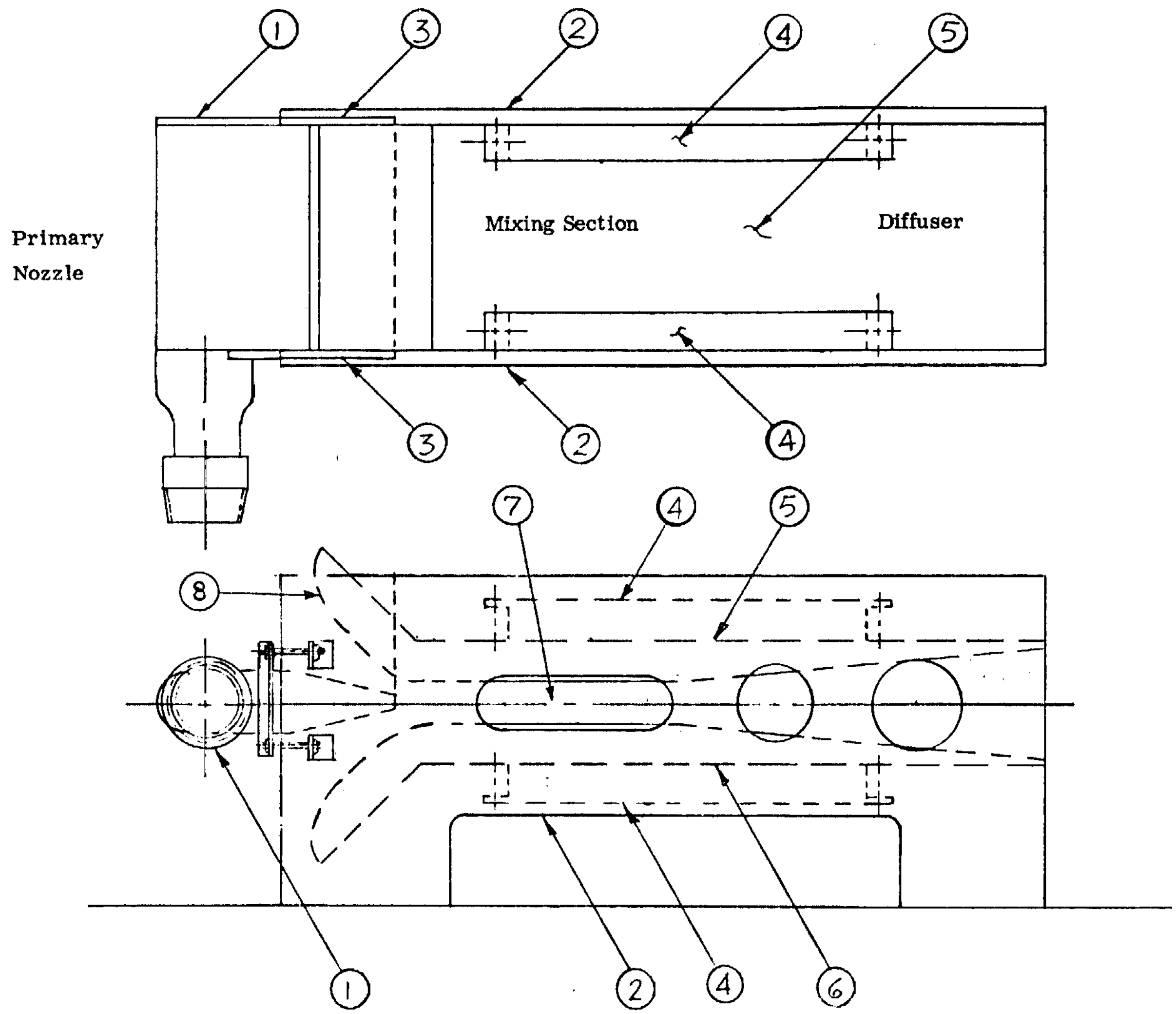

1 Primary Nozzle
2 Side Plates
3 Nozzle Holder
4 Suction Plenum
5 Upper Contoured Plate
6 Lower Contoured Plate
7 Plexiglass Windows
8 Inlet Bellmouth
9 Diffuser

Figure 1

Assembly Sketch of Two Dimensional Ejector Test Rig

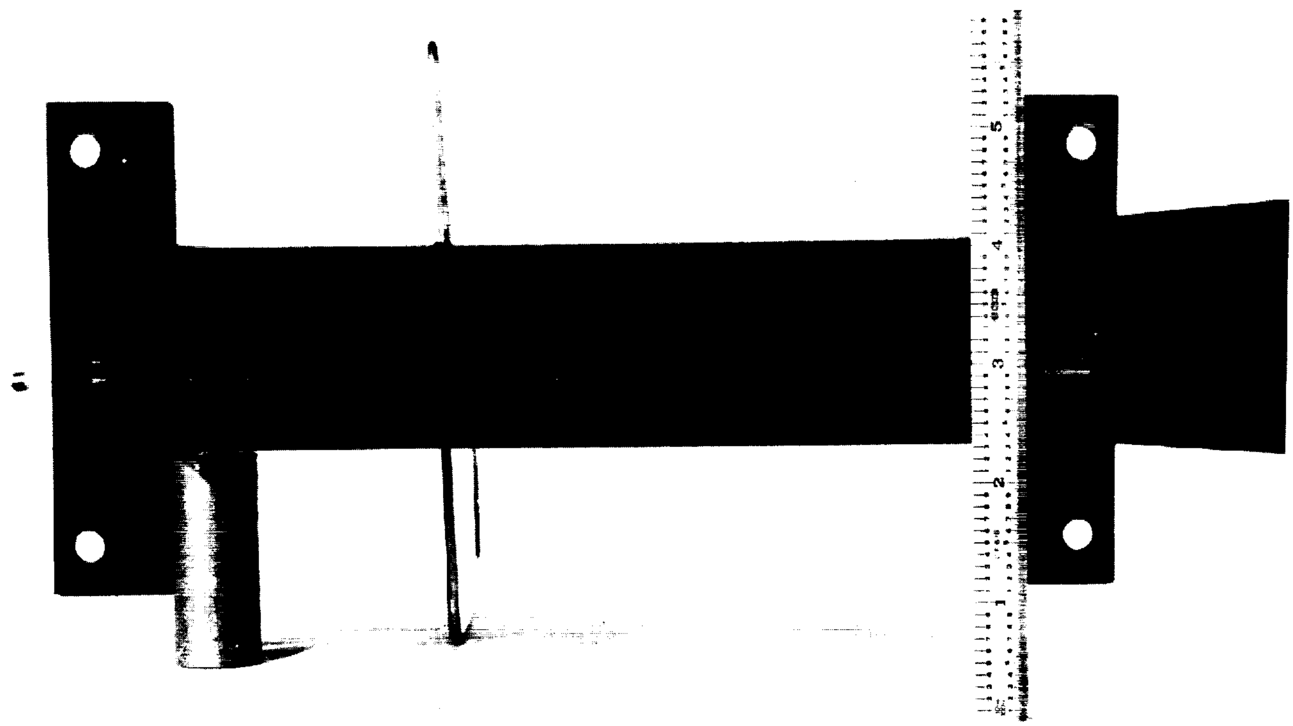

Figure 2

Picture of Primary Nozzle

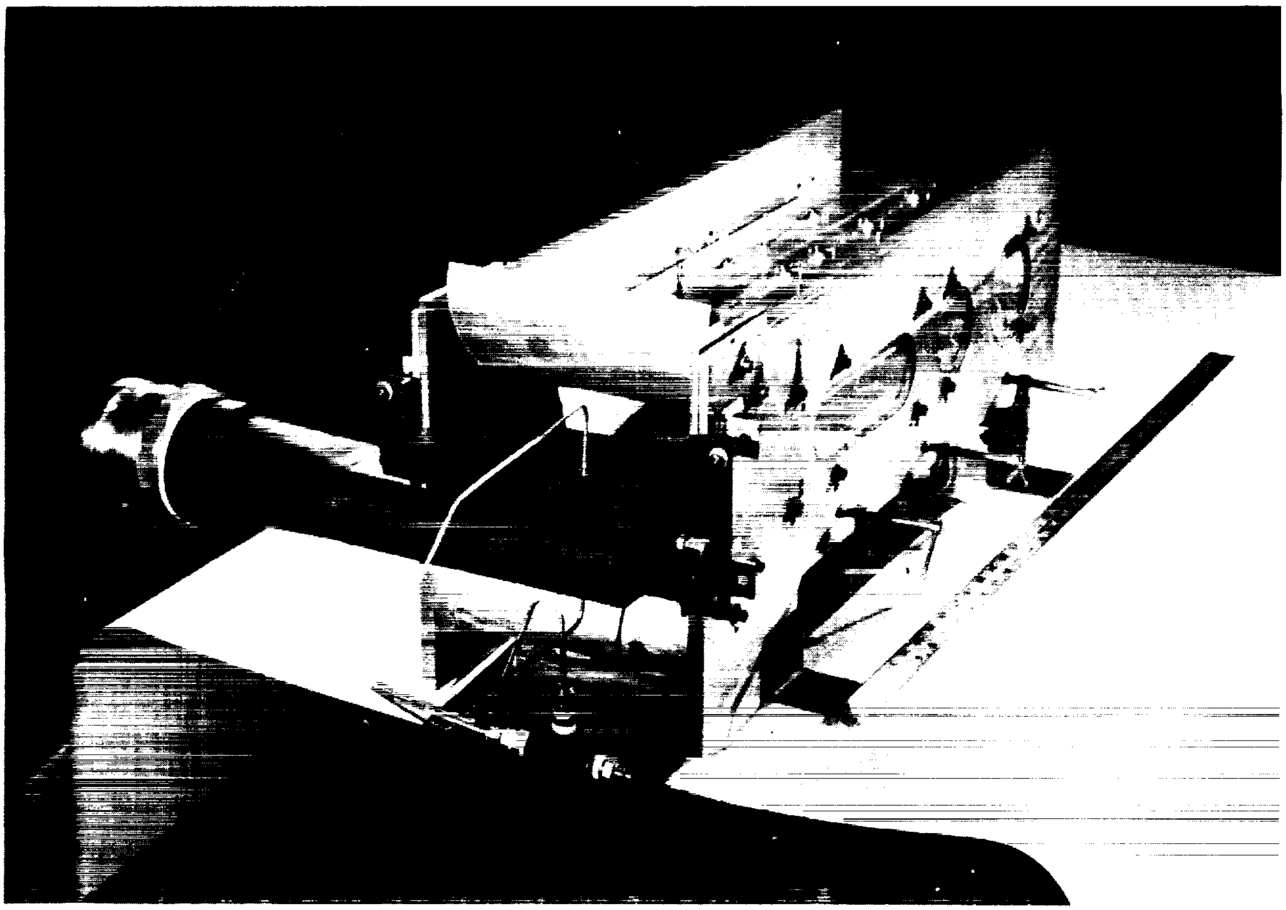

Figure 3

Picture of Nozzle Positioned in the Mixing Section

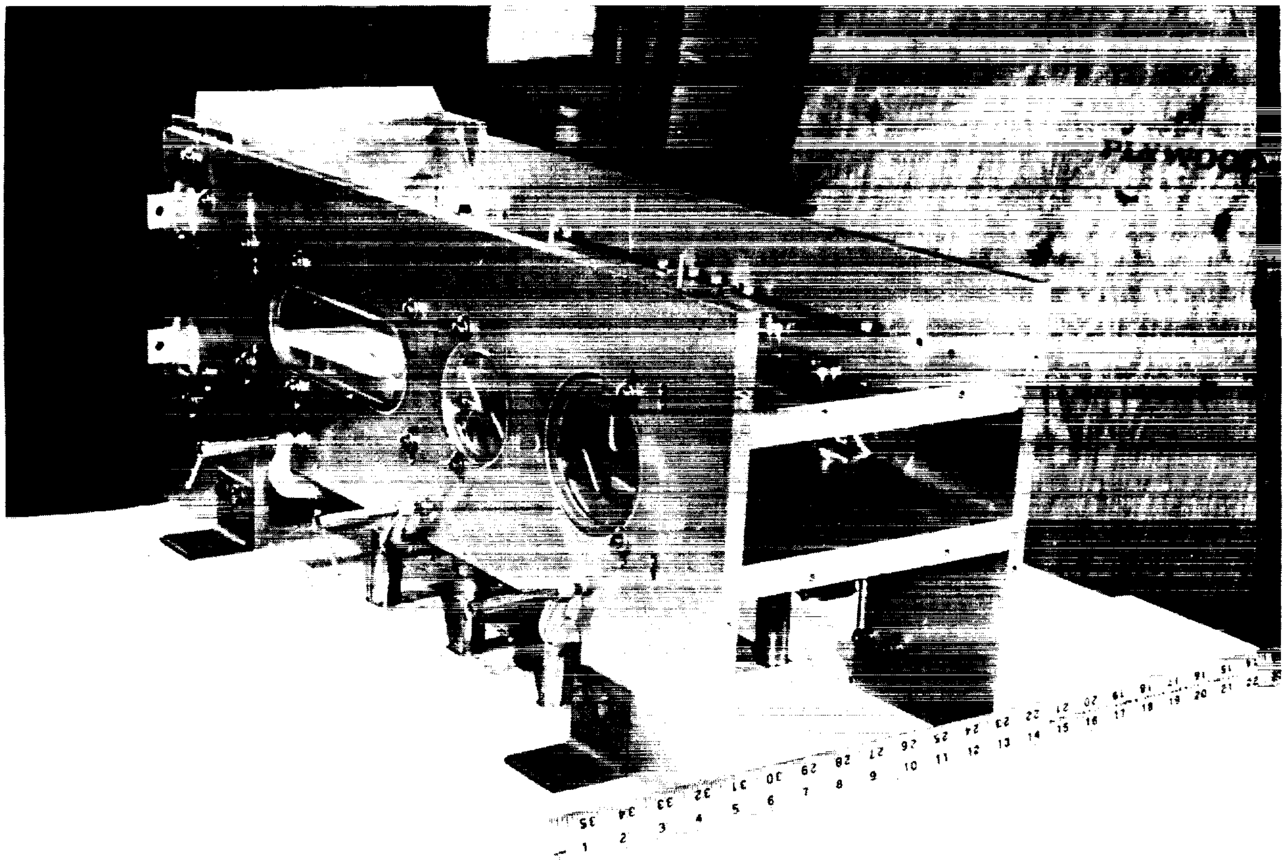

Figure 4

Picture of Mixing Section Discharge

1 Nozzle
2 Mixing Section Side Plate
3 Top-Contoured Plate
4 Bottom-Contoured Plate
5 Table Top
6 Screen
7 Solid Side Plates

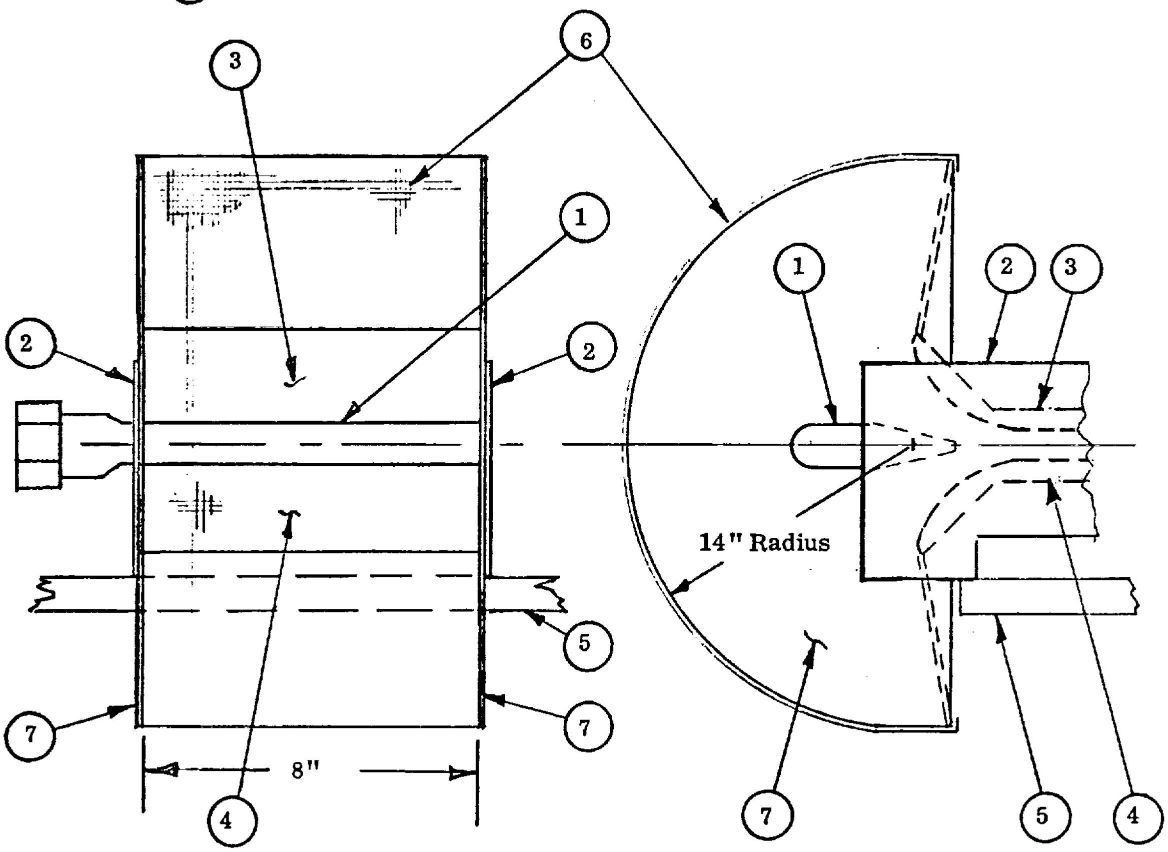

Figure 5

Extended Inlet on Ejector Test Rig

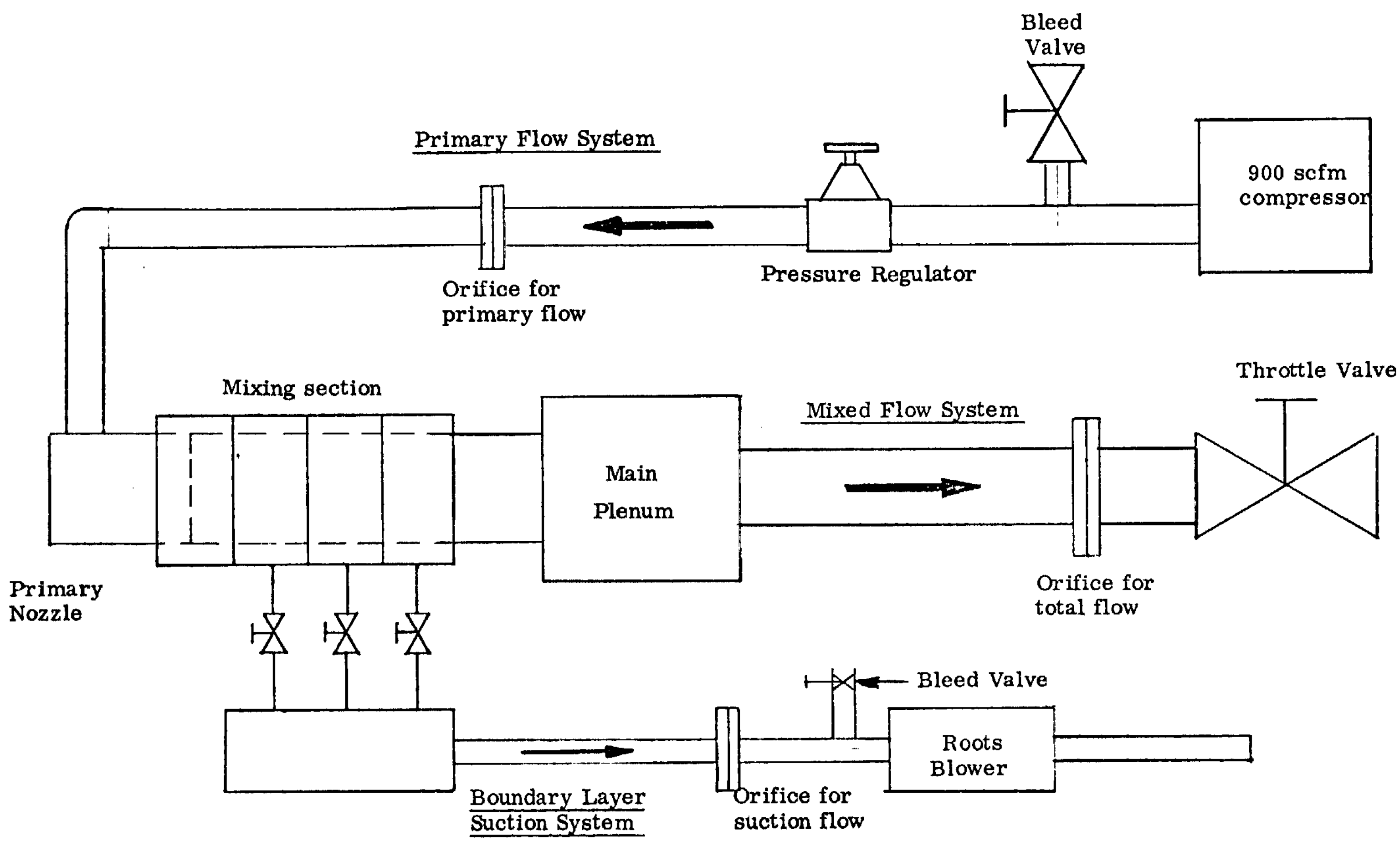

Figure 6

Schematic of Experimental Layout

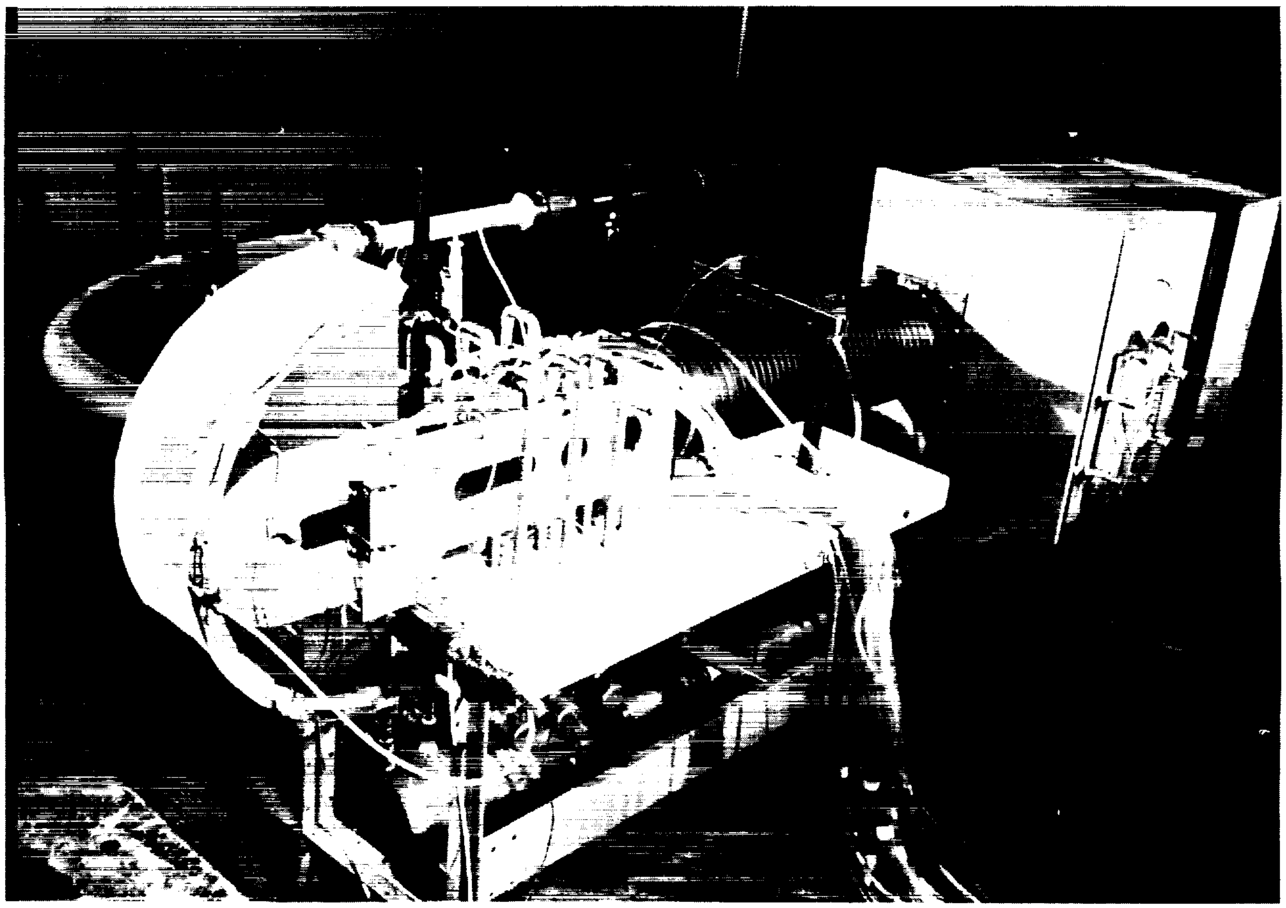

Figure 7

Picture of Right Side of Ejector Rig

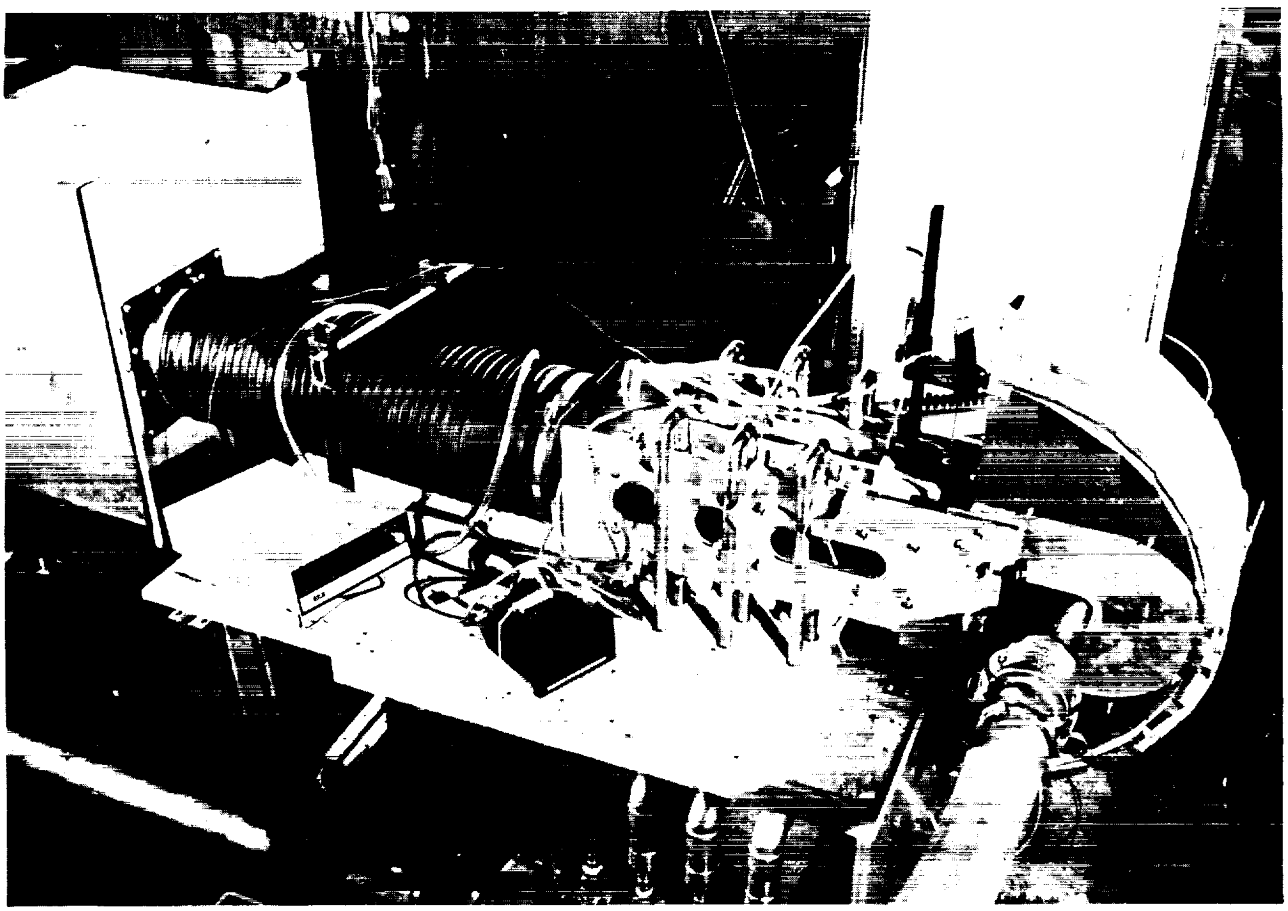

Figure 8

Picture of Left Side of Ejector Rig

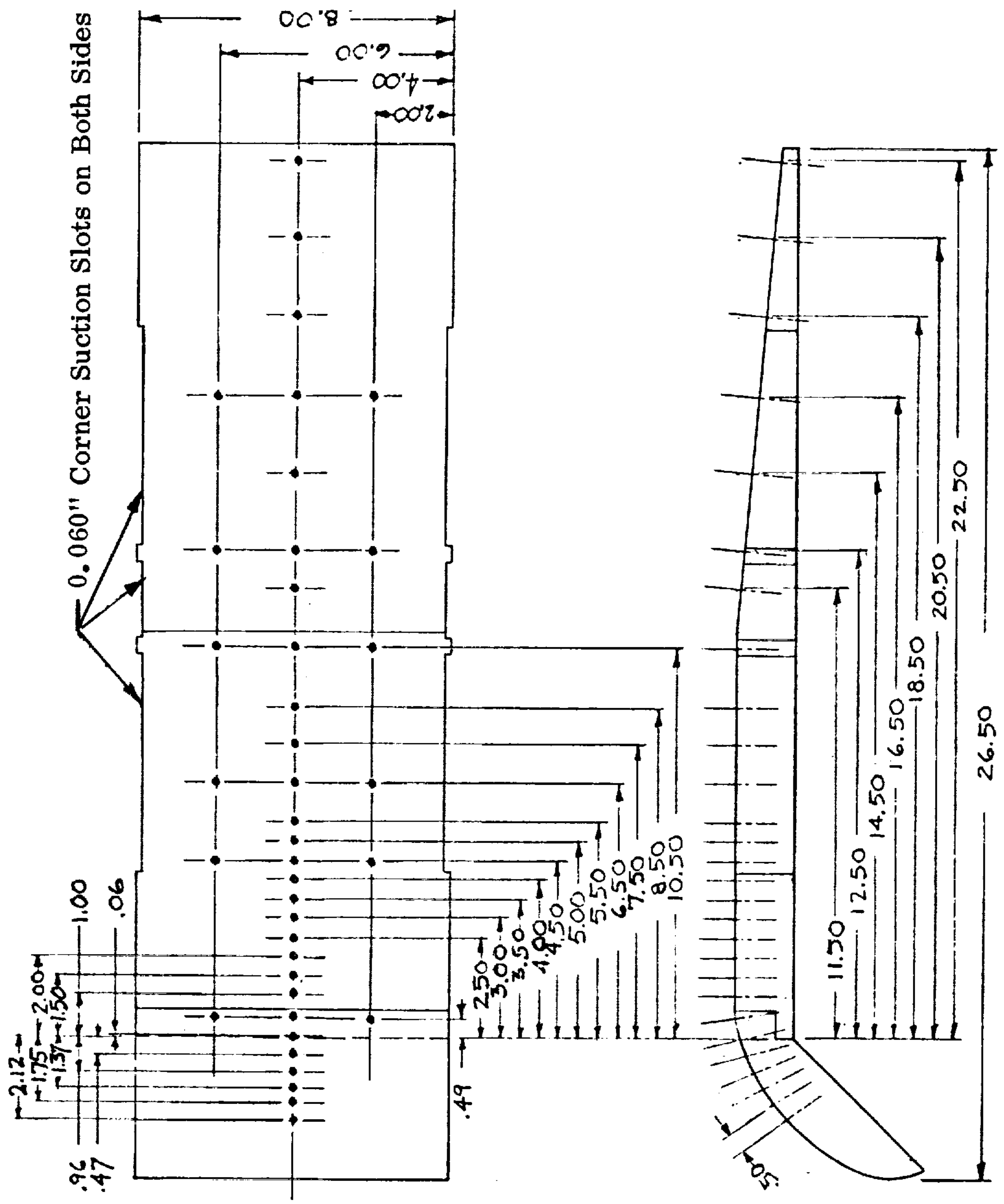

Figure 9

Mixing Section Static Pressures

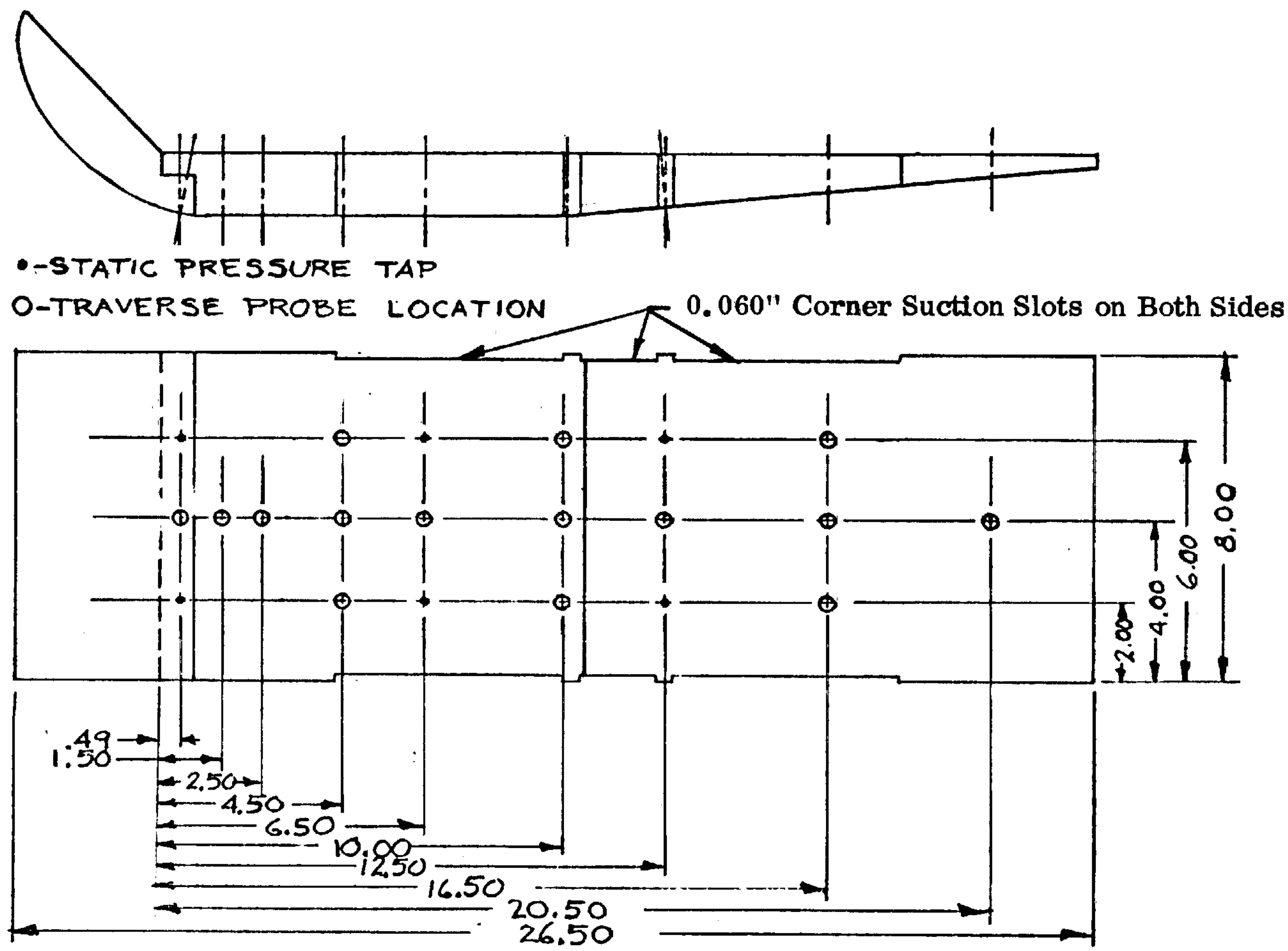

Figure 10

Mixing Section Traverse Locations

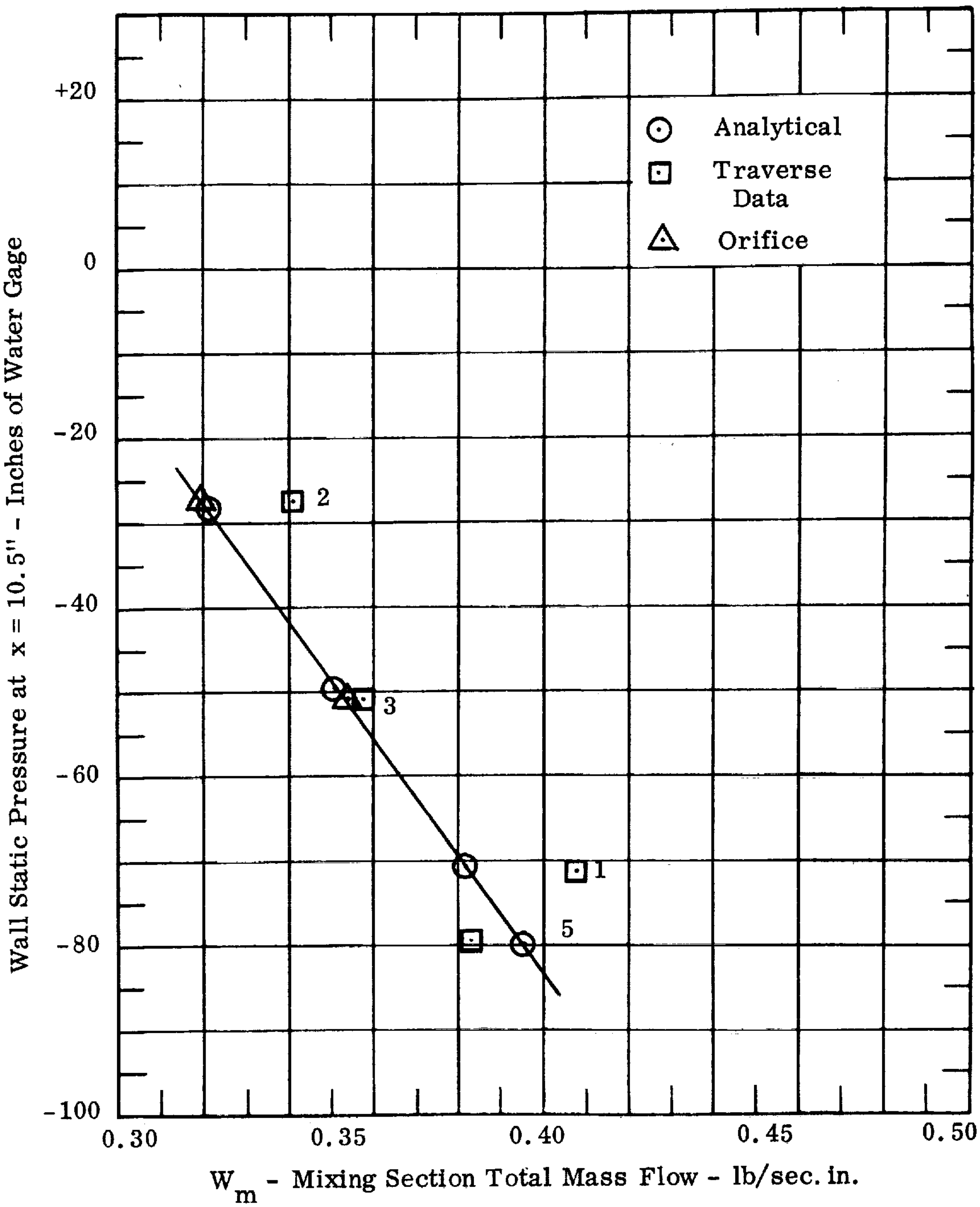

Figure 11 Comparison of Experimental and Analytical Mass Flow Rates for Runs 1, 2, 3 and 5

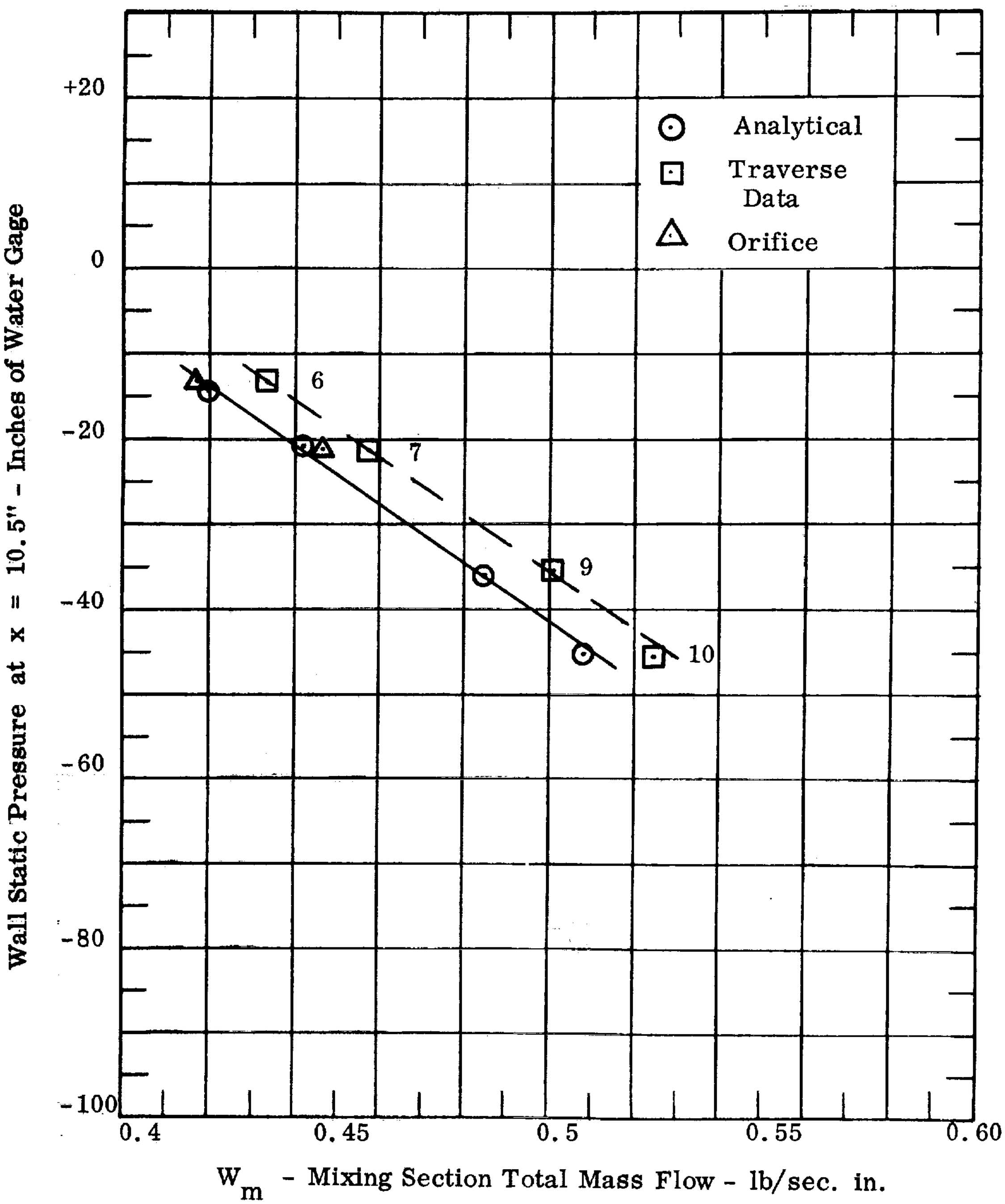

Figure 12 Comparison of Experimental and Analytical Mass Flow Rates for Runs 6, 7, 9, and 10

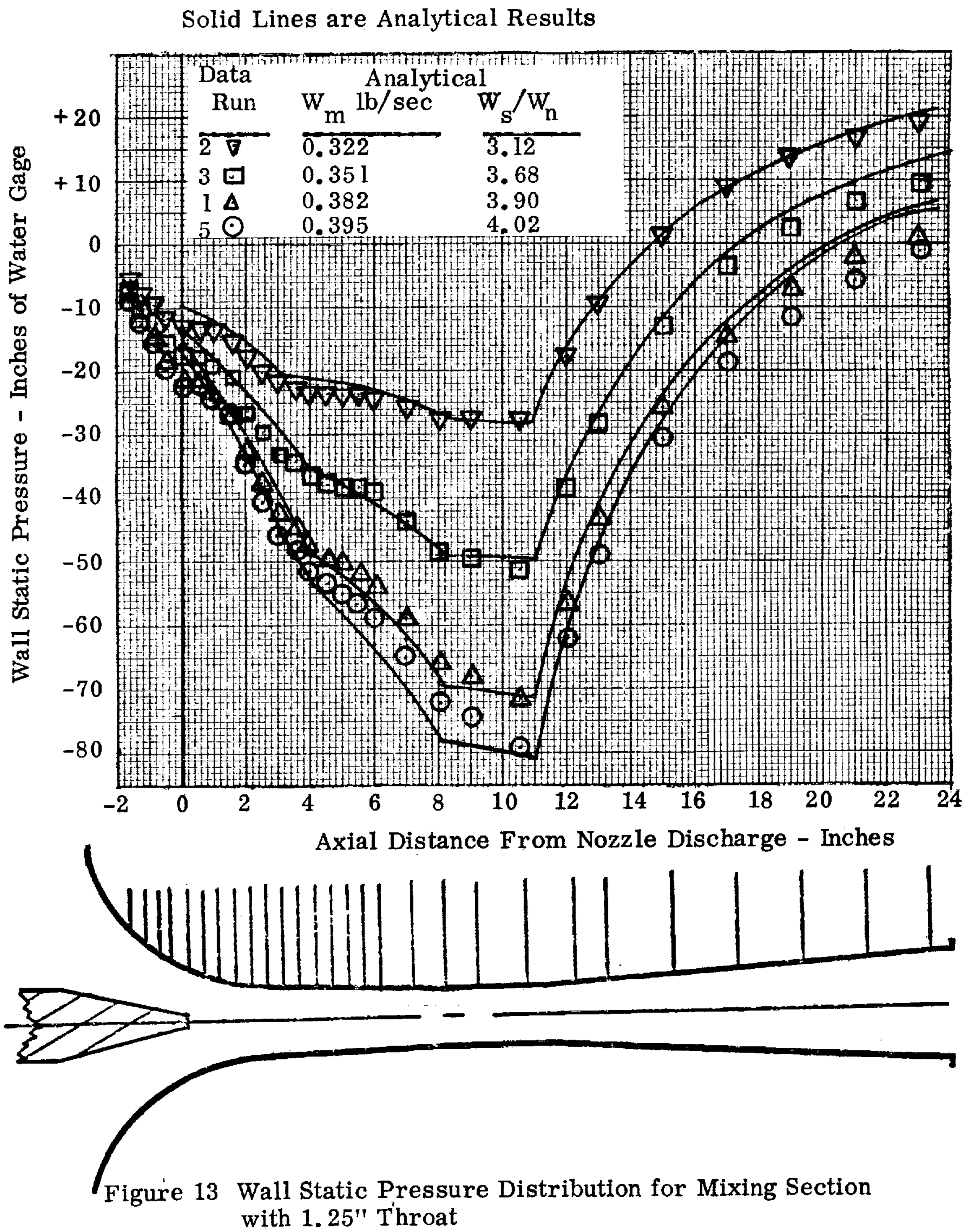

Figure 13 Wall Static Pressure Distribution for Mixing Section with 1.25" Throat

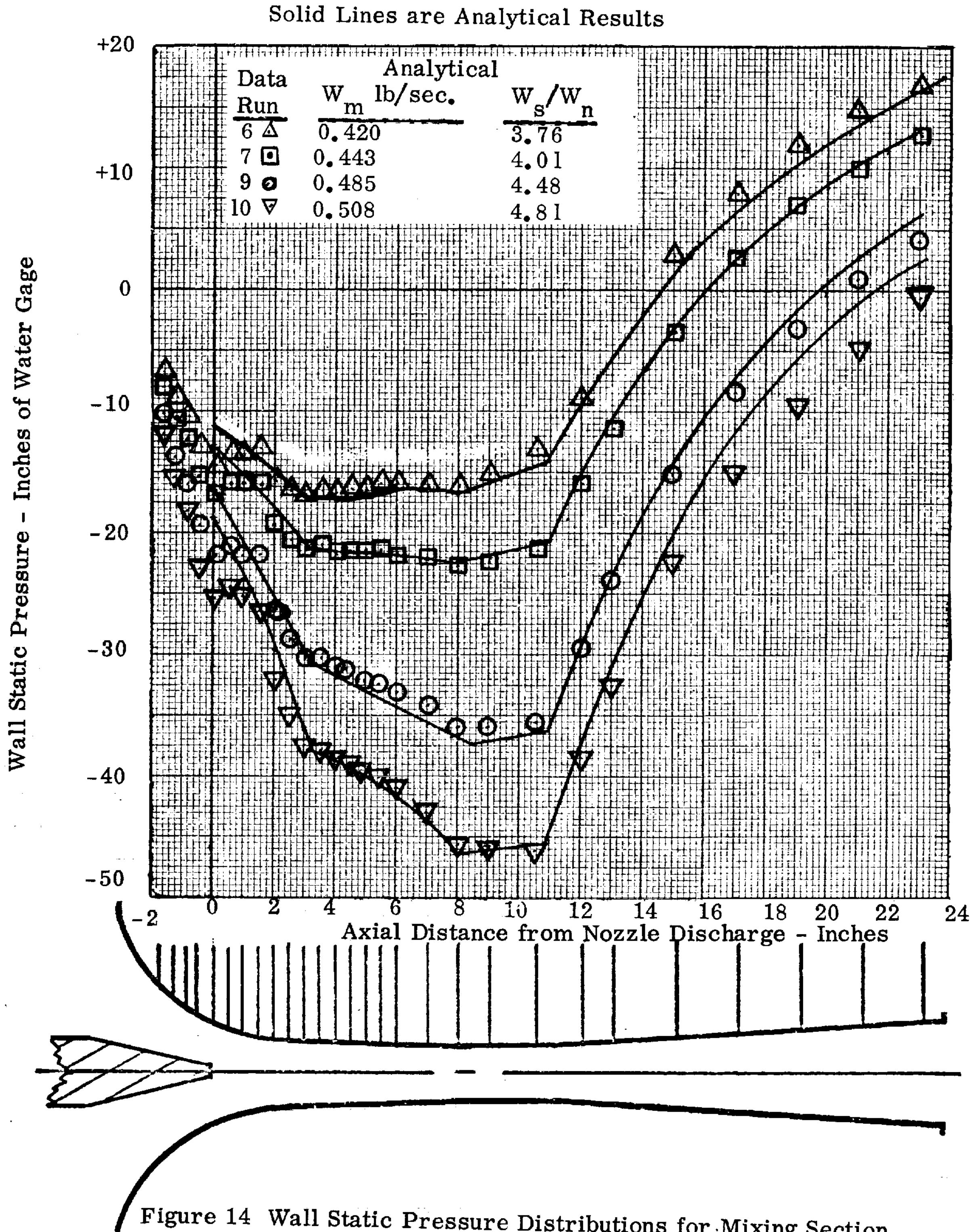

Figure 14 Wall Static Pressure Distributions for Mixing Section with 1.875" Throat

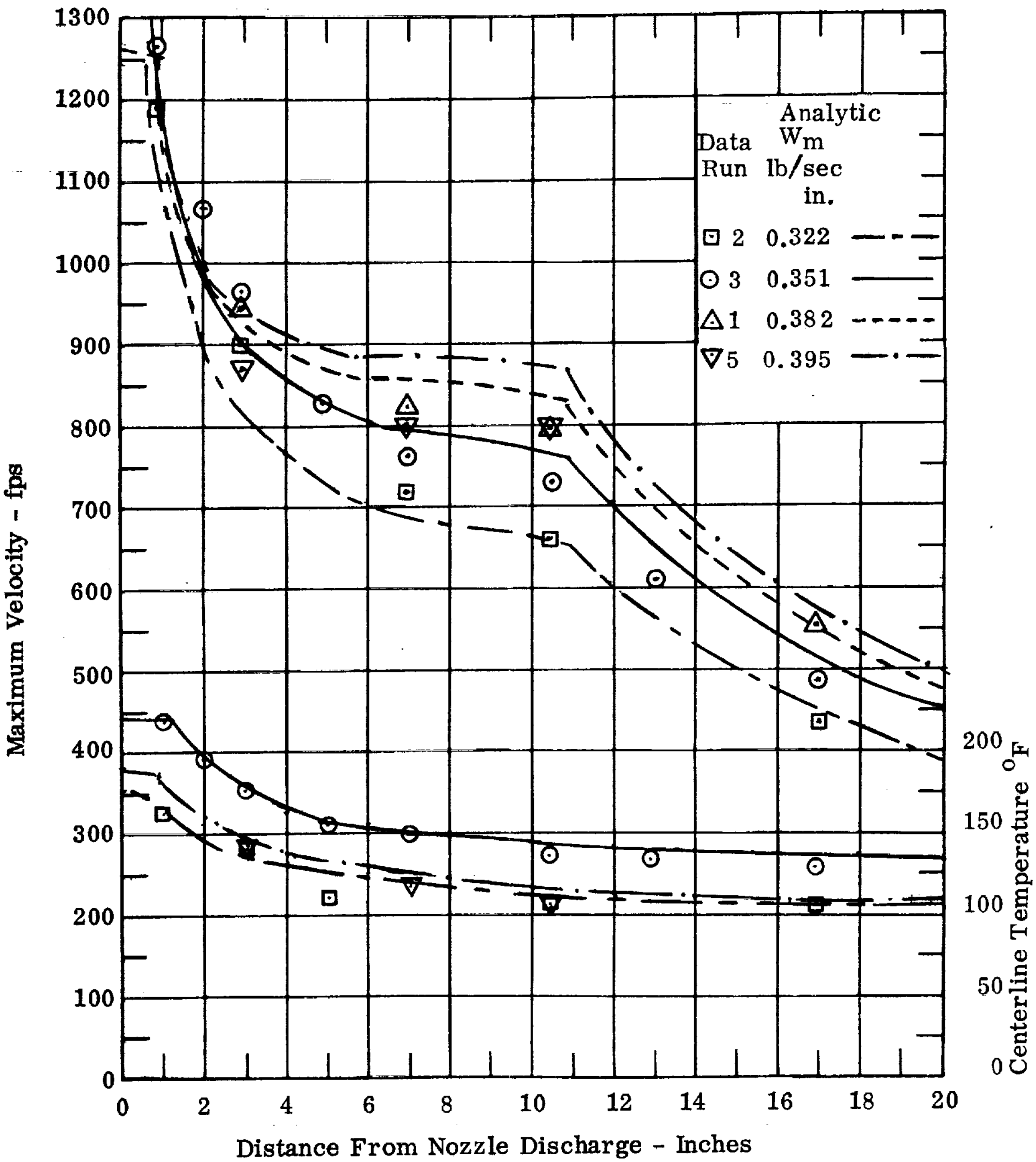

Figure 15 Maximum Velocities for 1.25" Throat Mixing Section

p_N = 17.0 psig

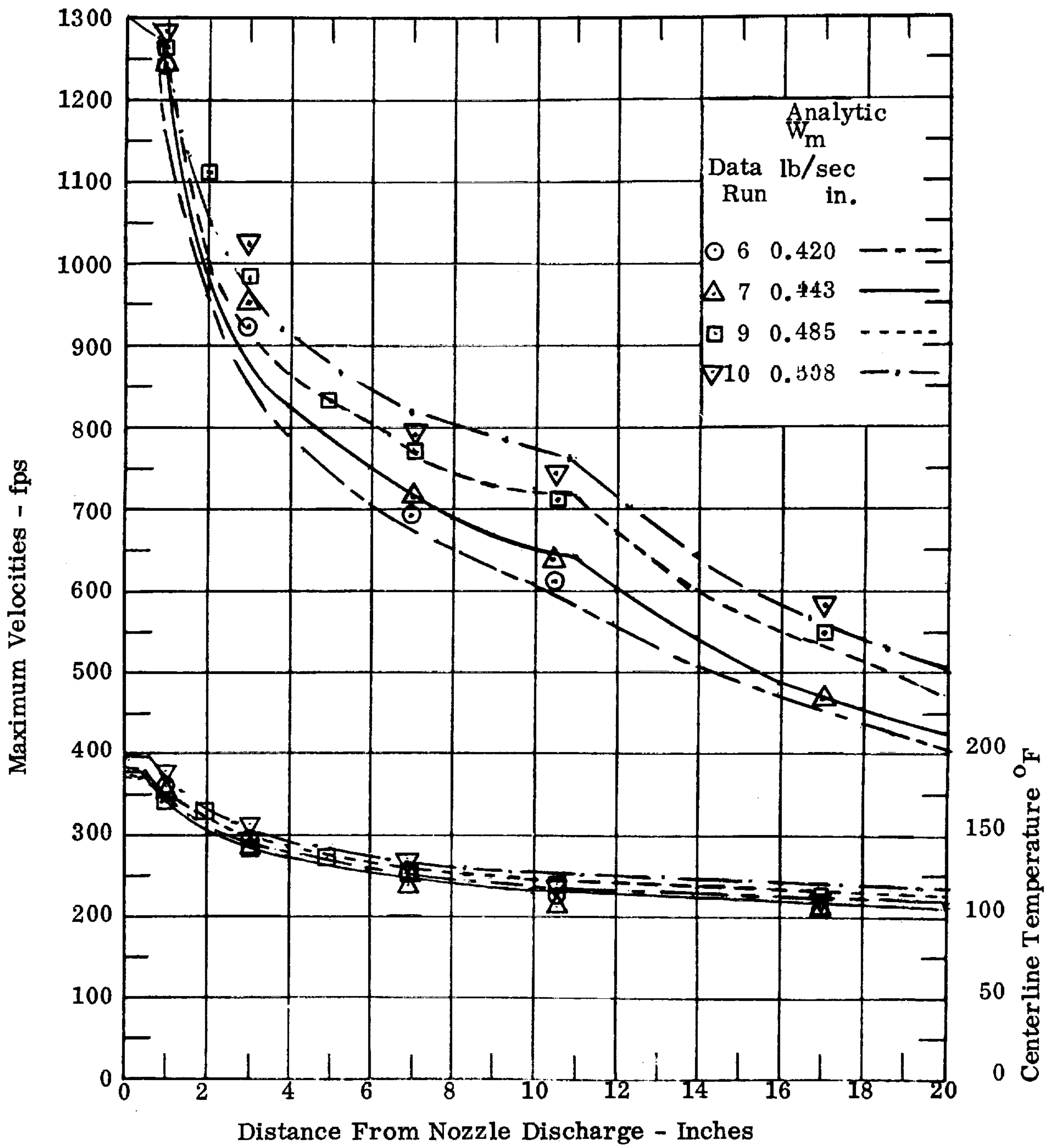

Figure 16 Maximum Velocities for 1.875" Throat Mixing Section

p_N = 21.0 psig

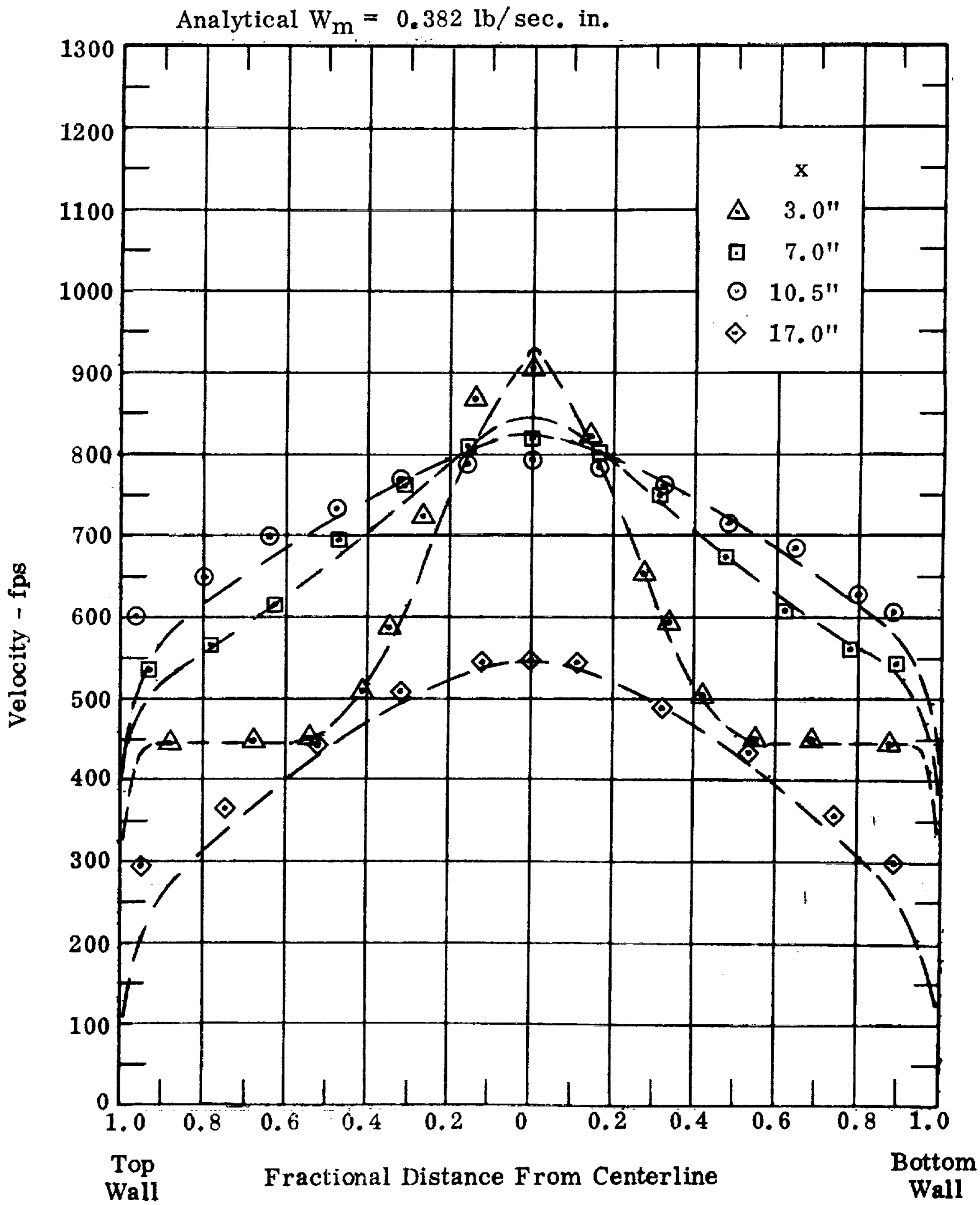

Figure 17 Velocity Profiles for Run 1 for 1.25" Throat Mixing Section
p_N = 17.0 psig, T_N = 181° F, W_N = .0780 lb/sec.in.

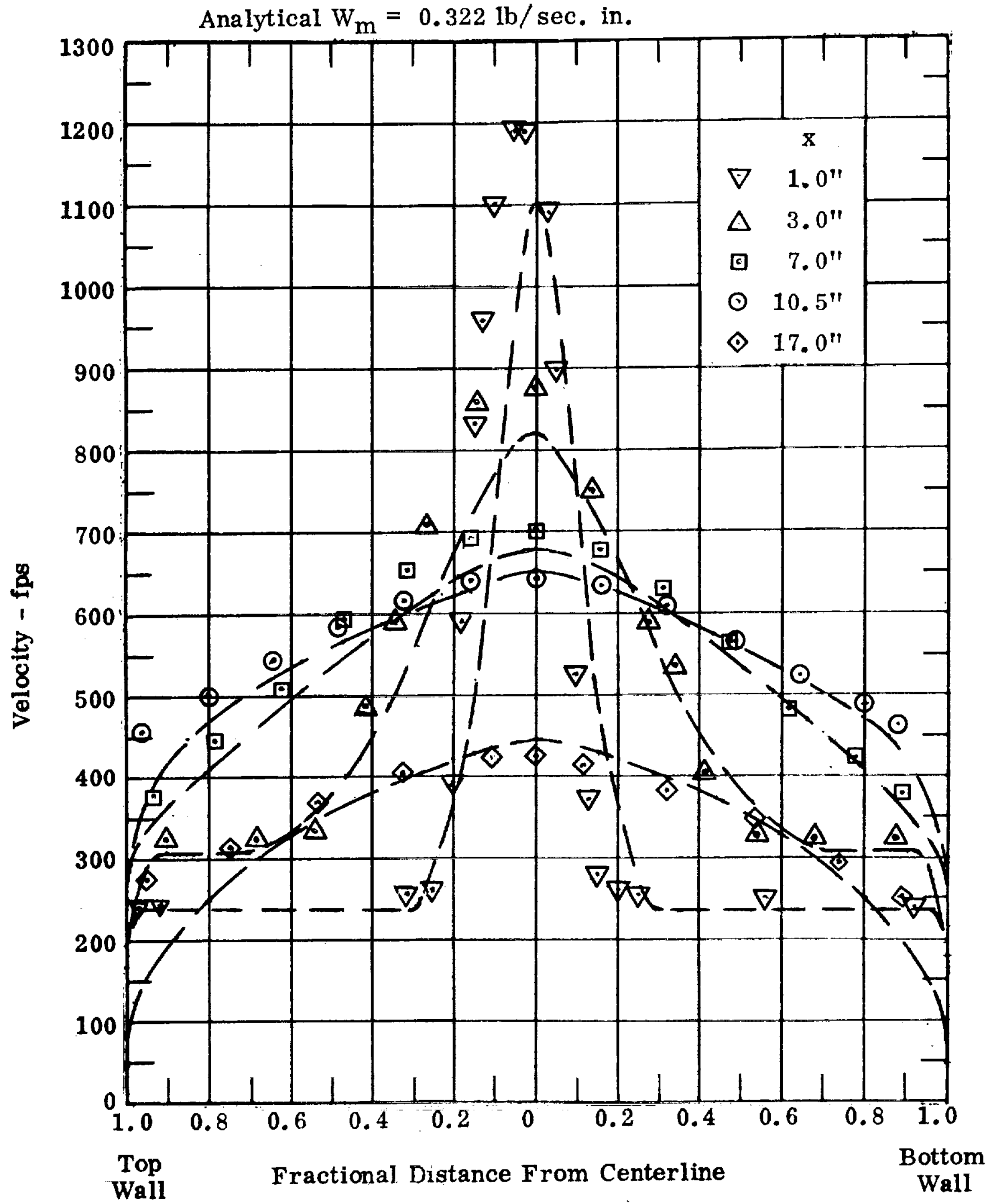

Figure 18 Velocity Profiles for Run 2 for 1.25" Throat Mixing Section
p_N = 17.0 psig T_N = 177° F, W_N = 0.0782 lb/sec. in.

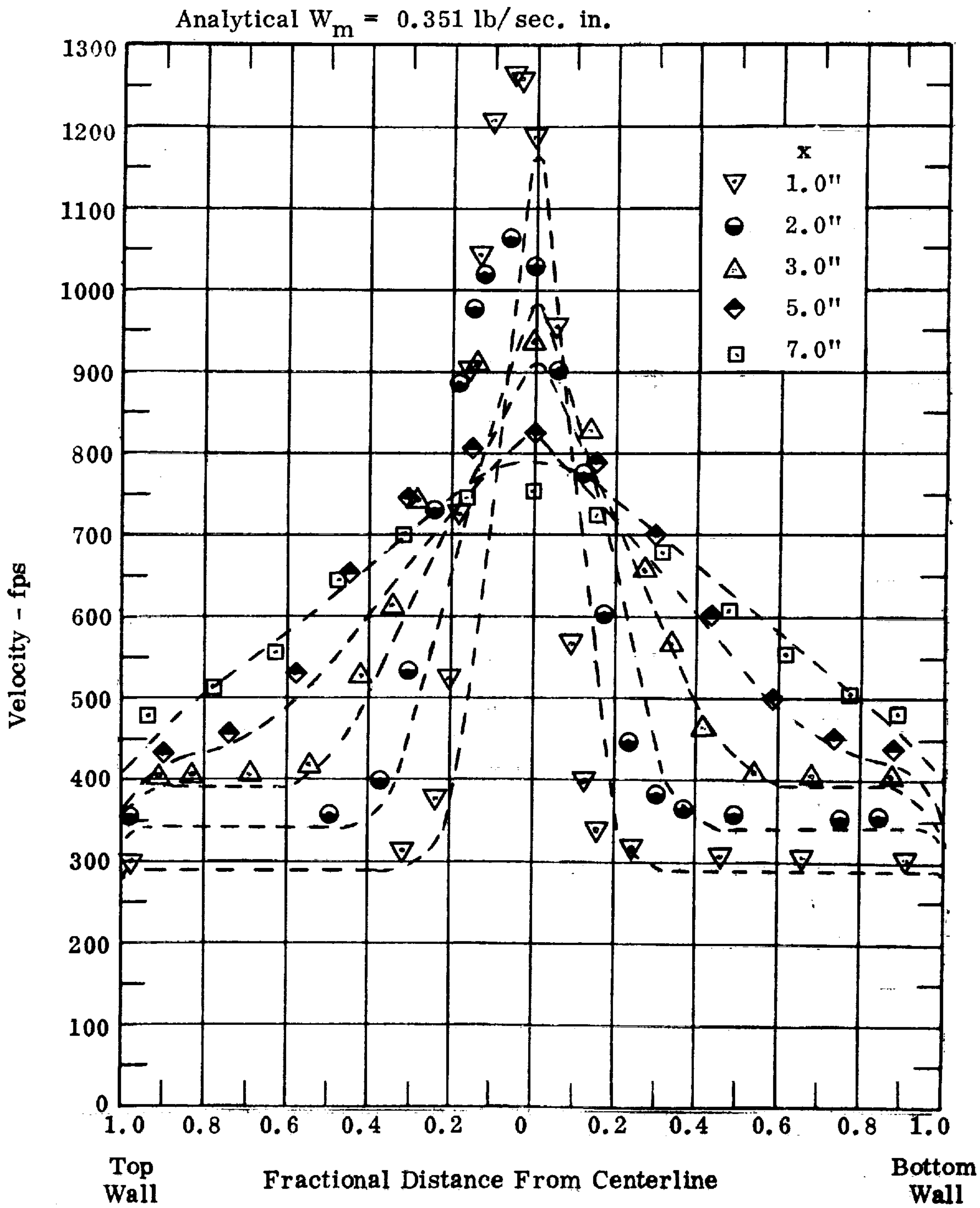

Figure 19a Velocity Profiles for Run 3 for 1.25" Throat Mixing Section

p_N = 17.0 psig, T_N = 246° F, W_N = 0.075 lb/sec. in.

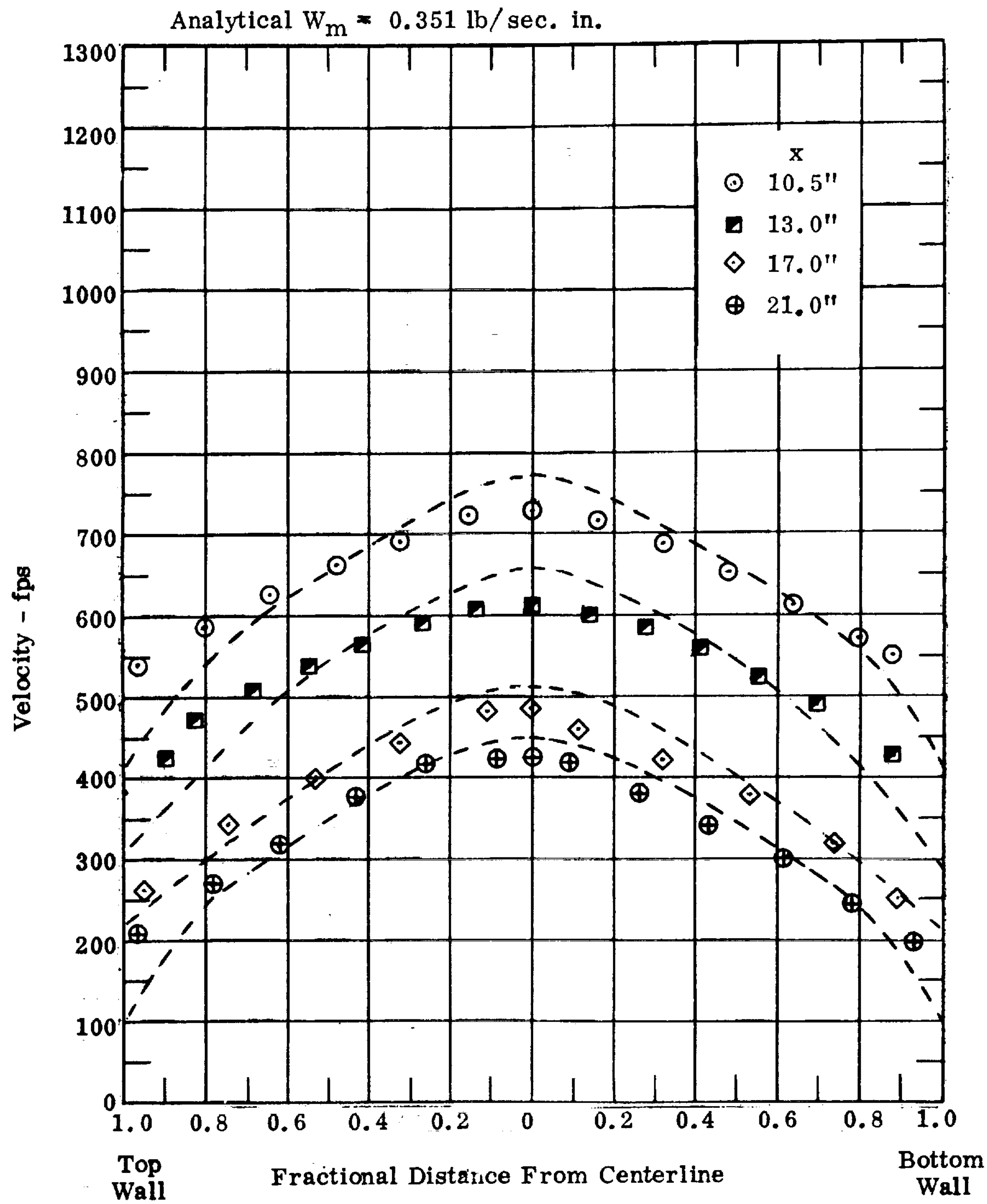

Figure 19b Velocity Profiles for Run 3 for 1.25" Throat Mixing Section

p_N = 17.0 psig, T_N = 246° F, W_N = 0.075 lb/sec. in.

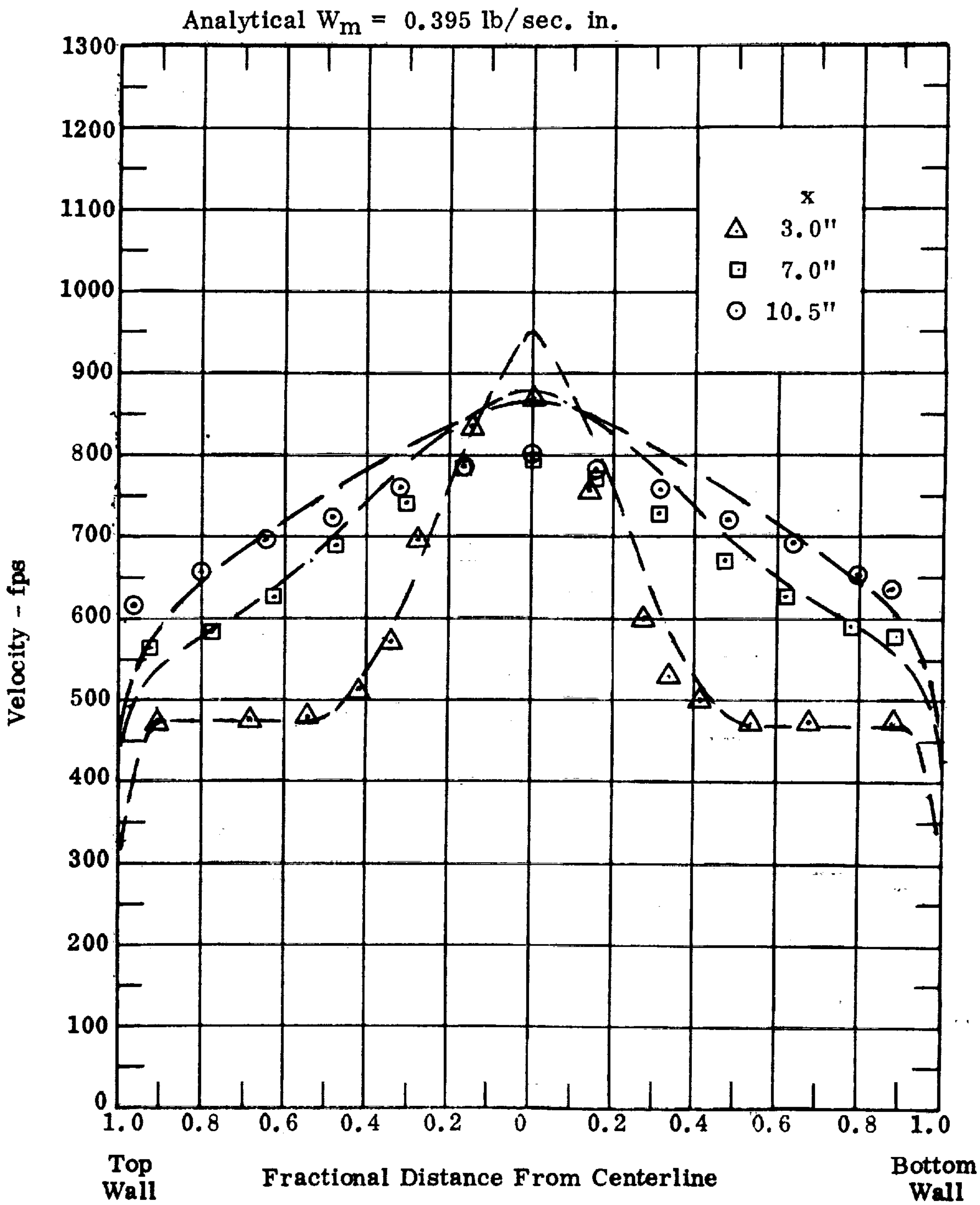

Figure 20 Velocity Profiles for Run 5 for 1.25" Throat Mixing Section

p_N = 17.0 psig, T_N = 188° F, W_N = .0787 lb/sec. in.

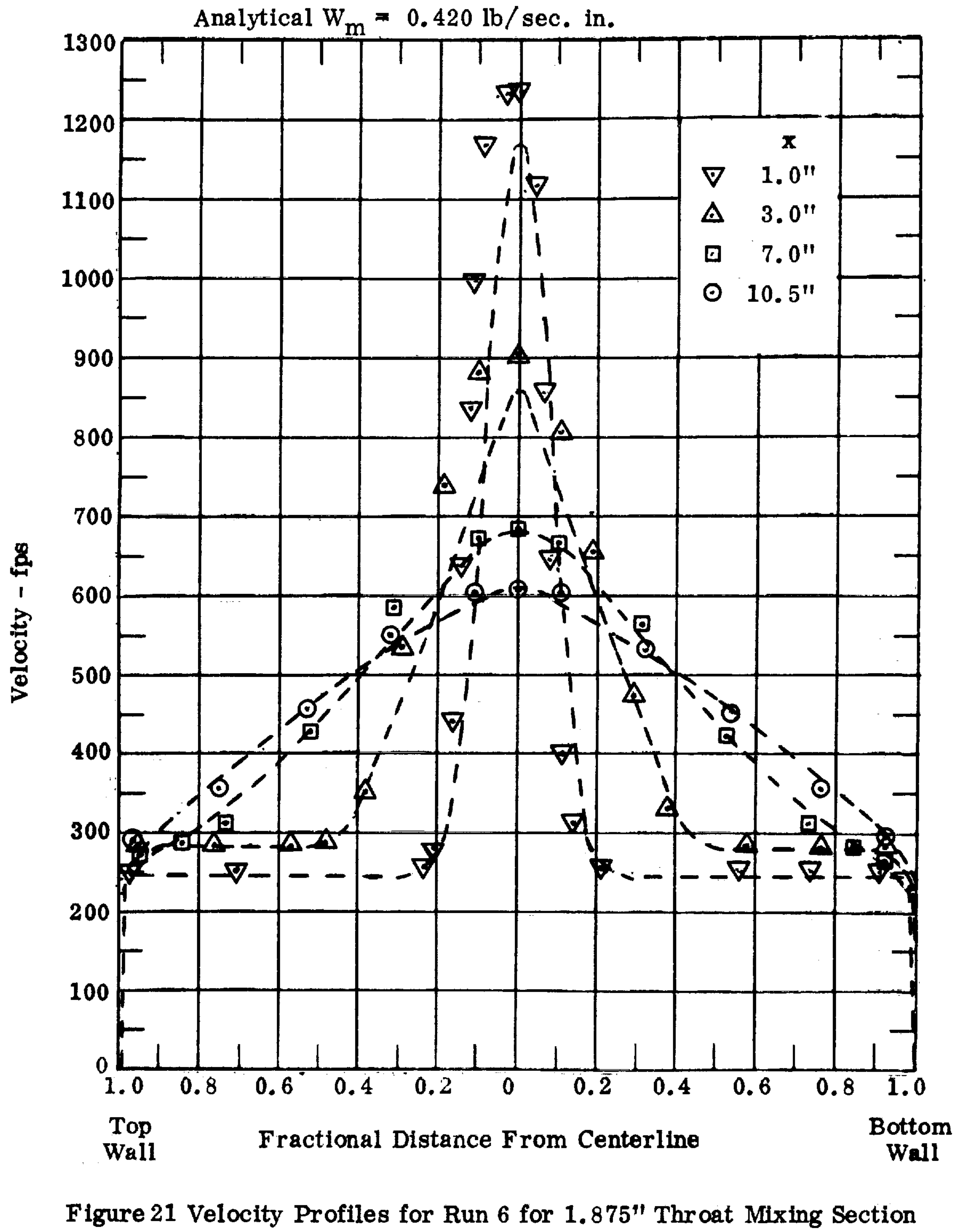

Figure 21 Velocity Profiles for Run 6 for 1.875" Throat Mixing Section

P_N=21.0 psig, T_N=189° F, W_N = .0882 lb/sec. in.

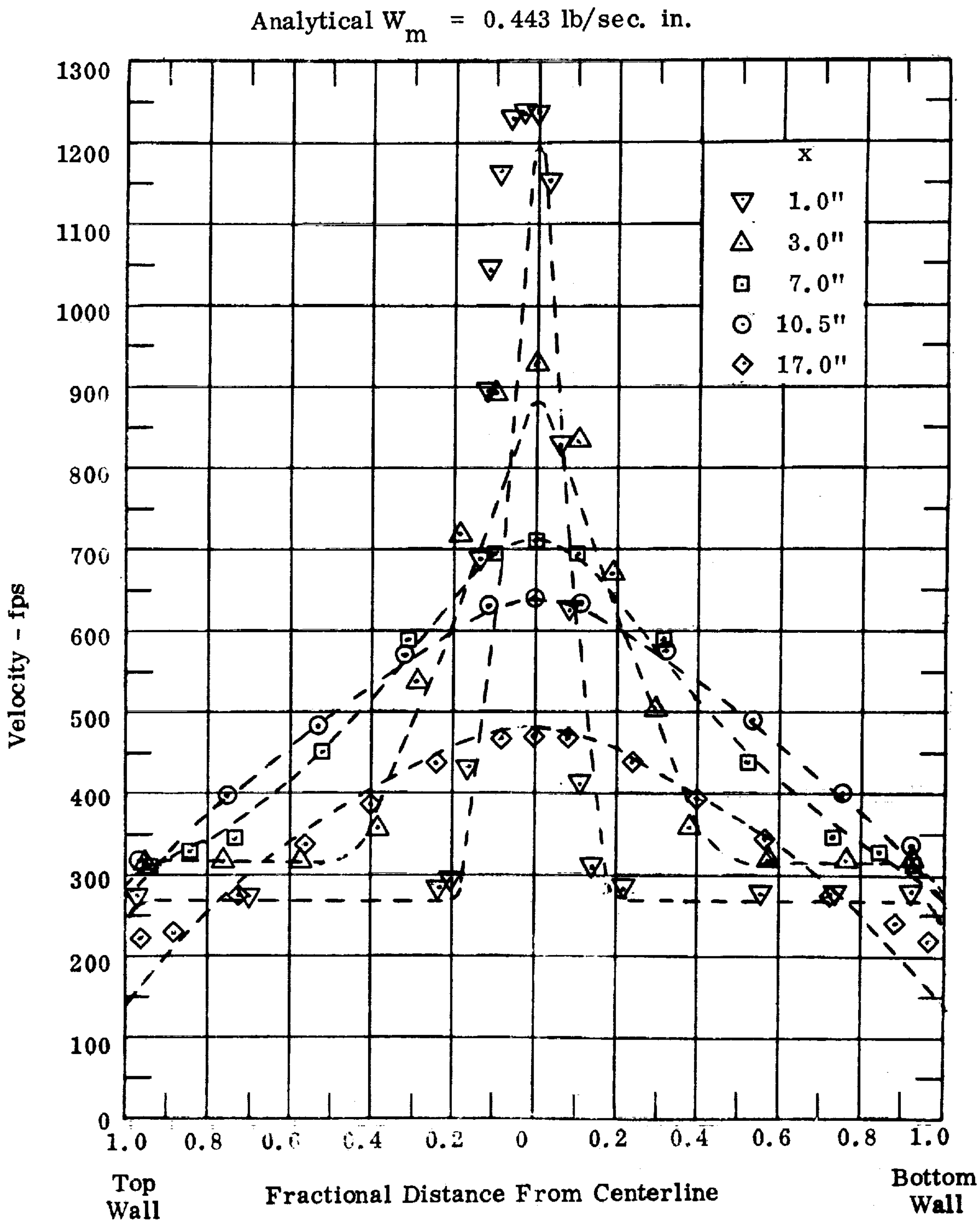

Figure 22 Velocity Profiles for Run 7 for 1.875" Throat Mixing Section p_N = 21.0 psig, T_N = 187°F, W_N = .0884 lb/sec. in.

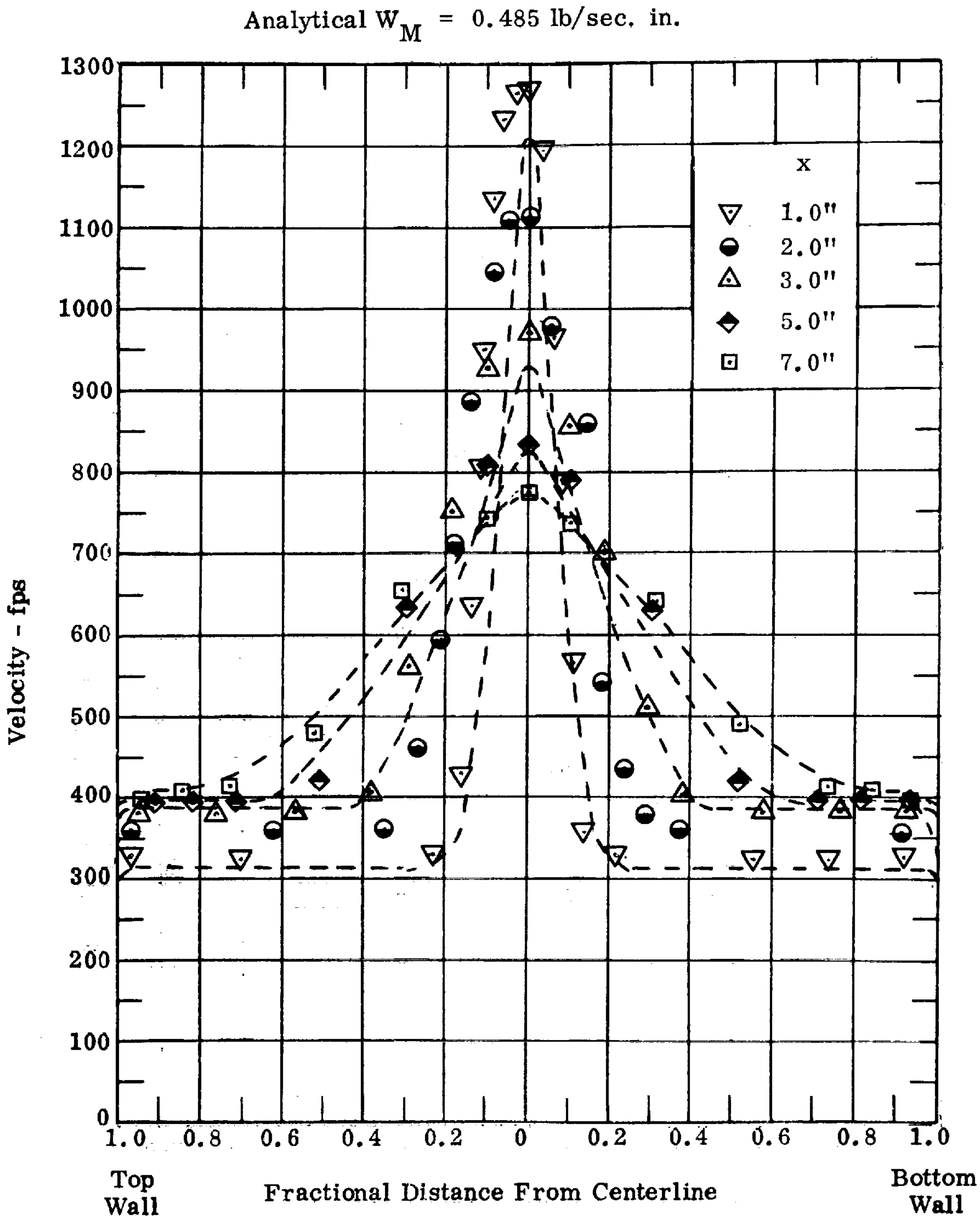

Figure 23a Velocity Profiles for Run 9 for 1.875" Width Mixing Section
p_N = 21.0 psig, T_N = 184°F, W_N = .0884 lb/sec. in.

Analytical W_m = 0.485 lb/sec. in.

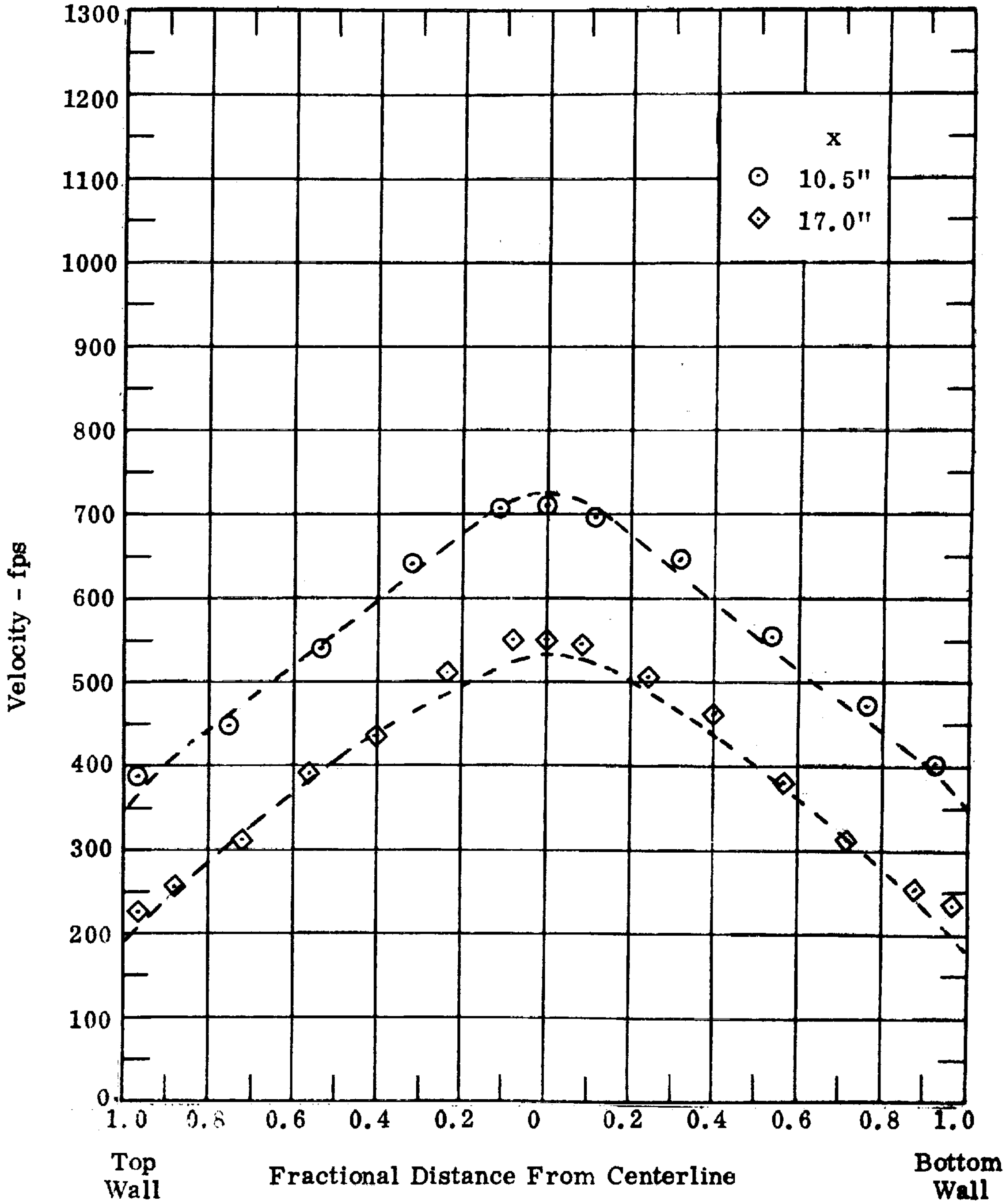

Figure 23b Velocity Profiles for Run 9 for 1.875" Throat Mixing Section
p_N = 21.0 psig, T_N = 184°F, W_N = .0884 lb/sec. in.

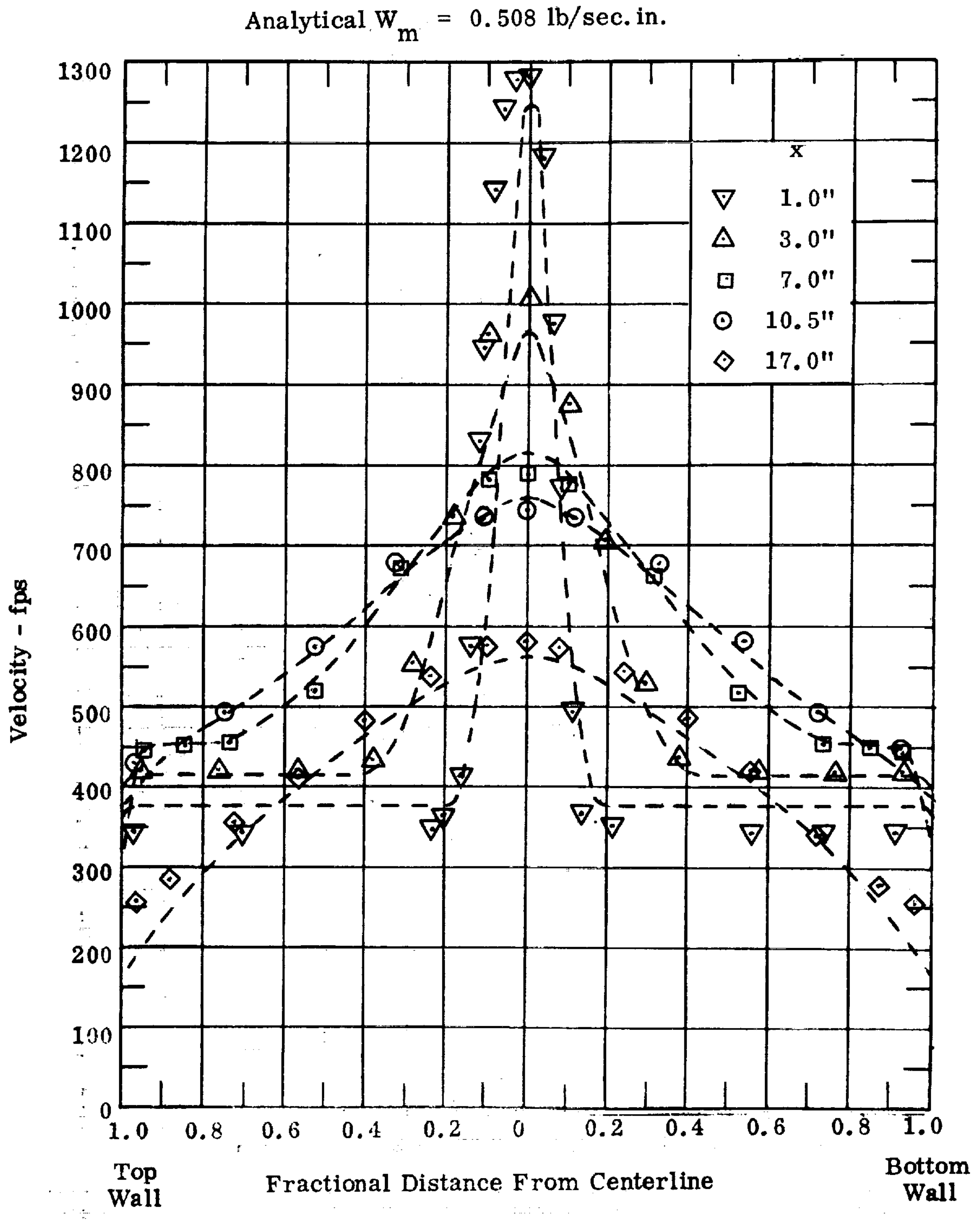

Figure 24 Velocity Profiles for Run 10 for 1.875" Throat Mixing Section
p_N = 21.0 psig, $T_N = 200^oF$, W_N = .0874 lb/sec. in.

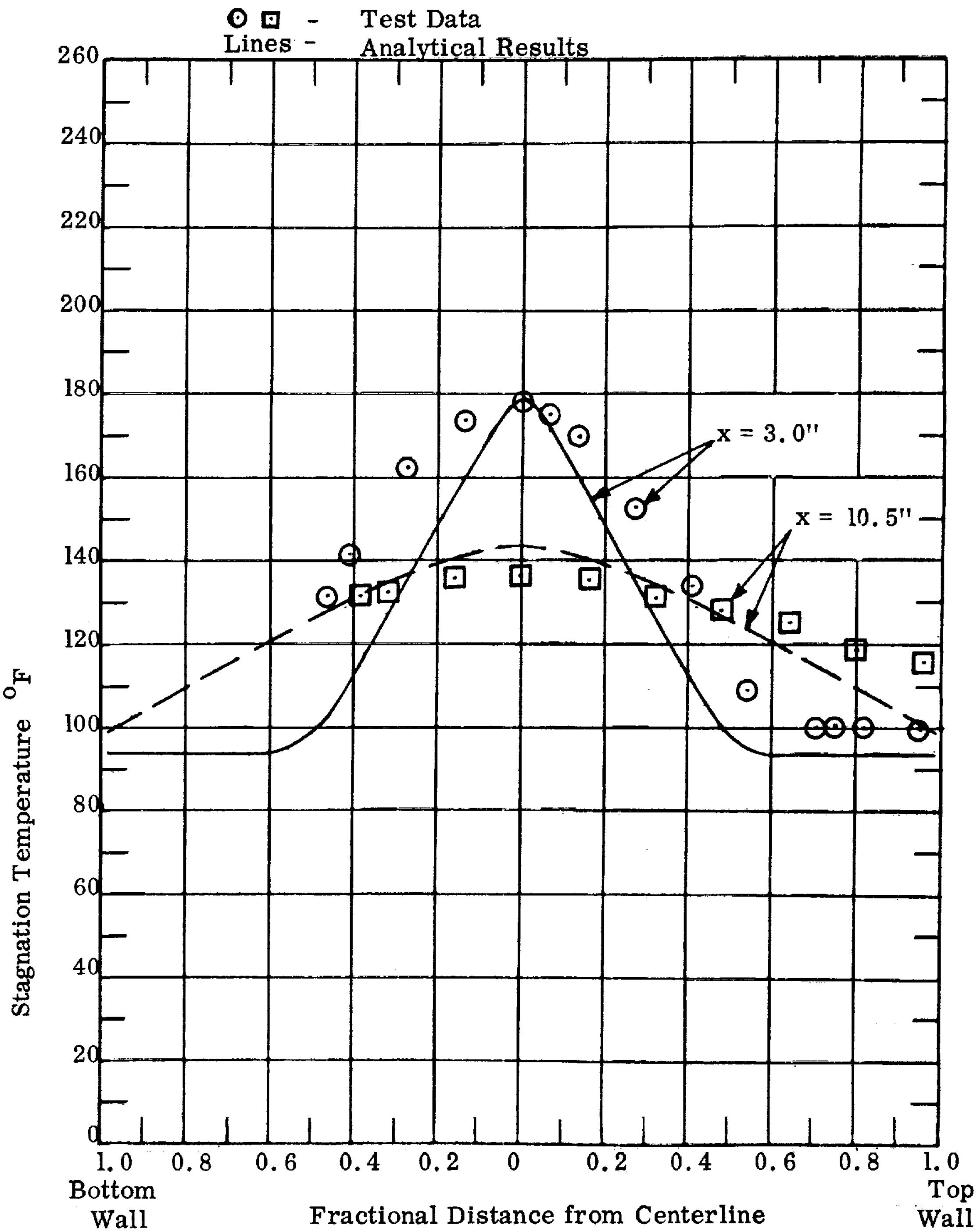

Figure 25 Temperature Profiles for Run 3 for 1.25" Throat Mixing Section

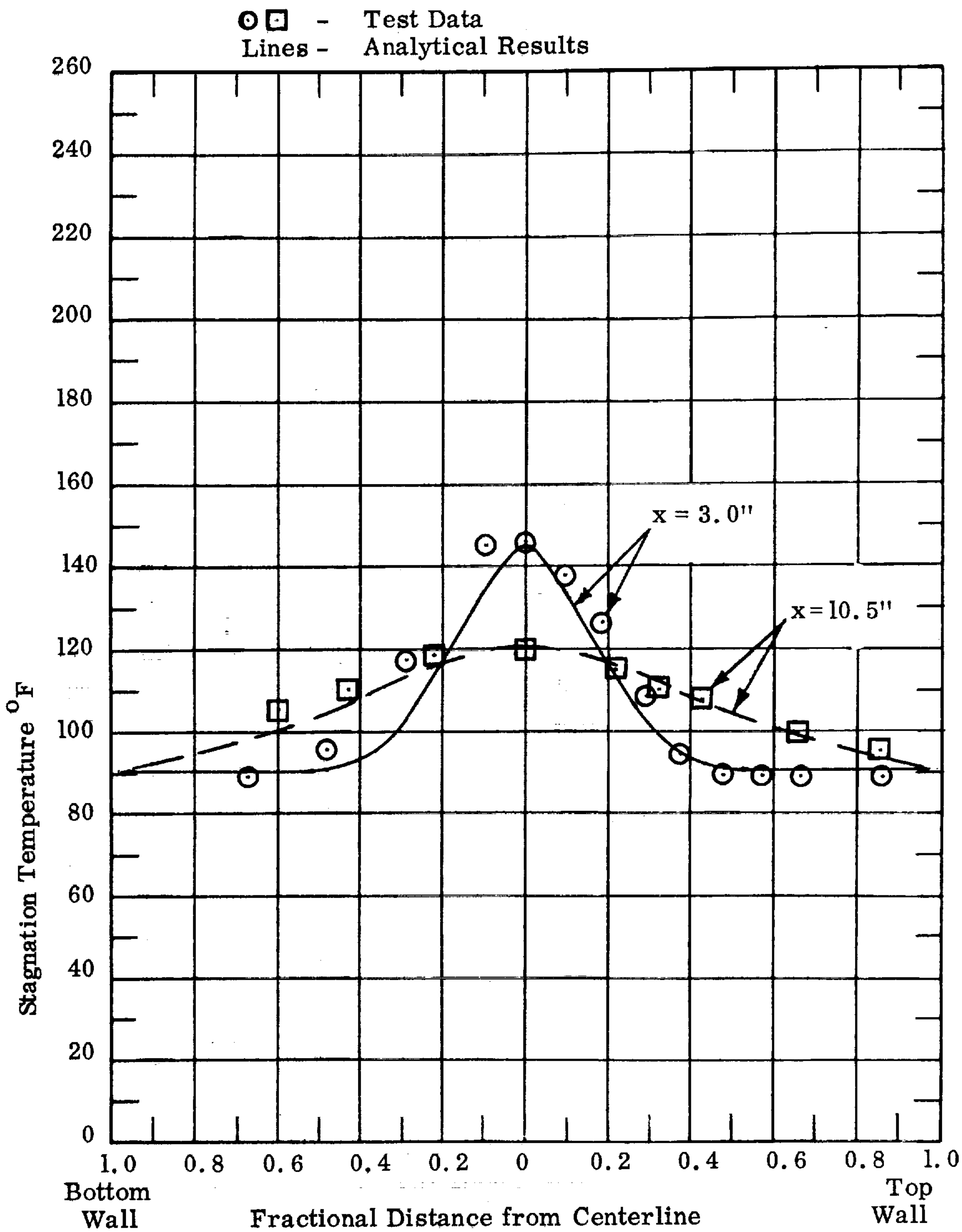

Figure 26 Temperature Profiles for Run 9 for 1.875" Throat Mixing Section

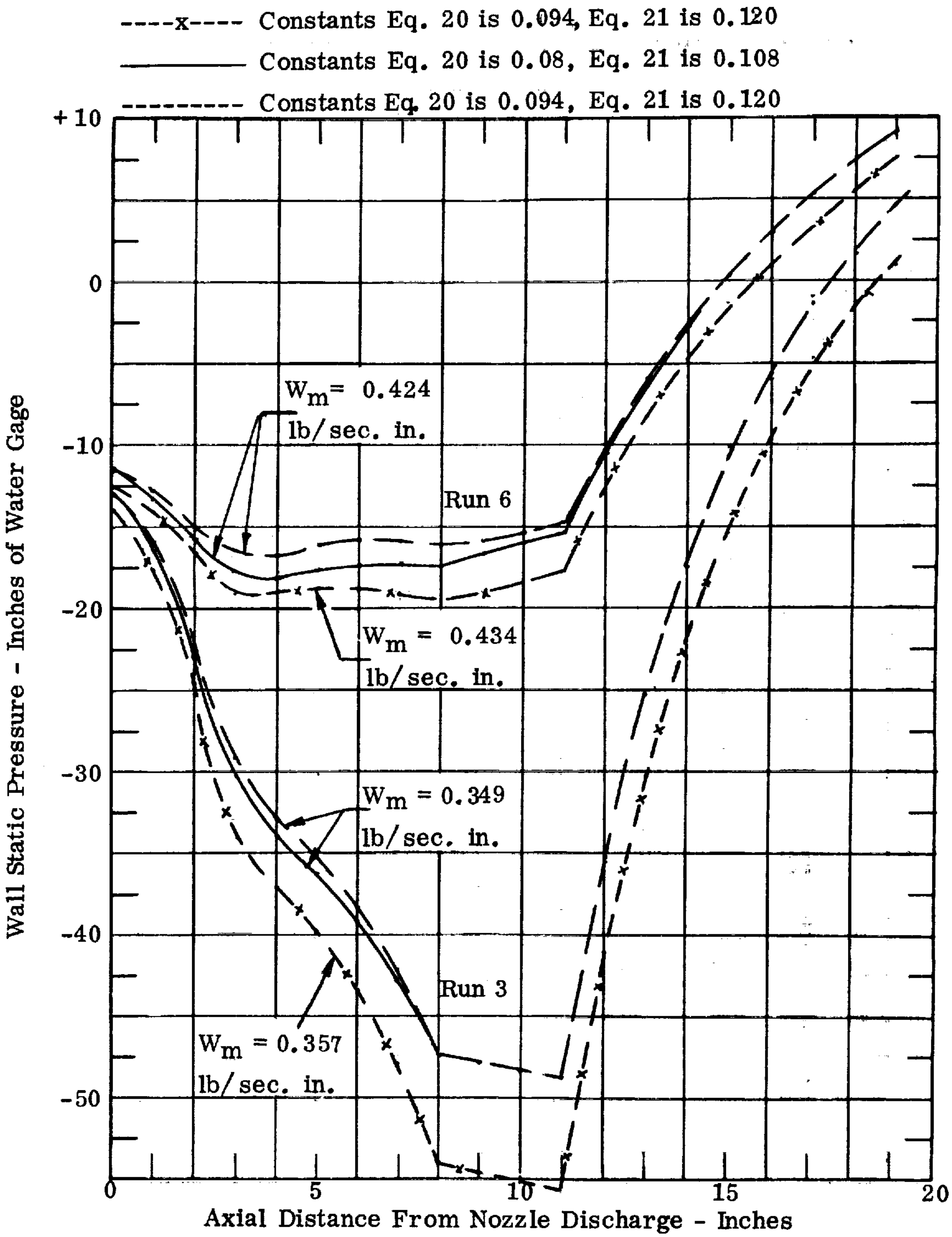

Figure 27 Wall Static Pressure Sensitivity to Flow Rate and Eddy Viscosity for Run 3 and Run 6

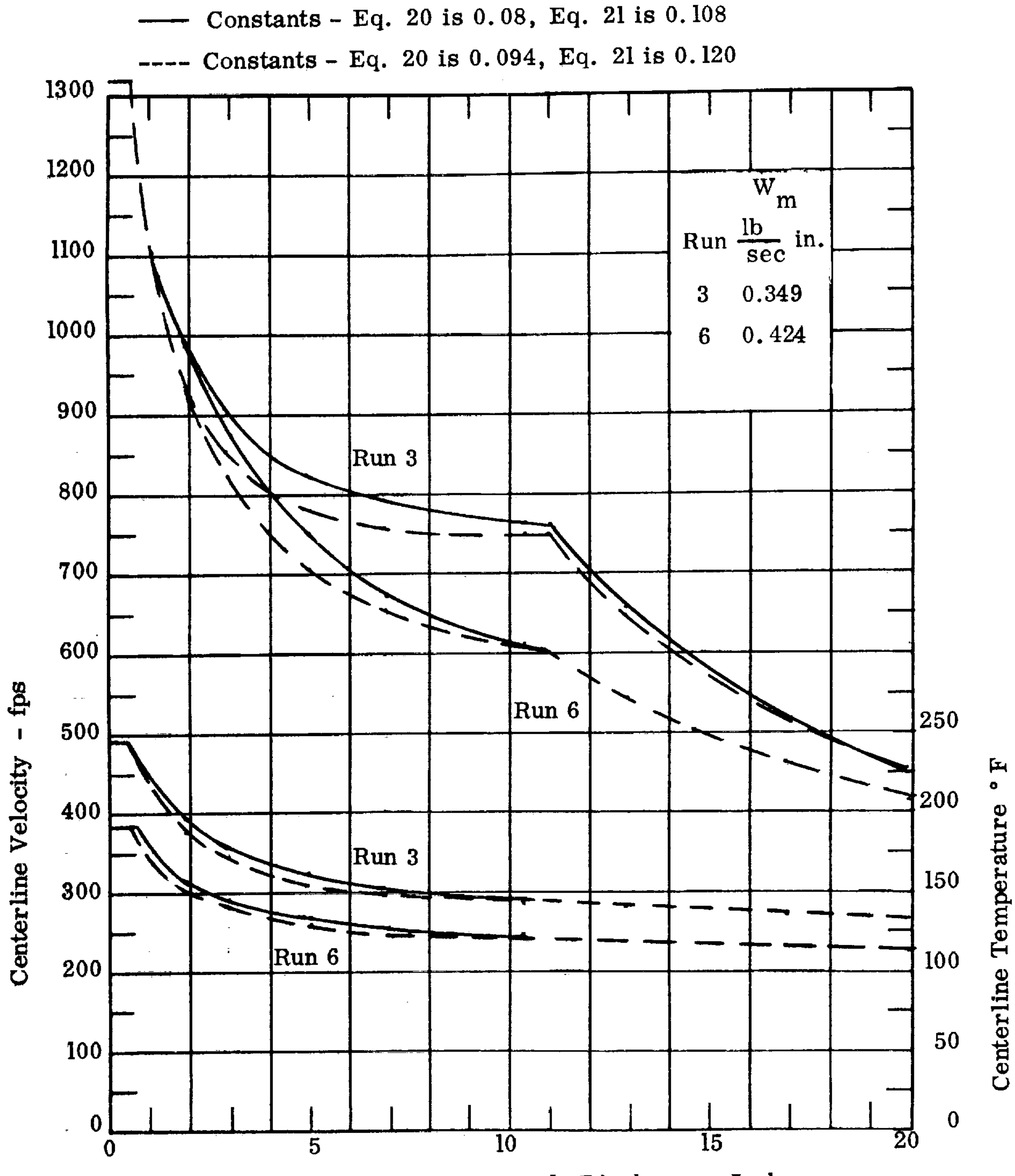

Figure 28 Centerline Velocity and Temperature Sensitivity to Eddy Viscosity for Run 3 and Run 6

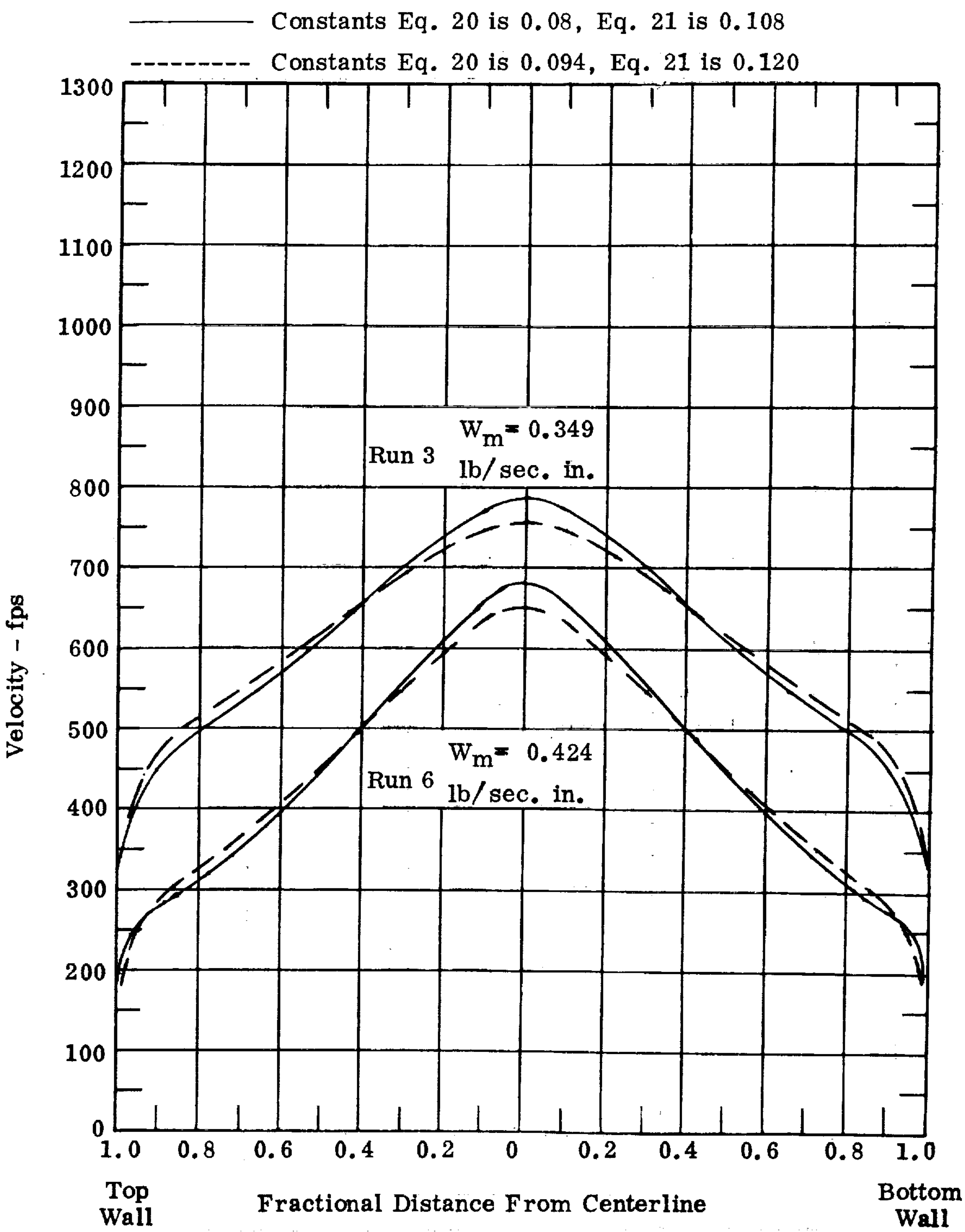

Figure 29 Velocity Profile Sensitivity to Eddy Viscosity For Run 3 and Run 6 at x = 7.0"

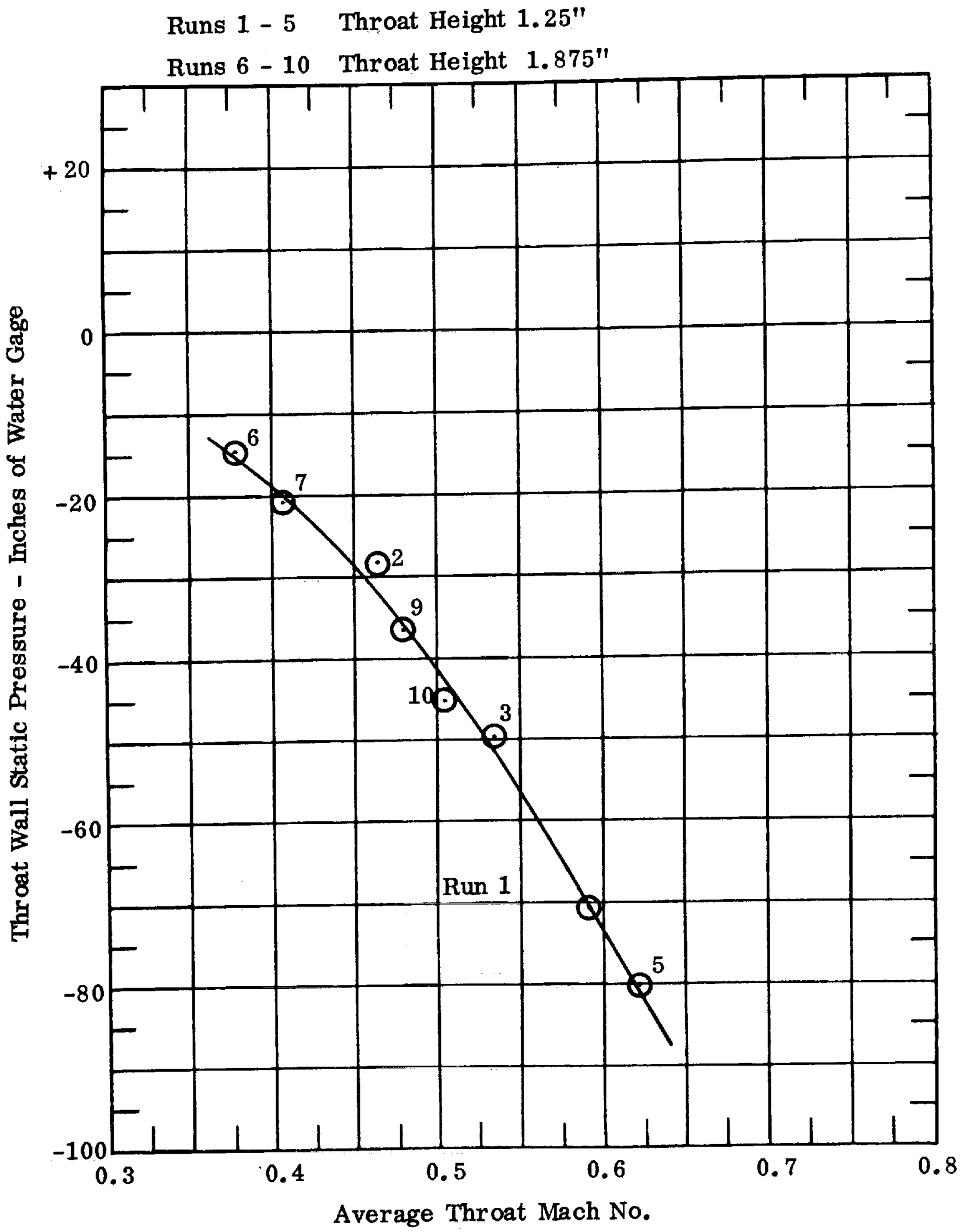

Figure 30 Mixing Section Throat Static Pressure As A Function of Throat Mach Number

*U.S. GOVERNMENT PRINTING OFFICE: 1973-739-026/19